Yasmin Faraji - Hoogvliet

The Development of TREYESCAN

An Eye Tracking Test for the Measurement of Compensatory Eye Movements for Driving with Visual Field Loss

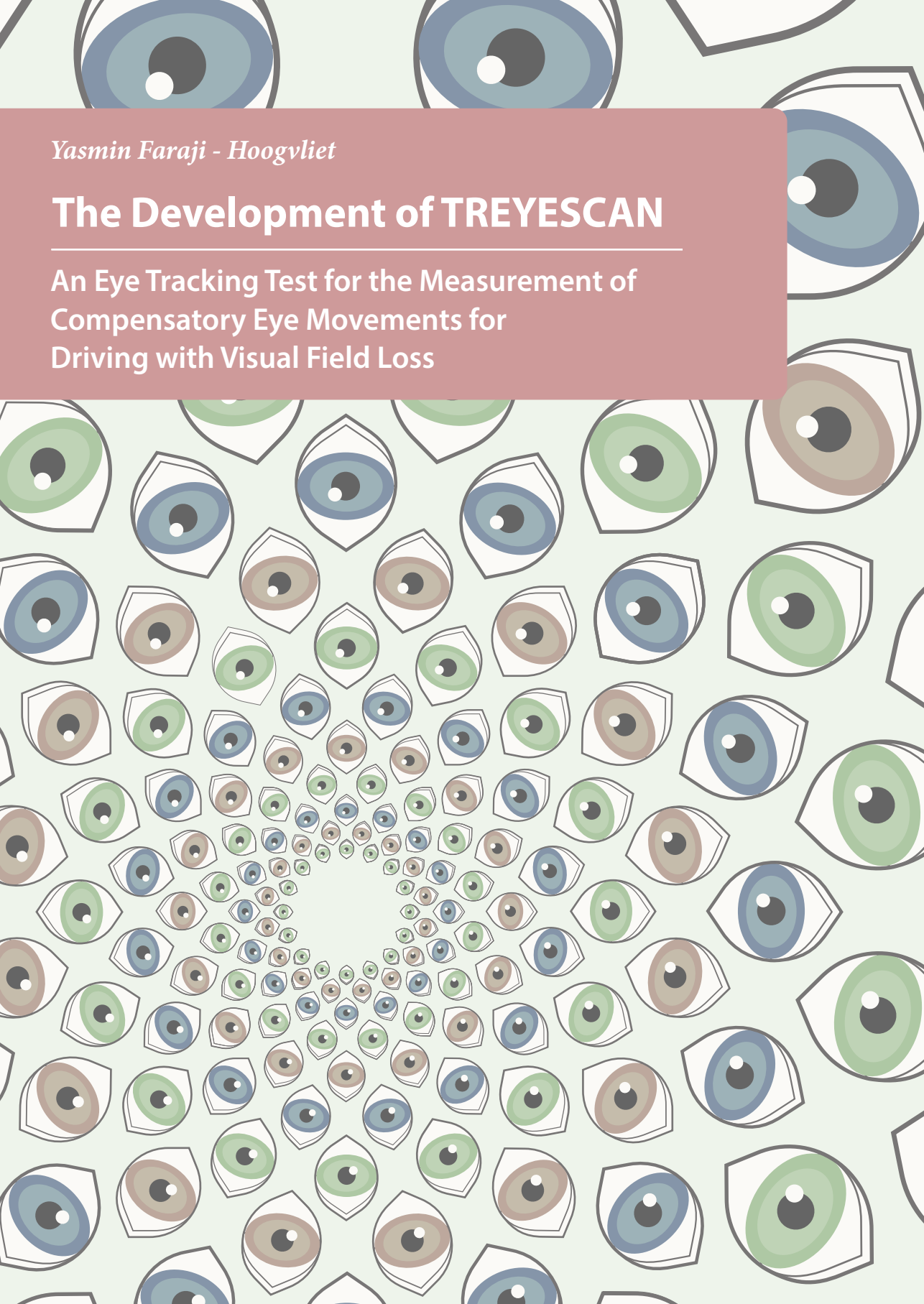

The Development of TREYESCAN

An Eye Tracking Test for the Measurement of Compensatory Eye Movements for Driving with Visual Field Loss

Y. Faraji-Hoogvliet

The studies presented in this thesis were conducted within the department of Ophthalmology, Amsterdam UMC, Vrije Universiteit Amsterdam and the Amsterdam Public Health research institute, Amsterdam, the Netherlands.

The research presented in this thesis was financially supported by Stichting Uitzicht, Algemene Nederlandse Vereniging Ter Voorkoming Van Blindheid, De Landelijke Stichting voor Blinden en Slechtzienden, Oogfonds, Visio Foundation, Stichting tot Verbetering van het Lot der Blinden, COVID Amsterdam UMC Financial Support Voucher, and Vision 2017 Conference Revenues.

Additional financial support for printing this thesis was kindly provided by Stichting Blindenhulp, Tramedico, Landelijke Stichting voor Blinden en Slechtzienden, Chipsoft, Rotterdamse Stichting voor Blindenbelangen, Synga Medical, Ergra Low Vision, Bayer, Stichting tot Verbetering van het Lot der Blinden, Thea Pharma, Koninklijke Visio, and Santen.

Lay-out & Printing:	Ridderprint | www.ridderprint.nl
Cover:	Y Faraji
ISBN:	978-94-6506-394-2
DOI:	http://doi.org/10.5463/thesis.788

VRIJE UNIVERSITEIT

The Development of TREYESCAN

An Eye Tracking Test for the Measurement of Compensatory Eye Movements for Driving with Visual Field Loss

ACADEMISCH PROEFSCHRIFT

ter verkrijging van de graad Doctor
aan de Vrije Universiteit Amsterdam,
op gezag van de rector magnificus
prof.dr. J.J.G. Geurts,
in het openbaar te verdedigen
ten overstaan van de promotiecommissie
van de Faculteit der Geneeskunde
op vrijdag 15 november 2024 om 13.45 uur
in een bijeenkomst van de universiteit,
De Boelelaan 1105

door

Yasamin Faraji
geboren te Sari, Iran

promotoren:	prof.dr. G.H.M.B. van Rens prof.dr. R.M.A. van Nispen
copromotoren:	dr. L.J. van Rijn dr. J. Koopman
promotiecommissie:	prof.dr. A.C. Moll prof.dr. H.J.M. Beckers prof.dr. F.W. Cornelissen dr. H.H.L.M. Goossens prof.dr. D. de Waard

To praise the sun is to praise your own eyes

— Rumi

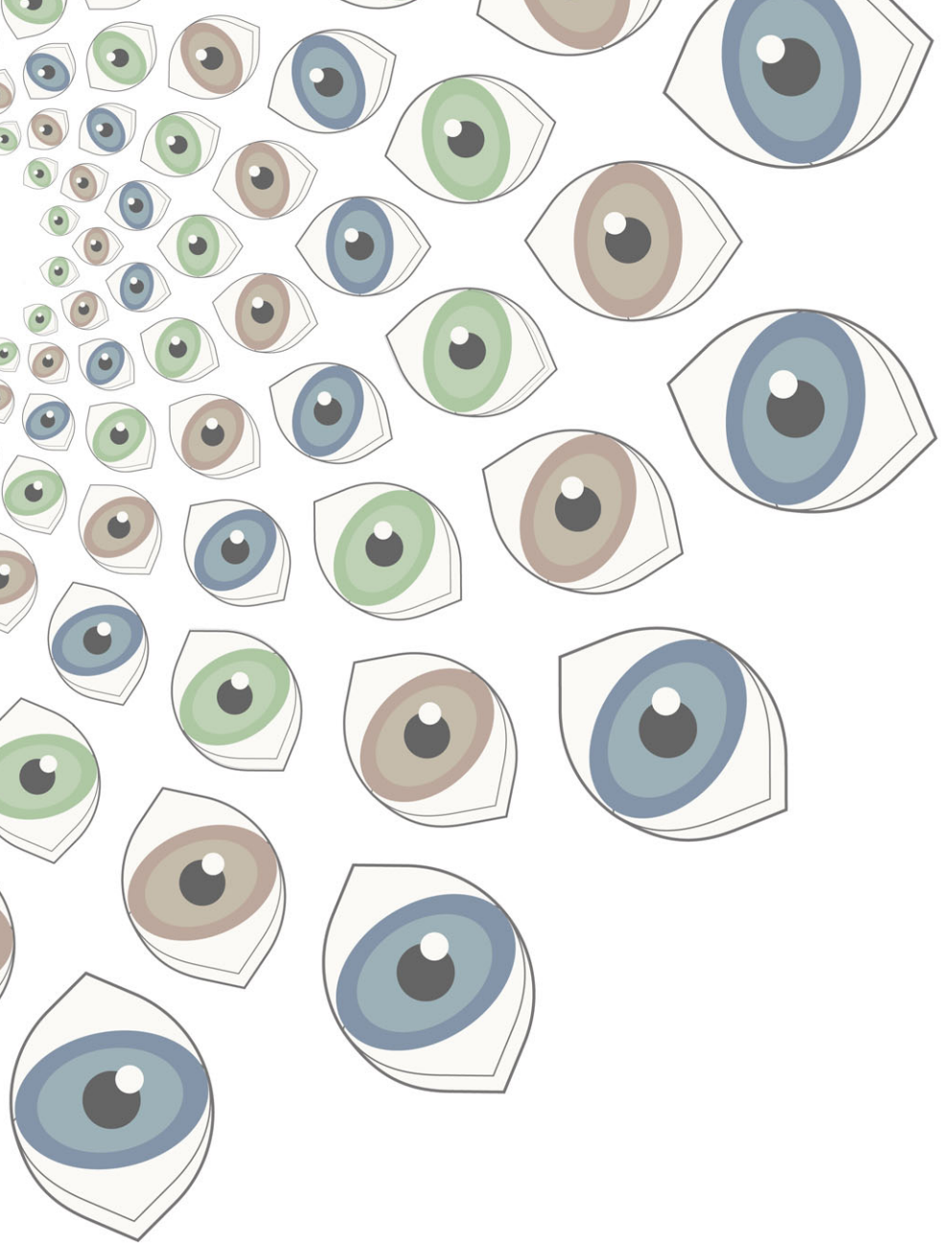

Table of Contents

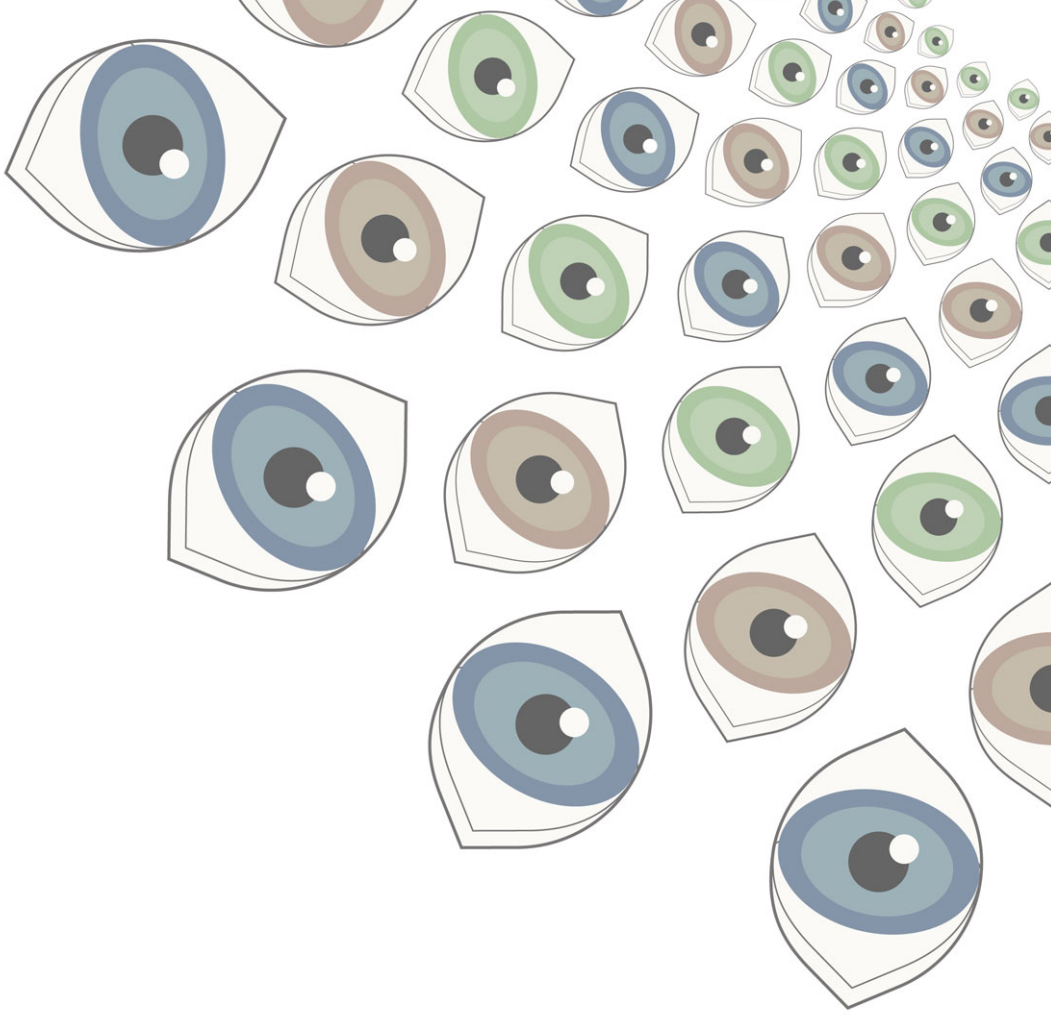

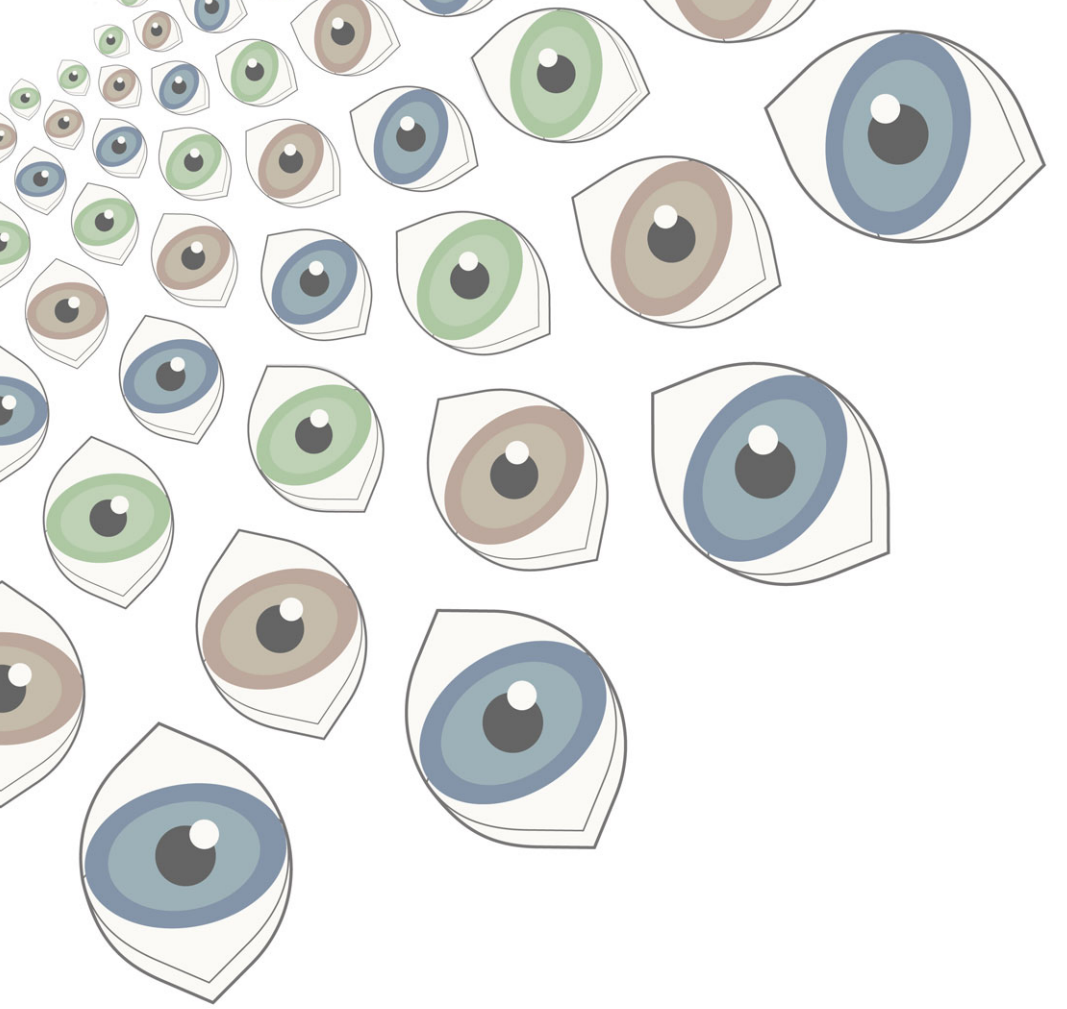

Chapter 1

General Introduction

Glaucoma

Glaucoma, a prevalent ocular disorder, is the leading cause of irreversible blindness and the second leading cause of blindness worldwide.[1] The most common form of glaucoma, known as primary open-angle glaucoma (POAG), often manifests with increased intraocular pressure (IOP), leading to the gradual deterioration of the optic nerve fibers. POAG represents a significant public health concern with a global prevalence of 2.4% in the population over 40 years old, affecting 68.56 million individuals in 2021.[2] Additionally, other forms of glaucoma exist, such as angle-closure glaucoma, normal-tension glaucoma, and secondary glaucoma, which is associated with other ocular or systemic conditions. Glaucoma is characterized by progressive damage to the optic nerve (Fig. 1 & Fig. 2), a vital structure responsible for transmitting visual information from the eye to the brain.[3] As the disease progresses, this damage results in the development of characteristic visual field defects, primarily peripheral vision (Fig. 3). If left untreated or inadequately managed, glaucoma can lead to irreversible vision loss, with advanced stages potentially ending in tunnel vision or even complete blindness. Therefore, timely detection and intervention are vital to minimize the impact of glaucoma on visual function.[4]

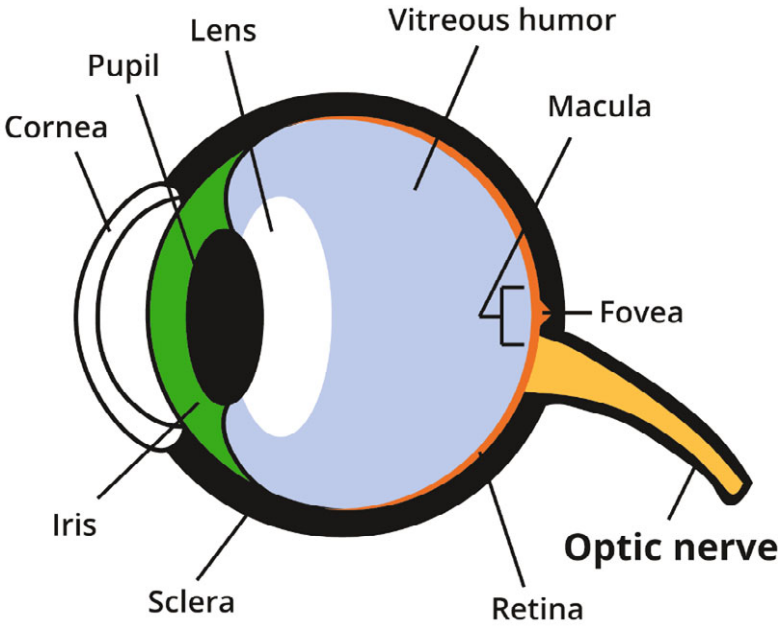

Figure 1. Schematic representation of the major eye structures. The optic nerve is highlighted.

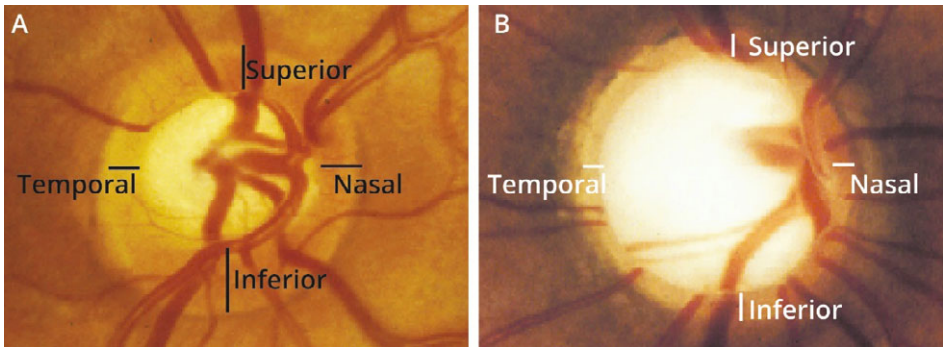

Figure 2. Ophthalmoscopic photographs of a healthy and glaucomatous optic disk of the right eye. **A.** In the healthy optic disc, the neuroretinal rim has its normal shape with its widest part in the inferior region. **B.** In the glaucomatous optic disc, the neuroretinal rim is strikingly thinner than in the healthy optic disc, and the optic cup is subsequently larger and deeper.
Adapted from Jonas, et al.[3] Glaucoma (2017) *The Lancet*.

Visual Field Testing

Static visual field testing can provide insights into visual field function in clinical and research settings. A standard automated perimeter, typically the Humphrey Field Analyzer (Zeiss) or Octopus (Haag-Streit), consists of a concave dome with a central fixation target and multiple stimulus points arranged in a grid pattern.[5] During the test, patients keep their head still on a chinrest and maintain fixated on the central target while the testing protocol presents small stimuli at various locations within the grid. When a threshold test is done, the minimum detectable intensity of light at different locations within the visual field is determined. The stimuli are typically presented briefly, and patients are required to respond whenever they detect them by pressing a button. The responses are then recorded, and a comprehensive map of the patient's visual field sensitivity is generated. This allows for the identification and characterization of visual field defects, such as scotomas or areas of reduced sensitivity, which may indicate the presence of ocular or neurological disorders. Both monocular and binocular testing approaches can be used to evaluate the visual field function.

Monocular threshold testing is used to monitor each eye separately, which provides information about the individual eye's sensitivity and detects any eye-specific abnormalities (Fig. 3). This is particularly useful when assessing the progression of visual field loss in one eye.[6]

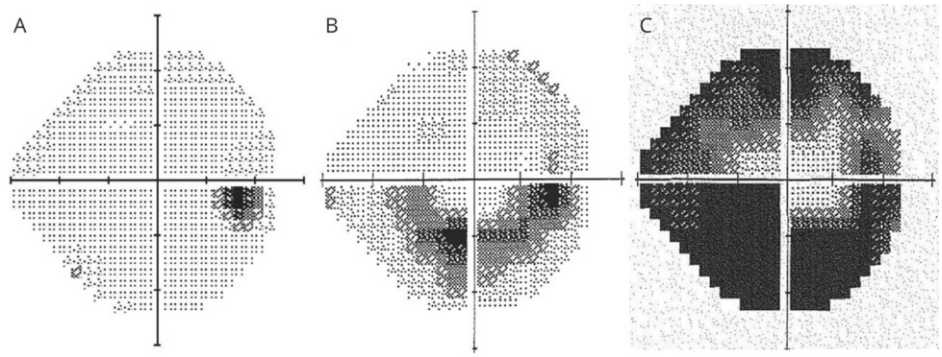

Figure 3. Characteristics of visual field loss in glaucoma as evaluated through a monocular 24-2 visual field test. **A.** Visual field within normal limits. Blind spot appears black, which is physiological. This occurs because there are no photoreceptors in the optic disc of the retina where the optic nerve exits the eye. The brain usually compensates for the blind spot, filling in the missing information based on surrounding visual input, so individuals are generally unaware of this gap in their vision under normal circumstances. **B.** Arcuate scotoma, due to damage to the arcuate fibers. Darker gray and black areas represent loss of vision in the visual field. **C.** Advanced stage of glaucomatous field loss, with a central/temporal island of vision remaining. Nasal fibers and the maculopapular bundle are typically spared until late in the disease process. Photos Courtesy of Pradeep Ramulu, MD, PhD, Wilmer Eye Institute, EyeWiki: Standard Automated Perimetry, *American Academy of Ophthalmology*.

Binocular suprathreshold testing, on the other hand, evaluates the visual field by measuring both eyes simultaneously. This is highly relevant, since the brain integrates the visual input received from each eye (Fig. 4). The optic nerve carries visual information to the optic chiasm from each eye, where a partial crossing of optic nerve fibers occurs. Subsequently, the left and right optic tracts, transmit information to the occipital cortex. The integration of the two fields occurs in the higher visual processing centers, where the views from each eye are compared and combined, enabling the perception of depth, stereopsis, and accurate spatial judgment.[7] In the case of individuals with glaucoma who have visual field loss, the fusion of the fields of each eye could lead to a normal binocular visual field, if the visual field loss in one eye corresponds with an area of intact visual field perception in the other eye.[8]

The Esterman visual field test is typically used for binocular testing (Fig. 5).[9] Utilizing a suprathreshold approach, this test employs a grid with 120 stimuli covering about 160 degrees horizontally. Notably, the central 10 degrees are excluded from the testing grid. In a suprathreshold visual field test, patients are presented stimuli that are deliberately set above the threshold level, ensuring they are easily visible. The goal of such a test is to quickly identify abnormalities or significant deficits within the visual field. Typically employed for screening purposes, a suprathreshold test

offers a rapid assessment. However, it is less sensitive in detecting subtle changes or early signs of visual field abnormalities. By measuring the inputs from both eyes, binocular testing provides an assessment of the patient's overall visual field function and the integration from both eyes. This test is particularly suitable when a patient's visual field needs to be evaluated in relation to the functional impact on tasks, such as driving.[10,11]

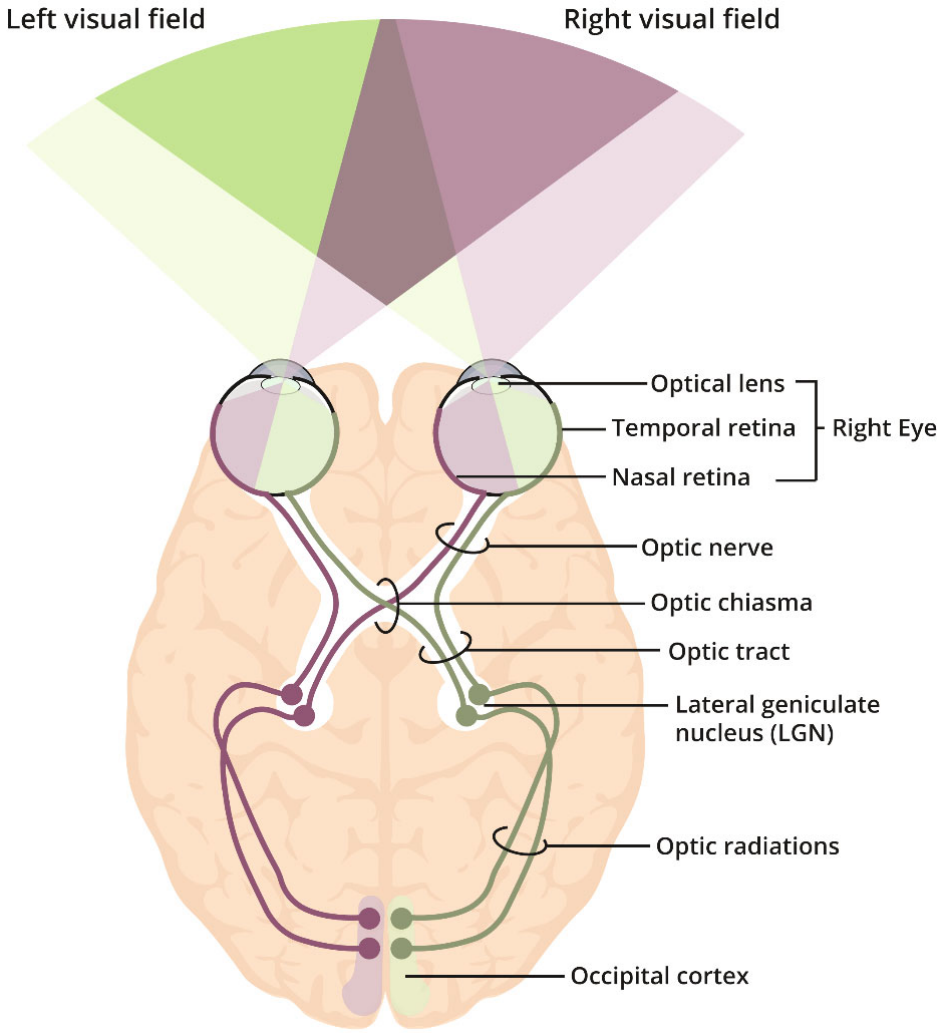

Figure 4. Schematic representation of the visual pathways. The overlapping sections of the visual fields, represents the section of the visual field perceived with both eyes.

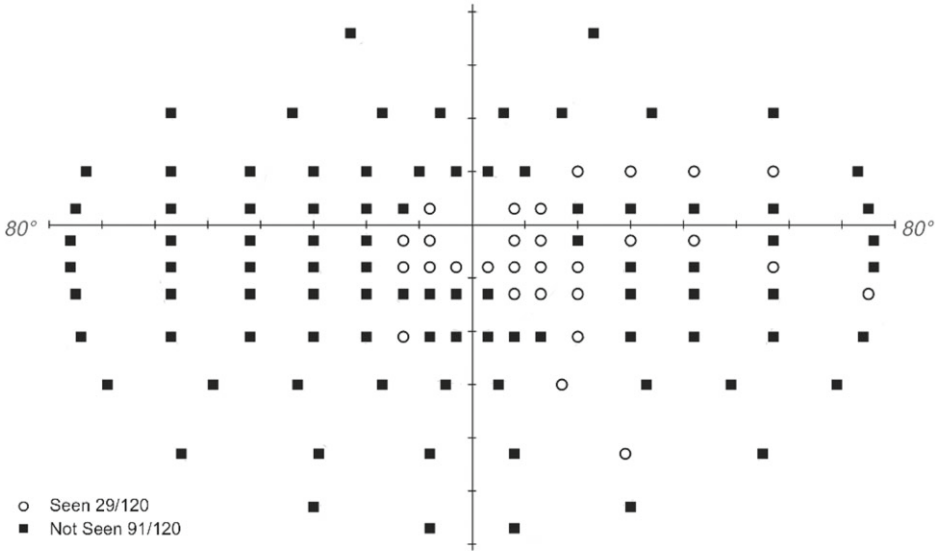

Figure 5. An Esterman visual field test of a person with advanced glaucomatous visual field loss.

Undergoing a visual field test can be difficult for some individuals.[12] It requires an understanding of what is asked, an ability to perform tasks quickly, and high levels of concentration.[13] Especially maintaining strict fixation on a central target while stimuli are presented at various locations within the visual field, requires a high level of concentration and visual attention.[14] This can be particularly demanding for patients with attention deficits or those experiencing fatigue during the testing session.

A visual field test is one example of a visual function test, with others including visual acuity measurements, color vision assessments, and tests for glare and contrast sensitivity. These tests evaluate how effectively the eye and visual system perform. On the other hand, functional vision refers to how well an individual performs in vision related tasks, such as reading or driving.[15] Most diagnostic visual field tests use small, threshold-level stimuli presented against an empty field. However, functional and real-world vision typically involve detecting larger, often moving objects against complex backgrounds. The peripheral field is especially sensitive to motion, yet standard automated perimetry typically relies on static stimuli. Additionally, these tests do not evaluate the binocular visual field and measure eye movements, both of which are crucial for assessing functional vision. In daily life, effective scanning habits are essential for good spatial awareness.[16]

Unawareness of Visual Field Loss

Glaucoma patients often remain unaware of their visual field loss until the disease reaches an advanced stage. This lack of awareness can potentially be attributed to the phenomenon in which visual field defects are filled-in by the brain, leading to concealment of these defects (Fig. 6).[17] The plasticity of the visual cortex allows it to reorganize itself in response to damage in the retina or visual pathways, by activating existing but typically ineffective synapses.[18] As a result, glaucomatous field defects are likely masked by the surrounding colors and patterns until the visual input diminishes to a level where the brain can no longer construct a coherent visual image (Fig. 6C). This phenomenon could explain the delayed detection of glaucoma-related visual impairments by the affected individual.[19]

Figure 6. Images and corresponding visual field examinations. **A.** Normal vision. **B.** Early stage of glaucoma. **C.** Advanced stage of glaucoma. The yellow symbols in Figures **B** and **C** represent the patient's fixation point. Objects located completely in the blind areas are not seen. These areas are filled-in with colors and patterns of the surroundings.

Adapted from Hoste [17] New insights into the subjective perception of visual field defects (2003) *Bull Soc Belge Ophtalmol*

In the early stages of glaucoma, the brain is probably able to compose a very plausible image, by combining the input of both eyes and filling-in the field defect with the colors, forms and textures of the surroundings areas. However, objects located in the foreground that fall entirely within the blind area cannot be perceived, as the brain lacks any information to form an image of such objects (Fig. 6B). This not only poses challenges in daily life, but might also lead to hazardous situations. For instance, while driving, a glaucoma patient may fail to detect the sudden presence of children crossing the street if their visual image falls entirely within the field defect of the affected eye, while remaining unseen by the other eye. The risk is further amplified by the patient's lack of awareness regarding any visual impairment. When the disease advances, fewer objects are visible in the periphery, as an increasing proportion of them become entirely situated within expanding blind areas.

Compensatory Eye Movements

In Figures 6B and 6C, the illustration portrays a scene where the fixation point of the glaucoma patient is situated at the center of the scene, resulting in the children being located within the blind area of the visual field. However, the gaze of a glaucoma patient is not solely fixed straight ahead but can encompass both head and eye movements to scan the entire scene. When these movements are executed appropriately, glaucoma patients can perceive a greater extent of the visual scene, as illustrated in Figures 7A and 7B.[20,21]

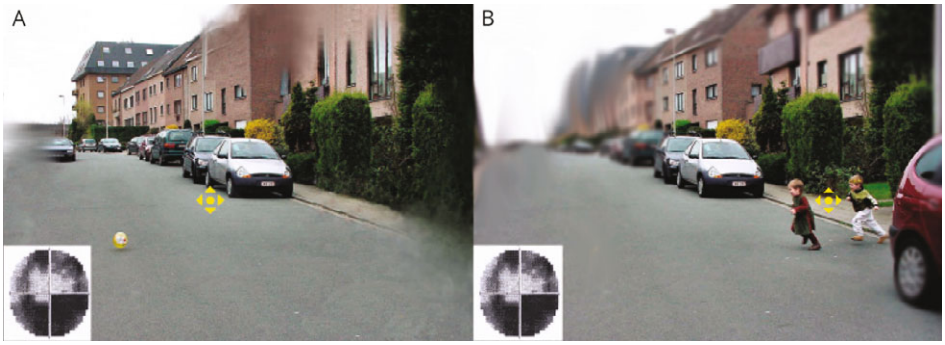

Figure 7. The yellow symbols represent the patient's fixation point. **A.** Original image.[17] Objects located completely in the blind areas are filled-in with colors and patterns of the surroundings. **B.** Illustration depicting the same scene with a compensatory eye movement towards the right. Adapted from Hoste [17] New insights into the subjective perception of visual field defects (2003) Bull *Soc Belge Ophtalmol.*

By focusing their attention on central targets and employing systematic scanning strategies, individuals with glaucoma may effectively utilize their remaining visual field. Active scanning could allow them to explore their environment more comprehensively, bringing relevant objects and areas of interest into their remaining visual field. One important aspect of compensatory eye movements in glaucoma is the utilization of saccadic eye movements. Saccades involve rapid shifts of gaze from one point to another and are instrumental in directing the line of sight towards specific targets or objects. Understanding these compensatory mechanisms and incorporating them into rehabilitation programs can help individuals with glaucoma make the most efficient use of their available visual resources and maintain functional independence.

Driving with Visual Field Defects

Driving with visual field defects can pose significant challenges and safety concerns when the remaining visual field is limited or not adequately compensated for.[22] The leading cause of visual field loss in the elderly population is glaucoma;[23] other causes include stroke, diabetic retinopathy, retinal vascular occlusive disease, and age-related macular degeneration. As these conditions are age-related, and considering the increasing number of older drivers,[24] it is crucial to accurately determine which individuals can safely participate in traffic. Even hemianopia, a visual field impairment caused by stroke, where half of the visual field is missing in both eyes, should not be considered a definite contraindication for holding a drivers' license, as research has shown that not all patients fail the on-road driving test.[25] Tant, et al.[26], found that hemianopic scanning behavior is primarily driven by the visual field defect itself, rather than by the accompanying brain damage. Additionally, visuo-spatial driving performance can be improved with visual scanning training.[27]

To obtain or retain a driver's license when visual field abnormalities are present or suspected, visual field testing, generally the binocular Esterman visual field test, is required.[9] In The Netherlands, legal requirements follow the EU regulations,[28] which mandates a minimum horizontal visual field of 120 degrees with a minimum left/right reach of 50 degrees, along with a vertical visual field extending 20 degrees above and below the center. Within the central 20 degrees (radius), all points on the Esterman test must be detected, except for the physiologic blind spot in monocular drivers.[29] However, the establishment of criteria to assess the safety risk associated with visual field defects while driving remains limited.

Many studies have examined the relationship between visual field defects and driving performance, yet the available evidence remains inconclusive.[30] Several studies indicate that visual field impairment is associated with a higher risk of motor vehicle collisions.[31-34] However, there are also studies that do not find a correlation between visual field defects and increased collision risk.[35-38]

Due to these inconsistent findings and to prevent unwarranted denial of licenses, certain countries, including The Netherlands, have implemented an "exceptional case" program. Under this initiative, the CBR (Dutch driving test organization) offers an on-road driving test to individuals who do not fully meet the visual field criteria. This practical fitness to drive test allows them to demonstrate their ability to adapt to their visual field defects and show their competence in real-world driving conditions.

In the Dutch context, the Royal Dutch Visio (Centers of Expertise for Blind and Partially Sighted People), have implemented a program known as "AutO&Mobiliteit".[39,40] Under this initiative, individuals with a visual impairment can apply for a comprehensive assessment, facilitated by information provided by their ophthalmologists. Participants referred to the program undergo an one-day consultation, encompassing examinations that evaluate various aspects, including visual functions, inquiries into driving experience and history, and, when deemed necessary, a neuropsychological examination. Practical observations, such as walking and cycling, are conducted outdoors to assess real-world functionality and compensatory mechanisms.

The conclusion of the "AutO&Mobiliteit" program leads to a personalized recommendation based on the outcome of the assessments. These recommendations could categorize individuals into four groups: those considered eligible to drive based on legal standards, those advised to undergo driving lessons with subsequent application for an on-road driving test, those recommended for specific training programs such as bioptic telescopic spectacles training or saccadic visual search training,[41-44] and those for whom driving is deemed inadvisable. Importantly, in instances where driving is discouraged, guidance is provided on alternatives and solutions to maintain personal mobility. The program's tailored approach not only outlines the individual's current driving capabilities but also provides guidance that reflects a broad perspective on mobility extending beyond the act of driving.

While on-road driving tests are effective in discriminating between capable and incapable drivers, their high cost and time-consuming nature underscore the importance to identify more accessible methods for assessing compensatory viewing

abilities in individuals with visual field loss. Within the context of the "AutO&Mobiliteit" program, obtaining an objective indication of how clients with visual field defects scan their surroundings might be crucial.

Eye Tracking

Eye tracking refers to the technology and methodology used to monitor and analyze eye movements. By employing specialized cameras or sensors, eye tracking systems can precisely track the movements and gaze patterns of a person's eyes, and can give valuable insights into the allocation of visual attention as eye movements are linked to cognitive processing.[45] This technology has various applications, including research in healthcare, psychology, biomedical applications, and neuroscience.[46] It enables researchers to understand how individuals interact with visual stimuli. Various types of eye trackers exist, each employing different technologies and methodologies. Two types of commonly used eye trackers are remote and wearable eye trackers. Firstly, remote or video-based eye trackers, use cameras attached to a monitor to track the position and movements of the eyes whilst showing stimuli on the monitor. These trackers are non-intrusive and can be used for various different tasks. Secondly, wearable eye trackers consist of glasses or headsets equipped with cameras or sensors to capture eye movements. A scene camera takes the role of recording the stimulus, which is the scene that the participant is exploring. They offer portability, unrestricted head movements, and enable researchers to study eye movements in real-world scenarios.

Measuring Compensatory Eye Movements

Previous studies have examined how individuals with glaucoma compensate for their visual field defects during on-road driving,[47,48] driving simulator tests,[20,49,50] and hazard perception tests.[21,51]

A dynamic hazard perception test is a mandatory component of obtaining a driver's license in some countries, such as the UK and Australia, serving as a crucial assessment of a candidate's ability to anticipate and respond to potential hazards while driving.[52-54] Consisting of a series of video clips depicting various driving scenarios that are shown on a small screen, this test evaluates the candidate's ability for identifying and clicking on developing hazards on the road, such as pedestrians crossing, or vehicles changing lanes. By determining hazard perception skills, this test aims to ensure that new drivers possess the necessary awareness essential for safe driving.

Driving simulators are technological systems designed to replicate real-world driving experiences in a controlled environment. Utilized for training purposes, research, and assessments, driving simulators provide a safe and immersive tool for learners to develop their driving skills without the risks associated with on-road practice. These simulators typically feature realistic vehicle controls, animated visual displays, and simulated traffic scenarios, allowing users to navigate virtual roads, highways, and urban environments.

However, there is a gap in the existing testing methodologies, as shown in Table 1. Specifically, there is a lack of a test tailored to measure compensatory eye movements on a wide screen, with the capability of objectively quantifying compensatory eye movements.

Table 1. Comparison of Esterman Visual Field Test, Dynamic Hazard Perception Test (HPT), Driving Simulator, On-Road Driving Test, and TREYESCAN.

	Esterman Visual Field Test	HPT	Driving Simulator	On-Road Driving Test	TREYESCAN
Allowing for compensatory eye movements	−−	+	+	++	++
Duration of test	+	+	+/−	+/−	+
Legal embedding	+	−	−	+	−
Measuring driving capability	−−	−	+	++	−
Naturalistic conditions	−−	+	+/−	++	+
Numerical analysis of results	+	+	+	−−	+
Objective measure of viewing and compensation	−−	−−	−−	−−	++
Statistical analysis of compensation	−−	+	+	−−	++
Wide field of view	++	−	+	++	+

This is particularly relevant in the context of dynamic areas of interest (AOIs) within traffic scenes, which are specific regions of a stimulus that are relevant for the research objective (Fig. 8). AOIs are used to measure metrics like AOI hits, which occur when gaze coordinates fall within an AOI.[45] Dynamic AOIs – moving regions of interest that emerge during video presentations or animated elements on a screen – present a challenge due to the movement of these objects relative to the coordinate system in which the gaze position data is recorded.[55] Existing research has primarily

focused on fixations and saccades, without exploring the importance of viewing AOIs. Investigating these compensatory eye movements is important, as they play a crucial role in helping individuals with visual field defects in overcoming visual limitations and maintaining functional performance in visually demanding situations, like driving.

Figure 8. A snapshot of a traffic scene with areas of interest highlighted with rectangles, including five cyclists, one car and two traffic lights. The red rectangles denote "Must-Be-Seen" objects, signifying objects that demand active or passive consideration by the driver, provoking actions like speed reduction, lane change, or delayed acceleration. The blue rectangles represent "May- Be-Seen" objects, which are relevant to be seen by the driver, but do not necessitate a change in driving behavior, such as pedestrians on the sidewalk and oncoming traffic in the other lane. In this depicted scene, one cyclist is classified as a Must-Be-Seen object due to an upcoming situation where the cyclist approaches to cross the road.

Potential Benefits for the Patient Group

The evaluation of compensatory eye movements in patients with visual field loss can offer several benefits to the patient group. Firstly, it provides valuable insights, allowing healthcare professionals to understand how individuals adapt their gaze behavior to compensate for their impaired vision. By gaining a better understanding of the compensatory eye movements, rehabilitation services can tailor interventions to optimize the client's viewing strategies and overall quality of life. Additionally, this assessment can aid in the acceptance of driver's license revocation, as it provides objective evidence regarding the individual's ability to compensate for their visual field loss. When individuals perceive withdrawals as unjust, it could result in a diminished trust in the authorities, particularly when withdrawals are determined by vision tests that inadequately predict individual driving capabilities.[56] Individuals who have their driving license withdrawn due to visual field loss also experience welfare loss on several domains, such as work, income, housing, and health.[57] Moreover, the measurement of compensatory eye movements can serve as a potential predictor for referral to a driving test. Coeckelbergh, et al.[58] found that the predictive power of current vision requirements for driving was low, but it could be improved by taking compensatory viewing efficiency into account. By evaluating an individual's ability

to compensate for visual field defects, healthcare professionals could potentially identify those who are more likely to be safe drivers. This information can assist drivers to make informed decisions about their continued driving suitability despite their visual field loss. For individuals not yet demonstrating sufficient compensation, participation in compensatory vision training offers an option for improvement before reevaluation. Notably, this approach may lead to the referral of patients who might have otherwise been excluded from on-road driving evaluation based on the Esterman visual field test, thereby providing a more comprehensive and accurate assessment of their capabilities.

Aim and Outline of This Thesis

The primary objective of this research is to develop an innovative eye tracking test called the Traffic Eye Scanning and Compensation Analyzer (TREYESCAN) to investigate and analyze compensatory eye movements in individuals with glaucoma. The TREYESCAN is designed to quantitatively measure compensatory eye movements employed by individuals with visual field defects, while viewing videos of traffic scenes on a wide screen. By analyzing the gaze behavior of individuals with glaucoma in relation to AOIs, we aim to understand the compensatory mechanisms employed at various stages of disease progression, and fill the gap in testing methodologies as described in Table 1.

Chapter 1 provides a general introduction to the research background, objectives, and methodology. **Chapter 2** presents the results of a retrospective matched case-control study which analyses the predictive value of the Esterman visual field test on the outcome of on-road driving tests offered by the CBR. **Chapter 3** describes a validation study for the TREYESCAN setup and software, introducing a toolkit developed for the Pupil Core eye tracker to facilitate gaze analyses of dynamic AOIs on a wide screen with unrestricted head movements. Moving forward, **chapter 4** outlines the development of the TREYESCAN, encompassing the selection of suitable traffic scenes and relevant AOIs within them by conducting a pilot study with normally-sighted individuals. Subsequently, the TREYESCAN was administered in a case-control study involving glaucoma patients at various stages of disease progression and control participants. In **chapter 5**, the results from the case-control study are compared between glaucoma patients and the control participants and the relationship between visual field loss and compensatory eye movements is explored. Finally, this thesis will end with a summary and general discussion (**chapter 6**).

References

1. Flaxman SR, Bourne RRA, Resnikoff S, et al. Global causes of blindness and distance vision impairment 1990-2020: a systematic review and meta-analysis. *Lancet Global Health*. 2017;5(12):e1221-e1234. doi:10.1016/S2214-109X(17)30393-5
2. Zhang N, Wang J, Li Y, Jiang B. Prevalence of primary open angle glaucoma in the last 20 years: a meta-analysis and systematic review. *Scientific Reports*. 2021;11(1):13762. doi:10.1038/s41598-021-92971-w
3. Jonas JB, Aung T, Bourne RR, Bron AM, Ritch R, Panda-Jonas S. Glaucoma. *Lancet*. 2017;390(10108):2183-2193. doi:10.1016/S0140-6736(17)31469-1
4. Rein DB, Wittenborn JS, Lee PP, et al. The cost-effectiveness of routine office-based identification and subsequent medical treatment of primary open-angle glaucoma in the United States. *Ophthalmology*. 2009;116(5):823-32. doi:10.1016/j.ophtha.2008.12.056
5. Phu J, Khuu SK, Yapp M, Assaad N, Hennessy MP, Kalloniatis M. The value of visual field testing in the era of advanced imaging: clinical and psychophysical perspectives. *Clinical and Experimental Optometry*. 2017;100(4):313-332. doi:10.1111/cxo.12551
6. Wu Z, Saunders LJ, Daga FB, Diniz-Filho A, Medeiros FA. Frequency of Testing to Detect Visual Field Progression Derived Using a Longitudinal Cohort of Glaucoma Patients. *Ophthalmology*. 2017;124(6):786-792. doi:10.1016/j.ophtha.2017.01.027
7. Blake R, Wilson H. Binocular vision. *Vision Research*. 2011;51(7):754-70. doi:10.1016/j.visres.2010.10.009
8. Broadway DC. Visual field testing for glaucoma - a practical guide. *Community Eye Health*. 2012;25(79-80):66-70.
9. Esterman B. Functional scoring of the binocular field. *Ophthalmology*. 1982;89(11):1226-1234.
10. Jorstad OK, Jonsdottir TE, Zysset S, Rowe F. A traffic perimetry test that adheres to the European visual field requirements. *Acta Ophthalmologica*. 2021;99(4):e555-e561. doi:10.1111/aos.14633
11. Dow J. Visual field defects may not affect safe driving. *Traffic Injury Prevention*. 2011;12(5):483-90. doi:10.1080/15389588.2011.582906
12. Gardiner SK, Demirel S. Assessment of patient opinions of different clinical tests used in the management of glaucoma. *Ophthalmology*. 2008;115(12):2127-31. doi:10.1016/j.ophtha.2008.08.013
13. Dersu, II, Ali TK, Spencer HJ, Covey SM, Evans MS, Harper RA. Psychomotor vigilance and visual field test performance. *Seminars in Ophthalmology*. 2015;30(4):289-96. doi:10.3109/08820538.2013.859279
14. Glen FC, Baker H, Crabb DP. A qualitative investigation into patients' views on visual field testing for glaucoma monitoring. *BMJ Open*. 2014;4(1)
15. Colenbrander A. Aspects of vision loss–visual functions and functional vision. *Visual impairment research*. 2003;5(3):115-136.
16. Colenbrander A. Visual functions and functional vision. Elsevier; 2005:482-486.
17. Hoste AM. New insights into the subjective perception of visual field defects. *Bulletin de la Societe Belge d'Ophtalmologie*. 2003;(287):65-71.
18. Safran AB, Landis T. Plasticity in the adult visual cortex: implications for the diagnosis of visual field defects and visual rehabilitation. *Current Opinion in Ophthalmology*. 1996;7(6):53-64.
19. Prior M, Francis JJ, Azuara-Blanco A, Anand N, Burr JM, group GsPS. Why do people present late with advanced glaucoma? A qualitative interview study. *British Journal of Ophthalmology*. 2013;
20. Kubler TC, Kasneci E, Rosenstiel W, et al. Driving with Glaucoma: Task Performance and Gaze Movements. *Optom Vis Sci*. Nov 2015;92(11):1037-46. doi:10.1097/OPX.0000000000000702
21. Crabb DP, Smith ND, Rauscher FG, et al. Exploring eye movements in patients with glaucoma when viewing a driving scene. *PLoS One*. 2010;5(3):e9710. doi:10.1371/journal.pone.0009710
22. Patterson G, Howard C, Hepworth L, Rowe F. The Impact of Visual Field Loss on Driving Skills: A Systematic Narrative Review. *British and Irish Orthoptic Journal*. 2019;15(1):53-63. doi:10.22599/bioj.129

23. Ramrattan RS, Wolfs RC, Panda-Jonas S, et al. Prevalence and causes of visual field loss in the elderly and associations with impairment in daily functioning: the Rotterdam Study. *Archives of Ophthalmology*. 2001;119(12):1788-94. doi:10.1001/archopht.119.12.1788
24. Bourne R, Steinmetz JD, Flaxman S, et al. Trends in prevalence of blindness and distance and near vision impairment over 30 years: an analysis for the Global Burden of Disease Study. *The Lancet Global Health*. 2021;9(2):e130-e143.
25. Tant M, Brouwer W, Cornelissen F, Kooijman A. Driving and visuospatial performance in people with hemianopia. *Neuropsychological rehabilitation*. 2002;12(5):419-437.
26. Tant M, Cornelissen FW, Kooijman AC, Brouwer WH. Hemianopic visual field defects elicit hemianopic scanning. *Vision research*. 2002;42(10):1339-1348.
27. Tant ML, Brouwer WH, Cornelissen FW, Kooijman AC. Prediction and evaluation of driving and visuo-spatial performance in homonymous hemianopia after compensational training. *Visual impairment research*. 2001;3(3):133-145.
28. European Parliament. Directive 2006/126/EC of the European Parliament and of the Council of 20 December 2006 on driving licences (Recast). Official Journal of the European Union;L403:18–60. Accessed March, 2022, http://eur-lex.europa.eu/LexUriServ/LexUriServ.do?uri=OJ:L:2006:403:0018:0060:EN:PDF
29. Netelenbos T. Regeling eisen geschiktheid - BWBR0011362. Accessed March, 2022, https://wetten.overheid.nl/BWBR0011362/2021-04-17
30. Thorslund B, Strand N. Vision measurability and its impact on safe driving: a literature review. *Scandinavian Journal of Optometry and Visual Science*. 2016;9(1):1-9.
31. Huisingh C, McGwin G, Jr., Wood J, Owsley C. The driving visual field and a history of motor vehicle collision involvement in older drivers: a population-based examination. *Investigative Ophthalmology & Visual Science*. 2014;56(1):132-8. doi:10.1167/iovs.14-15194
32. Kwon M, Huisingh C, Rhodes LA, McGwin G, Jr., Wood JM, Owsley C. Association between Glaucoma and At-fault Motor Vehicle Collision Involvement among Older Drivers: A Population-based Study. *Ophthalmology*. Jan 2016;123(1):109-16. doi:10.1016/j.ophtha.2015.08.043
33. Haymes SA, Leblanc RP, Nicolela MT, Chiasson LA, Chauhan BC. Risk of falls and motor vehicle collisions in glaucoma. *Investigative Ophthalmology & Visual Science*. 2007;48(3):1149-55. doi:10.1167/iovs.06-0886
34. McGwin G, Jr., Huisingh C, Jain SG, Girkin CA, Owsley C. Binocular visual field impairment in glaucoma and at-fault motor vehicle collisions. *Journal of Glaucoma*. 2015;24(2):138-43. doi:10.1097/IJG.0b013e3182a0761c
35. McCloskey LW, Koepsell TD, Wolf ME, Buchner DM. Motor vehicle collision injuries and sensory impairments of older drivers. *Age and Ageing*. 1994;23(4):267-73. doi:10.1093/ageing/23.4.267
36. McGwin G, Jr., Mays A, Joiner W, Decarlo DK, McNeal S, Owsley C. Is glaucoma associated with motor vehicle collision involvement and driving avoidance? *Investigative Ophthalmology & Visual Science*. 2004;45(11):3934-9. doi:10.1167/iovs.04-0524
37. Yuki K, Asaoka R, Tsubota K. The relationship between central visual field damage and motor vehicle collisions in primary open-angle glaucoma patients. *PLoS One*. 2014;9(12):e115572. doi:10.1371/journal.pone.0115572
38. Okamura K, Iwase A, Matsumoto C, et al. Association between visual field impairment and involvement in motor vehicle collision among a sample of Japanese drivers. *Transportation research part F: traffic psychology and behaviour*. 2019;62:99-114.
39. Melis-Dankers BJ, Kooijman AC, Brouwer WH, et al. A demonstration project on driving with reduced visual acuity and a bioptic telescope system in the Netherlands. *Visual impairment research*. 2008;10(1):7-22.
40. Kooijman AC, Melis-Dankers BJ, Peli E, et al. The introduction of bioptic driving in the Netherlands. *Visual impairment research*. 2008;10(1):1-6.
41. Dougherty BE, Flom RE, Bullimore MA, Raasch TW. Vision, training hours, and road testing results in bioptic drivers. *Optometry and vision science: official publication of the American Academy of Optometry*. 2015;92(4):395.

42. Postuma E, Heutink J, Tol S, et al. A systematic review on visual scanning behaviour in hemianopia considering task specificity, performance improvement, spontaneous and training-induced adaptations. *Disability and Rehabilitation*. 2023:1-22. doi:10.1080/09638288.2023.2243590
43. Coeckelbergh TR, Brouwer WH, Cornelissen FW, Kooijman AC. Training compensatory viewing strategies: Feasibility and effect on practical fitness to drive in subjects with visual field defects. *Visual impairment research*. 2001;3(2):67-83.
44. Kooijman A, Brouwer W, Coeckelbergh T, et al. Compensatory viewing training improves practical fitness to drive of subjects with impaired vision. *Visual Impairment Research*. 2004;6(1):1-27.
45. Holmqvist K, Andersson R. Eye tracking: A comprehensive guide to methods, paradigms and measures. *Lund, Sweden: Lund Eye-Tracking Research Institute*. 2017;
46. Carter BT, Luke SG. Best practices in eye tracking research. *International Journal of Psychophysiology*. 2020;155:49-62. doi:10.1016/j.ijpsycho.2020.05.010
47. Kasneci E, Sippel K, Aehling K, et al. Driving with binocular visual field loss? A study on a supervised on-road parcours with simultaneous eye and head tracking. *PLoS One*. 2014;9(2):e87470. doi:10.1371/journal.pone.0087470
48. Lee SS, Black AA, Wood JM. Scanning Behavior and Daytime Driving Performance of Older Adults With Glaucoma. *Journal of Glaucoma*. 2018;27(6):558-565. doi:10.1097/IJG.0000000000000962
49. Prado Vega R, van Leeuwen PM, Rendon Velez E, Lemij HG, de Winter JC. Obstacle avoidance, visual detection performance, and eye-scanning behavior of glaucoma patients in a driving simulator: a preliminary study. *PLoS One*. 2013;8(10):e77294. doi:10.1371/journal.pone.0077294
50. Coeckelbergh TR, Brouwer WH, Cornelissen FW, Van Wolffelaar P, Kooijman AC. The effect of visual field defects on driving performance: a driving simulator study. *Archives of ophthalmology*. 2002;120(11):1509-1516.
51. Lee SS, Black AA, Wood JM. Effect of glaucoma on eye movement patterns and laboratory-based hazard detection ability. *PLoS One*. 2017;12(6):e0178876. doi:10.1371/journal.pone.0178876
52. Horswill MS. Hazard perception tests. *Handbook of Teen and Novice Drivers*. CRC Press; 2016:459-470.
53. Moran C, Bennett JM, Prabhakharan P. Road user hazard perception tests: A systematic review of current methodologies. *Accident Analysis & Prevention*. 2019;129:309-333.
54. Wetton MA, Hill A, Horswill MS. The development and validation of a hazard perception test for use in driver licensing. *Accid Anal Prev*. Sep 2011;43(5):1759-70. doi:10.1016/j.aap.2011.04.007
55. Hessels RS, Benjamins JS, Cornelissen THW, Hooge ITC. A Validation of Automatically-Generated Areas-of-Interest in Videos of a Face for Eye-Tracking Research. *Frontiers in Psychology*. 2018;9:1367. doi:10.3389/fpsyg.2018.01367
56. Nyberg J, Levin L, Larsson K, Strandberg T. Distrust of Authorities: Experiences of Outcome and Processes of People Who Had Their Driving License Withdrawn Due to Visual Field Loss. *Social Sciences*. 2021;10(2):76.
57. Nyberg J, Strandberg T, Berg H-Y, Aretun Å. Welfare consequences for individuals whose driving licenses are withdrawn due to visual field loss: a Swedish example. *Journal of Transport & Health*. 2019;14
58. Coeckelbergh TR, Brouwer WH, Cornelissen FW, Kooijman AC. Predicting practical fitness to drive in drivers with visual field defects caused by ocular pathology. *Human Factors*. 2004;46(4):748-760.

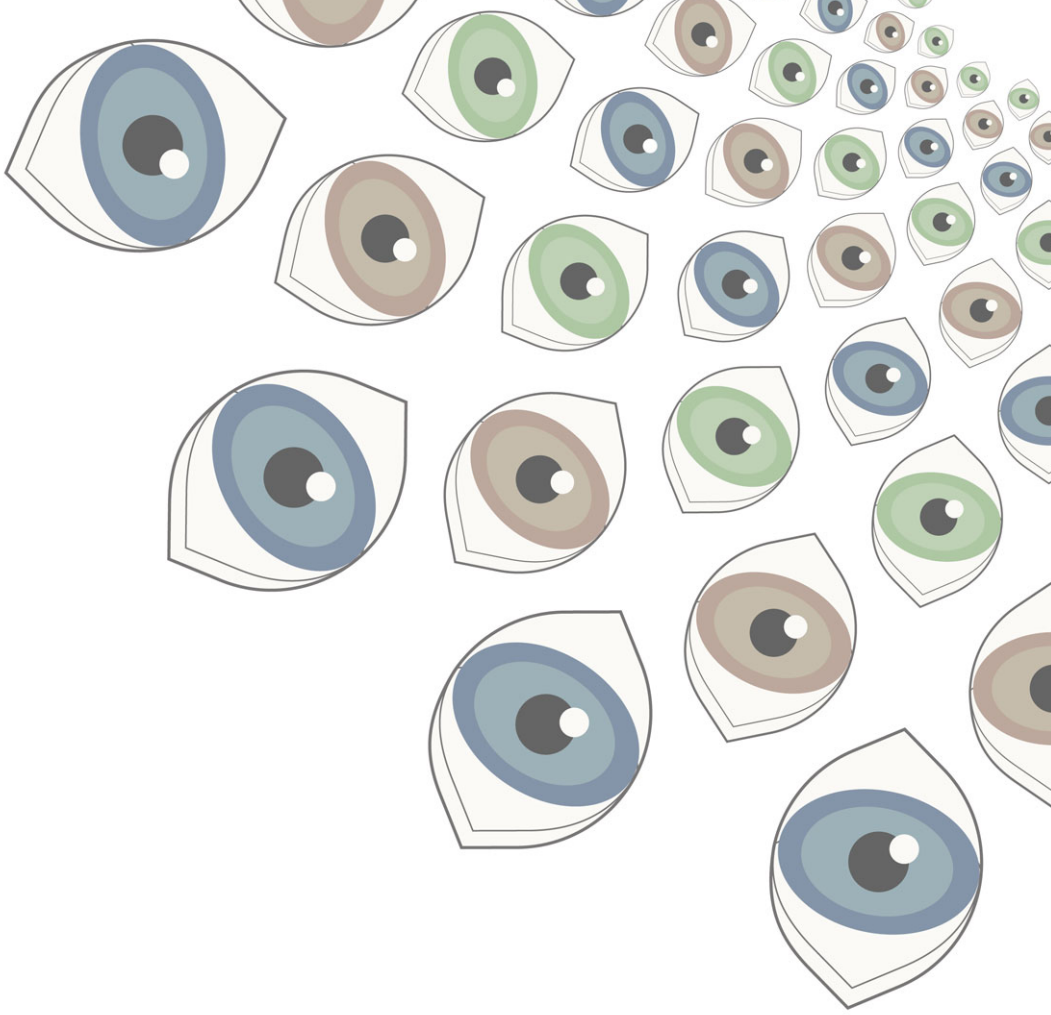

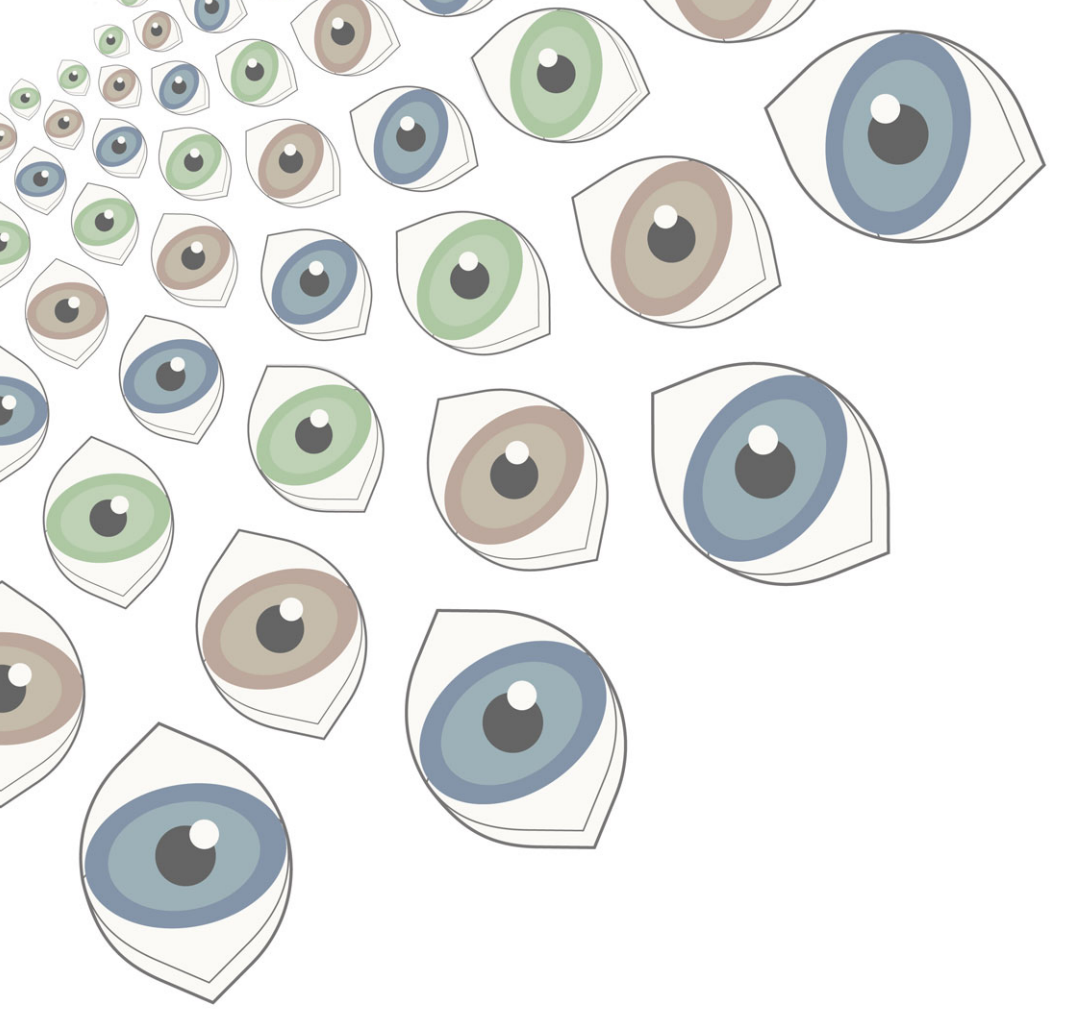

Chapter 2

Predictive Value of the Esterman Visual Field Test on the Outcome of the On-Road Driving Test

Y Faraji, MT Tan-Burghouwt, RA Bredewoud, RMA van Nispen & LJ van Rijn

Translational Vision Science & Technology, 2022; 11(3): 20

Abstract

Purpose

As the prevalence of age-related visual field disorders and the number of older drivers are rising, clear criteria on visual field requirements for driving are important. This article explores the predictive value of the Esterman visual field in relation to the outcome of an on-road driving test.

Methods

A retrospective chart review was performed for driver's license applicants who, based on their visual field, performed an on-road driving test. Cases (n = 101) with a failed on-road driving test were matched with 101 controls with a passed outcome. The Esterman visual field was divided in regions, and the number of points missed per region was counted. Logistic regression models and receiver operating characteristic (ROC) curves were computed for each region.

Results

Most regions presented a significantly increased odds for failing the driving test when more points were missed. The odds ratio for the whole visual field was 2.52 (95% confidence interval, 1.53–4.14, $p < 0.001$) for all the participants. However, ROC curves failed to reveal distinct fail–pass criteria based on the number of points missed, as revealed by a large amount of overlap between cases and controls.

Conclusions

These findings confirm the relation between visual field damage and impaired driving performance. However, the Esterman visual field results were not conclusive for predicting the driving performance of the individual driver with visual field defects.

Translational Relevance

In our group of participants, the number of on-road driving tests cannot be further reduced by a more detailed definition of fail–pass criteria, based on the Esterman visual field test.

Introduction

A driver's vision and visual field are vital for the assessment of driving performance in order to ensure public and road safety.[1] Hence, in most countries, visual field criteria apply for obtaining and retaining a driver's license. Research on this topic is becoming increasingly important, as the prevalence of age-related visual field disorders and the number of older drivers are rising.[2]

Many studies report on the relation between visual field defects and driving performance. Yet, the available evidence remains inconclusive.[3] Some studies find that visual field impairment is associated with an increased risk of being involved in a motor vehicle collision.[4-7] Other studies do not show such a correlation.[8-11]

This discrepancy may be explained by the fact that driving is a highly visual task involving visual sensory functions, such as spatial resolution, contrast sensitivity, and light sensitivity. Controlling a vehicle takes place in a visually cluttered environment with many distractions and involves the simultaneous use of central and peripheral vision, cognitive functions that a conventional visual field test does not measure.[12] Another aspect that is not measured by visual field tests is compensatory head and eye movements.[13,14] Some drivers may be better adapted to their visual field defect than others by better scanning toward blind areas.[15] Even some people with complete hemianopia have demonstrated to be safe drivers.[16,17]

Presently, formal visual field testing is still the first step for acquiring a driver's license when there are suspected visual field abnormalities. In The Netherlands, the legislation mandates a minimum horizontal visual field of 120 degrees and a minimum left/right reach of 50 degrees. The vertical visual field must extend to 20 degrees above and below. Within the central 20 degrees (radius), no points on the Esterman may be missed (apart from the physiologic blind spot in monocular drivers), since a single missed point may indicate a relevant binocular paracentral scotoma. However, fail–pass criteria for visual field defects are not well established as it is not clear what extent of visual field is necessary for safe driving. In order to avoid unnecessary license denial, some countries, including The Netherlands, offer an "exceptional case" program, mandating an on-road driving test for those candidates who do not quite fulfill the visual field criteria as mentioned above, in which they may demonstrate that they are well adapted to their visual field defects in natural driving conditions.[18]

Entry in this "exceptional case" program is based on visual acuity and visual field testing, generally the binocular Esterman visual field test.[19] This test was adopted by the American Medical Association for assessment of impairment.[20] It is a suprathreshold binocular test and includes peripheral points. It is fast and readily available on most commercial visual field testing devices. As a result, it has become the test of choice in The Netherlands and also in the United Kingdom, Norway, Sweden, and Ireland.[21] However, the Esterman visual field test has several flaws, such as that the distance between test points is not equal and that stimuli are not presented by the principle of the "hill of vision." The Dutch Society of Ophthalmology (NOG) recommends the use of the Esterman visual field in relation to driving until a tailor-made, well-evaluated screening tool is developed.[22]

Unclear fail–pass criteria for visual field defects might lead to more on-road driving tests than are required on the grounds of the visual field. The on-road driving tests, although providing high-quality discrimination between capable and incapable drivers, are costly and time-consuming. It would be desirable to reduce the number of cumbersome on-road driving tests offered to persons with visual field defects by redefining which "exceptional cases" would benefit from performing an on-road driving test while maintaining (or even improving) the quality of the discrimination.

Concurrently, it is important to give every potential driver the chance to obtain a license and to reduce the number of unjust license withdrawals for individuals with visual field defects. For elderly people, driving a motor vehicle may be the only option for autonomous mobility. Driving cessation in older drivers is related to poorer mental health, such as depression, declines in cognitive abilities, and diminished physical and social functioning.[23] Individuals who have their driving license withdrawn due to visual field loss also experience welfare loss on several domains, such as work, income, housing, and health.[24] Additionally, if withdrawals are experienced as unfair by those affected, it might lead to a decreased trust of the authorities, especially if withdrawals are based on vision tests that do not predict individual driving performance very well.[25]

Previous research on the predictive value of the visual field on driving performance was not conclusive. In the study by Silveira, et al.[26], the Esterman visual field 120-degree criterion could not predict the result of an on-road driving test. However, the nonsignificant results could have been due to the small proportion of people who failed the on-road driving test and the small number of participants with visual field

loss (8/94). Dow[27] found that failure to meet the formal visual field standards, based on the Esterman visual field, does not impede passing the on-road driving test, and no single factor or combination of factors could predict failure of the road test. Their study was not balanced: the number of failed candidates was much smaller than the number of passes, and there was no formal assessment between the extent of the visual field defects and the outcome of the on-road driving test. Another study found that the extent and location of visual field loss did not have significant impact on driving performance.[28] However, the extent of the visual field was obtained by confrontation testing, which can be considered less reliable than automated visual field testing.[29]

For this article, the aim is to explore the predictive value of the Esterman visual field in relation to the outcome of the on-road driving test by performing a matched case-control study containing balanced groups for pass and fail outcomes of the on-road driving test. Given the limited value of visual field testing, the question is if any prediction can be made about the results of the on-road driving test (or, for that matter, driving performance in general) based on the outcome of the visual field test. It may be possible to predict in which cases an individual Esterman visual field alone can warrant license renewal and avoid the on-road driving test. Some candidates could have severe visual field defects that predict a failed on-road driving test or, on the other hand, such mild defects that a passed result is expected. The location of the visual field defects could also have a relevant relation to the outcome of the on-road driving test. Possibly, the role of visual field testing, as a tool for preselection into the "exceptional case" program, could be optimized to limit the number of on-road driving tests.

Methods

Participants

A retrospective case-control study was performed. Participants were selected from a database provided by the CBR (Dutch driving test organization), the central office for driver's license administration in The Netherlands. The included participants applied for a renewal of their group 1 driving license (categories A, motor; B, passenger car; BE, trailer for passenger car; and T, tractor) and performed an on-road driving test, based on their visual field defects, between May 2010 and June 2015. When an on-road driving test is mandated based on an insufficient visual field, then the binocular (distance) visual acuity must be at least 0.30 (logarithm of the minimum angle of

resolution [logMAR]) and the binocular visual field must extend at least 90 degrees horizontally. Candidates with visual field defects with a binocular visual acuity above 0.30 (logMAR), a severely affected central visual field, and/or a minimal horizontal visual field extension below 90 degrees are not considered for an on-road driving test and not granted a license. See Supplementary Material S1 for more information about the driver's license application process in The Netherlands.

All included participants performed an on-road driving test, based on their visual field defects. Included cases were participants who did not pass the on-road driving test. For each case, a control participant was selected who did pass the driving test, matched on age (month of birth versus month of testing), gender, and the diagnosis code for their disorder in the CBR database. The codes referred to "visual field defect" (inclusion criterion for all participants in the database), "progressive eye disease" (e.g., glaucoma), and "central nervous system disorder" (e.g., occipital stroke).

Only participants were included in whom a visual field defect was the main (if not only) reason to mandate the on-road driving test. Furthermore, for inclusion, a binocular Esterman visual field (as provided by the referring ophthalmologist) had to be available. All Esterman visual fields were tested with the custom program available on a Humphrey Visual Field Analyzer (HFA; Carl Zeiss Meditec AG, Jena, Germany).

The On-Road Driving Test

All participants in this study underwent an on-road driving test on the public road, according to usual clinical practice in The Netherlands, where right-hand traffic and left-hand drive are common practice. The test has a duration of 60 minutes, with a minimal driving time of 30 minutes, and is administered by a practical fitness-to-drive expert of the CBR. There is not an obligatory fixed route for the test, but a specific protocol is in place in the presence of visual field defects (see Supplementary Materials S2). The on-road driving test always leads to a dichotomous pass or fail outcome. However, a passed driving test can be coupled with imposing restrictions, such as mandatory vehicle adaptations, and occasionally additional advice is given on a limited duration of license renewal.

Data Extraction

For each participant, the 120 points of the binocular Esterman visual field were scored if the point was "seen" (1) or "not seen" (0). The month and year of birth,

month and year of the driving test, (best-corrected) visual acuity of right and left eye, and relevant ocular comorbidity were listed (glaucoma, macular disease, cataract, stroke/brain tumor, diabetes mellitus, ocular vascular occlusion). Furthermore, data reported by the ophthalmologist, such as if the participant wore glasses or contact lenses, if the visual field condition was progressive or stable, and presence of diplopia or affected dark adaptation, were included in the database.

Analysis of Visual Field Data

The Esterman visual field was divided in regions for the statistical analysis. These regions were "all" (all points), "center" (points within a 20-degree radius), "European Union (EU) region" (a rectangle extending 20 degrees up and down and 50 degrees left and right, as mandated in the EU regulations[30]), "paracentral" (all 18 points adjacent to the center), and "periphery" (the points outside the EU region) (Fig. 1). Additionally, the visual field was divided by the midlines in "left," "right," "up," and "down" and the quadrants "left-up," "right-up," "left-down," and "right-down."

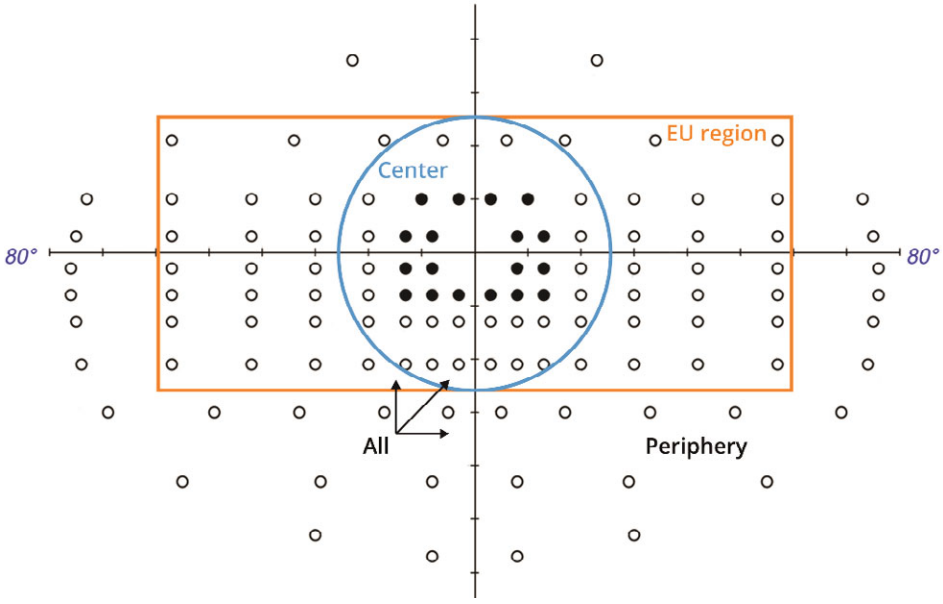

Figure 1. Visual field regions used for analysis. "All": all 120 points; "center": all points within 20 degrees (radius) from the center; "EU region": all points within a rectangle, extending 20 degrees up and down and 50 degrees left and right and "periphery" (the points outside the EU region). The black dots represent the paracentral region.

Statistical Analysis

Descriptive statistics were reported for the participant characteristics in the database. In addition, t-tests for continuous variables and $\chi 2$ tests for categorical variables were performed to verify if the matching was performed properly and if the groups did not vary significantly on the reported characteristics.

The relation between the factor (number of points seen) and the dichotomous outcome (fail or pass of the on-road driving test) was tested with a logistic regression model for each of the regions in Figure 1. The assumptions for logistic regression were checked. For skewed distributions, a ln-transformation was used. If this did not normalize the distribution, the variable was divided in tertiles. In case of tied values, the lowest rank was used. Besides conducting an uncorrected model, a corrected model was also performed, including best-corrected visual acuity (visual acuity of the best eye, in logMAR), age, and gender, to each visual field region to accommodate (minor) differences between cases and controls. Each model was also tested for the group of patients with glaucoma—since glaucoma is the main reason for driver's license issues at a higher age, from an ophthalmologic point of view—to investigate if the regions can predict the outcome of the on-road driving test for this group of patients. We decided to use the same tertiles in the group of patients with glaucoma as were used in the models for the total population. Other variables, such as presence of ocular comorbidities and progressive nature, were added to the univariate model of the whole field for the total population as these were potential confounders.

To investigate the predictive value of the Esterman visual field outcome for the outcome of the on-road driving test, receiver operating characteristic (ROC) curves were computed for each of the visual field regions, investigating the relation between the number of points seen and the outcome of the driving test. Pearson correlations for pairs of continuous variables were computed to explore the dependency of neighboring regions.

All analyses were performed with IBM SPSS Statistics for Windows, Version 26.0 (SPSS, Armonk, NY, USA). This research followed the tenets of the Declaration of Helsinki. Formal approval of an ethical committee was not necessary, because anonymized data were used for this retrospective analysis. A waiver was obtained from the Medical Ethical Committee of Amsterdam University Medical Centers—location VU University Medical Center.

Results

Demographic Description of Participants

In total, 101 cases and an equal number of controls were included. The participant characteristics are shown in Table 1, which reveals that the matching process based on age, gender, and diagnosis code was effective. Also, visual acuity, progressive nature, use of prescription glasses/contact lenses, and the presence of disease were not statistically different between fail and pass groups. Multiple comorbidities could be present in one participant. Forty-nine participants had cataract as reported by the referring ophthalmologist; this was in all cases accompanied by another diagnosis that explained the visual field loss. The average period between the Esterman visual field and the on-road driving test was 3.26 ± 2.87 months. This value did differ significantly, with a longer period for cases than for controls. The study population contained mainly elderly participants with a median age of 80.0 years (minimum, 18.4 years; maximum, 93.7 years). Of the 101 candidates who passed the driving test, 14 were given a license for 1 year, 31 for 3 years, 53 for 5 years, 2 for 10 years, and 1 unlimited.

Relation between Visual Field Defects and Outcome of Driving Test

Figure 2 presents the distributions of the number of points missed for the persons with a failed and a passed outcome of the on-road driving test. A wide range of overlap can be seen between the two groups, with the failed group showing a wider and lower normal curve.

Table 2 shows the outcome of the logistic regression analysis for the visual field regions (Fig. 1). A corrected model was also performed, adjusting for age, gender, and visual acuity (visual acuity of the best eye, in logMAR). However the difference with the uncorrected model was not noteworthy; hence, we decided to report the uncorrected model. Most regions presented a positive skew. To correct this, for the regions all, EU, left, right, and down, a ln-transformation was used, and for the other regions, the regression models were conducted with tertiles.

Table 1. Participant Characteristics

Characteristic	Fail (*n* = 101)	Pass (*n* = 101)	*P* Value
Age, mean ± SD, *y*	76.8 ± 12.7	77.9 ± 12.6	0.522
Number of female subjects	21	21	1
Corrected visual acuity, mean ± SD, *logMAR*	0.120 ± 0.114	0.109 ± 0.110	0.503
Visual field defect, *n*	101	101	1
Progressive eye disease, *n*	100	99	0.561
Central nervous system disorder, *n*	16	16	1
Presence of diseases,[a] *n*			
Glaucoma	60	54	0.395
Macular disease	9	12	0.489
Cataract	26	23	0.622
Stroke / brain tumor	18	13	0.329
Diabetes mellitus	19	18	0.856
Ocular vascular occlusion	5	5	1
Progressive disease, *n*	49	46	0.672
Prescription eyeglasses, *n*	78	76	0.837
Contact lenses, *n*	2	2	1
Affected dark adaptation, *n*	0	0	—
Diplopia, *n*	0	1	0.314
Time between field test and on-road driving test, mean ± SD, *mo*	3.97 ± 2.45	2.42 ± 1.59	**<0.001**

"Fail" and "pass" reflect the outcome of the on-road driving test. *P* values are outcomes of independent-samples *t*-tests for continuous variables and χ^2 tests for categorical variables. Bold value highlights a significant value ($p < 0.05$).
[a] Multiple comorbidities could be present in one participant.

The logistic regressions show that for most visual field regions, there was a significant increased odds for not passing the driving test when more points were missed. The relation was somewhat stronger for the center of the visual field, and the left side had more significant outcomes than the right side.

The logistic regression analysis for the group with a glaucoma diagnosis similarly showed that for the whole field, EU region, and center and paracentral regions, a significant increased odds for not passing the driving test was found when more points were missed. The visual field regions, right, up, down, and right-up quadrant, showed a significant relation, which were regions in the center and the right side of the visual field.

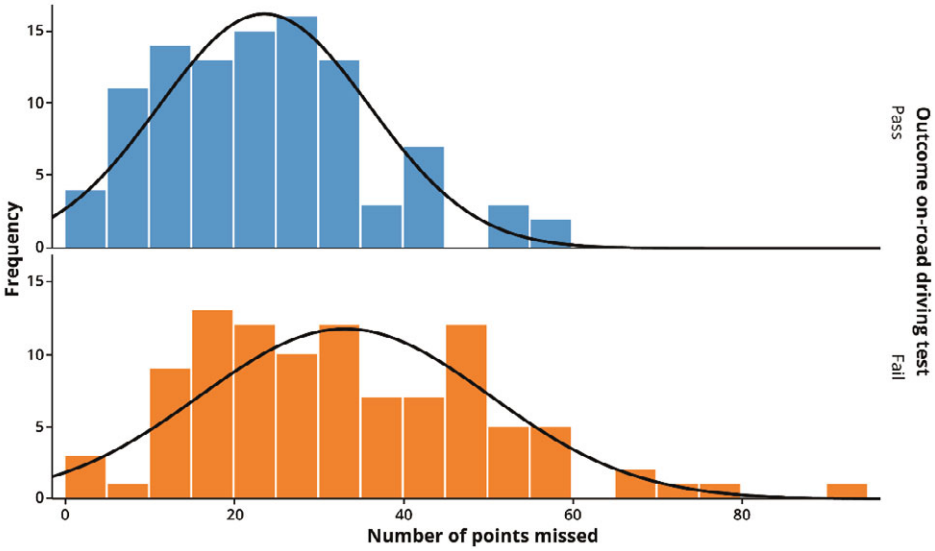

Figure 2. Distributions of the number of points missed for those who passed and failed the on-road driving test. The normal curve is also displayed.

The analyses of additional variables showed that only the time between the Esterman visual field based on the whole field data and the on-road driving test was a significant confounder and slightly increased the odds of a failed outcome (2.61; 95% confidence interval [CI], 1.53–4.47; $p < 0.001$).

Predictive Value of the Visual Field Outcome for the Outcome of the Driving Test

Figure 3 shows the ROC curves for the relation between a failed outcome for the on-road driving test and the number of points seen in the visual field regions. For all the regions, the predictive value, as measured by the AUC of the ROC curve, was below 0.7, which indicates no discriminative ability for the outcome of the test.[31] The EU region had the highest predictive value for the total population (0.674) and the glaucoma population (0.676). This implies that the results of the Esterman visual field test are not suitable for distinguishing between participants who will fail or pass the on-road driving test in our population.

Table 2. Number of Points Missed in Visual Field Regions (mean ± SD) and Odds of a Failed Outcome

Characteristic	Total Population						Glaucoma Population					
	Fail (*n* = 101)		Pass (*n* = 101)		Odds Ratio	*P* Value	Fail (*n* = 60)		Pass (*n* = 54)		Odds Ratio	*P* Value
	Mean ± SD	*n*	Mean ± SD	*n*			Mean ± SD	*n*	Mean ± SD	*n*		
Whole field (120)	32.68 ± 17.15	101	23.13 ± 12.46	101	**2.52 (1.53-4.14)**[a]	**<0.001**	33.12 ± 17.46	60	23.65 ± 13.22	54	**2.51 (1.30-4.86)**[a]	**0.006**
EU region (86)	17.32 ± 11.88	101	10.35 ± 6.86	101	**2.45 (1.61-3.73)**[a]	**<0.001**	17.77 ± 12.16	60	10.72 ± 7.61	54	**2.48 (1.41-4.33)**[a]	**0.002**
Center (42)												
Tertile 1	0.45 ± 0.51	31	0.31 ± 0.47	45	—	—	0.50 ± 0.52	16	0.26 ± 0.45	19	—	—
Tertile 2	3.41 ± 1.12	27	3.03 ± 1.06	39	1.01 (0.51-1.97)	0.988	3.50 ± 1.02	14	3.17 ± 1.13	24	0.69 (0.27-1.77)	0.442
Tertile 3	11.60 ± 6.29	43	9.18 ± 3.13	17	**3.67 (1.78-7.58)**	**<0.001**	12.27 ± 6.93	30	10.09 ± 3.53	11	**3.24 (1.24-8.45)**	**0.016**
Paracentral (18)												
Tertile 1	0.00 ± 0.00	34	0.00 ± 0.00	58	—	—	0.00 ± 0.00	16	0.00 ± 0.00	28	—	—
Tertile 2	1.41 ± 0.50	27	1.42 ± 0.50	24	1.92 (0.96-3.84)	0.066	1.46 ± 0.52	13	1.50 ± 0.52	12	1.90 (0.70-5.14)	0.208
Tertile 3	5.55 ± 2.52	40	4.11 ± 1.45	19	**3.59 (1.80-7.17)**	**<0.001**	5.55 ± 2.72	31	4.21 ± 1.67	14	**3.88 (1.61-9.35)**	**0.003**
Periphery (34)	15.37 ± 6.88	101	12.78 ± 7.44	101	**1.05 (1.01-1.10)**	**0.013**	15.35 ± 6.46	60	12.93 ± 7.46	54	1.05 (1.00-1.11)	0.068
Left (60)	15.49 ± 10.38	101	10.90 ± 7.72	101	**1.75 (1.22-2.51)**[a]	**0.002**	14.93 ± 10.43	60	11.85 ± 7.91	54	1.37 (0.85-2.22)[a]	0.198
Right (60)	17.20 ± 12.55	101	12.23 ± 8.63	101	**1.38 (1.02-1.88)**[a]	**0.039**	18.18 ± 12.34	60	11.80 ± 9.33	54	**1.82 (1.18-2.81)**[a]	**0.007**
Up (38)	11.29 ± 6.51	101	8.05 ± 4.70	101	**1.11 (1.05-1.17)**	**<0.001**	11.75 ± 6.76	60	7.89 ± 4.69	54	**1.12 (1.05-1.20)**	**0.001**
Down (82)	21.40 ± 13.15	101	15.08 ± 10.36	101	**1.91 (1.30-2.82)**[a]	**0.001**	21.37 ± 13.72	60	15.76 ± 10.95	54	**1.76 (1.06-2.92)**[a]	**0.030**
Left-up quadrant (19)												
Tertile 1	1.61 ± 1.18	36	1.49 ± 1.19	49	—	—	1.60 ± 1.14	20	1.71 ± 1.20	24	—	—
Tertile 2	4.88 ± 0.78	33	4.88 ± 0.84	34	1.32 (0.69-2.52)	0.397	4.75 ± 0.79	20	4.83 ± 0.86	18	1.33 (0.56-3.18)	0.517
Tertile 3	10.41 ± 2.95	32	8.67 ± 1.88	18	**2.42 (1.18-4.97)**	**0.016**	10.50 ± 2.78	20	8.50 ± 2.02	12	2.00 (0.79-5.07)	0.144

Table 2. Continued

Characteristic	Total Population						Glaucoma Population					
	Fail (*n* = 101)		Pass (*n* = 101)		Odds Ratio	*P* Value	Fail (*n* = 60)		Pass (*n* = 54)		Odds Ratio	*P* Value
	Mean ± SD	*n*	Mean ± SD	*n*			Mean ± SD	*n*	Mean ± SD	*n*		
Right-up quadrant (19)												
Tertile 1	1.46 ± 1.15	35	1.40 ± 1.23	45	—	—	1.63 ± 1.21	19	1.44 ± 1.25	27	—	—
Tertile 2	4.88 ± 0.83	25	4.81 ± 0.79	36	0.89 (0.46-1.75)	0.742	4.88 ± 0.89	16	4.72 ± 0.75	18	1.26 (0.52-3.09)	0.608
Tertile 3	10.12 ± 2.82	41	9.10 ± 2.00	20	**2.64 (1.32-5.27)**	**0.006**	10.36 ± 2.90	25	8.00 ± 1.00	9	**3.95 (1.51-10.33)**	**0.005**
Left-down quadrant (41)												
Tertile 1	2.15 ± 1.51	27	1.45 ± 1.25	42	—	—	2.11 ± 1.45	18	1.63 ± 1.34	19	—	—
Tertile 2	7.09 ± 1.79	35	7.67 ± 2.15	36	1.51 (0.77-2.96)	0.227	6.86 ± 1.62	21	7.61 ± 2.10	23	0.96 (0.40-2.31)	0.934
Tertile 3	18.10 ± 5.67	39	16.04 ± 4.20	23	**2.64 (1.30-5.35)**	**0.007**	17.95 ± 6.36	21	17.00 ± 5.27	12	1.85 (0.71-4.82)	0.210
Right-down quadrant (41)												
Tertile 1	2.03 ± 1.32	35	1.59 ± 1.46	37	—	—	2.37 ± 1.26	19	1.38 ± 1.53	21	—	—
Tertile 2	7.72 ± 2.49	25	8.05 ± 2.00	41	0.65 (0.33-1.27)	0.205	7.67 ± 2.41	15	7.55 ± 1.85	20	0.83 (0.33-2.07)	0.687
Tertile 3	21.59 ± 5.86	41	18.61 ± 5.36	23	1.88 (0.95-3.75)	0.071	21.65 ± 6.83	26	20.08 ± 5.33	13	2.21 (0.89-5.49)	0.088

The total number of points behind the field region demonstrates the number of points tested in the regions as defined in Figure 1. "Fail" and "pass" reflect the outcome of the on-road driving test. Odds ratios and *P* values are outcomes of univariate logistic regression models using untransformed variables, ln-transformed variables, or dummy variables. The second model only included the participants with a glaucoma diagnosis. Tertile 1 was used as the reference group in the logistic regression models. Bold values highlight significant values ($p < 0.05$).

[a] Odds ratio is computed with ln-transformed number of points missed. Mean ± SD is presented as untransformed variable.

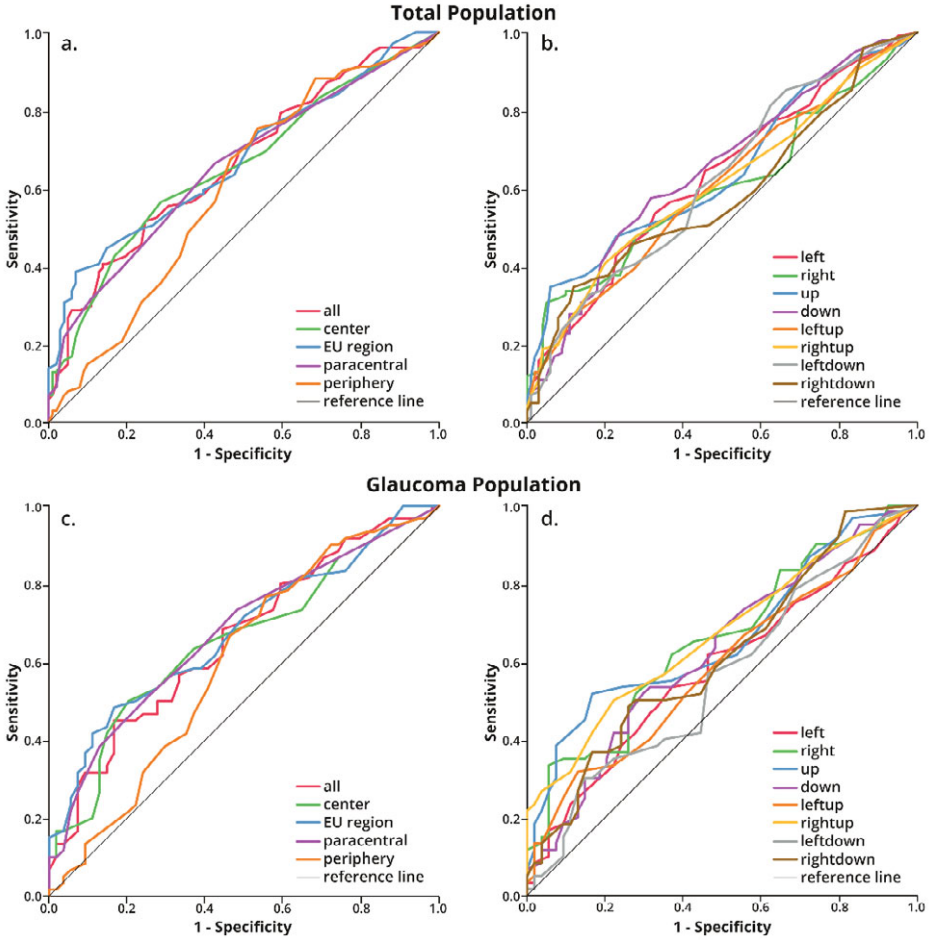

Figure 3. ROC curves for the relation between number of points seen per visual field region and outcome of on-road driving test for the total population **(A, B)** and the glaucoma population **(C, D)**. **A.** The area under the curve was 0.664 (whole field), 0.655 (central 20 degrees), 0.674 (EU region), 0.655 (paracentral points), and 0.601 (periphery). **B.** The area under the curve varied between 0.585 (right-down) and 0.648 (down). **C.** The area under the curve was 0.659 (whole field), 0.655 (central 20 degrees), 0.676 (EU region), 0.675 (paracentral points), and 0.598 (periphery). **D.** The area under the curve varied between 0.560 (left-down) and 0.665 (right-up).

Table 3 shows the intracorrelations between the visual field regions. It shows that the number of points missed is independent of neighboring regions, as the correlations between nonoverlapping visual field regions were well below 0.7.

Table 3. Intracorrelations for the Visual Field Regions

	All	EU	Cen	Par	Per	Le	Ri	Up	Do	LU	RU	LD	RD
All		.93**	.59**	.40**	.85**	.72**	.81**	.71**	.94**	.52**	.60**	.69**	.77**
EU	.94**		.74**	.57**	.59**	.66**	.76**	.72**	.85**	.52**	.60**	.61**	.70**
Cen	.63**	.76**		.87**	.22**	.45**	.45**	.40**	.56**	.34**	.29**	.42**	.45**
Par	.47**	.61**	.89**		.06	.32**	.30**	.37**	.34**	.33**	.25**	.25**	.27**
Per	.86**	.64**	.28**	.15		.62**	.68**	.52**	.84**	.38**	.44**	.63**	.67**
Le	.73**	.68**	.47**	.34**	.63**		.18*	.55**	.67**	.75**	.13	.94**	.17*
Ri	.82**	.78**	.50**	.39**	.70**	.21*		.55**	.77**	.10	.74**	.18*	.95**
Up	.70**	.70**	.36**	.37**	.53**	.60**	.49**		.43**	.77**	.80**	.33**	.35**
Do	.94**	.86**	.62**	.42**	.84**	.63**	.81**	.40**		.30**	.38**	.73**	.82**
LU	.49**	.52**	.31**	.33**	.34**	.74**	.09	.81**	.24*		.23**	.48**	.03
RU	.65**	.63**	.28**	.29**	.52**	.26**	.70**	.83**	.42**	.35**		.05	.50**
LD	.70**	.63**	.46**	.28**	.66**	.94**	.23*	.37**	.71**	.46**	.17		.21**
RD	.76**	.71**	.51**	.37**	.66**	.15	.96**	.27**	.84**	-.03	.46**	.21*	

Above the diagonal: total population (n = 202); below the diagonal: glaucoma population (n = 114). Pearson correlations for pairs of continuous variables. Shaded cells represent correlations between nonoverlapping regions. Cen, center; Par, paracentral; Per, periphery; Le, left; Ri, right; Do, down; LU, left-up; RU, right-up; LD, left-down; RD, right-down.
*$p < 0.05$
**$p < 0.01$

Discussion

In this research, we investigated the relation between the Esterman visual field test and the outcome of the on-road driving test. We found that, for most regions of the visual field, there is a significantly increased odds for failing the driving test when more points are missed. This underlines the importance of the visual field for driving performance. We found that the center may be more important than the periphery and that the left side may be more important than the right side. This could be attributed to the practice of right-hand traffic and left-hand drive in The Netherlands. It is also consistent with current opinions about the relative importance of the various visual field regions.[4]

We found that the period between the Esterman visual field and the on-road driving test was approximately 1.5 months longer for cases than for controls, with a wider

standard deviation for cases. A probable explanation is that a failed on-road driving test is often followed by a second on-road driving test, after the candidate takes additional driving lessons. We used data of the driving test that defined the candidate as suitable or unsuitable; hence, the time between the visual field test and the on-road driving test is longer for cases than for controls. The wide standard deviation can be explained by a variety in amount of driving lessons between the two failed on-road driving tests. We had no access to data about the number of failed on-road driving tests and the number of driving lessons.

The predictive value of visual field defects for the outcome of the driving test provided poor results. There was a large overlap between the visual field outcomes of failed and passed driving tests (see Fig. 2), making it virtually impossible to predict the outcome of the driving test, based on the visual field test alone. The poor predictive value illustrates that laboratory visual field testing and on-road driving tests measure different entities/capacities of the visual (visual field) and motor and cognitive (on-road driving test) system.

The Esterman visual field test was adopted for the assessment of impairment,[20] for which the central part of the field is considered more valuable than the periphery, the lower hemisphere is more useful than the upper, and the central 10 degrees is not measured. However, this is not necessarily applicable for driving. Typically, most traffic events occur within the central 25 degrees of the visual field. The front windshield of a car usually allows for visual field extension to the left of about 20 degrees and 50 degrees to the right. Side windows and mirrors are located more into the periphery. Moreover, the stimuli of the Esterman visual field do not follow the "hill of vision" but have size III and an intensity of 10 dB. This is far above the suprathreshold in the center of the visual field.[22] A new traffic perimetry test has recently been proposed,[21] removing some of the limitations of the Esterman visual field, such as emphasizing all parts of the field equally, equidistant test points, and following the hill of vision. The question remains if a static test would be able to predict the outcome of the on-road driving test. An alternative approach allowing a free gaze, with dynamic stimuli and cognitive screening, could be useful in minimizing the cumbersome on-road driving tests.

To the best of our knowledge, this is the first study to examine the relationship of the Esterman visual field with the outcome of an on-road driving test in a systematic manner using balanced and matched groups for the fail and pass outcome. The

use of various subdivisions of the Esterman visual field and statistical analysis with odds ratios and ROC curves provides a comprehensive exploration of the research question.

This study has several limitations. The number of participants in this study (*n* = 202) was acceptable for the statistical tests conducted. However, the group of patients with glaucoma (*n* = 114) is a smaller sample size, probably resulting in more nonsignificant results.

We assume the on-road driving test as the gold standard for driving performance. Although this is generally accepted, it may be debated.[32] The expert on practical fitness to drive who administered the on-road driving test was not blinded to the candidate's diagnoses and visual field defects; otherwise, planning a suitable on-road driving test is not possible. This could have biased the outcome of the on-road driving test. It has been found that driver status (active versus inactive driver) was a predictor for on-road driving performance.[17] In our retrospective study, we had no data on driver status or experience. Also, information on cognitive function, former rehabilitation, and the time since defect was missing in the provided data, which could have influenced our data and been attributed to a better predictive ability of our model.

Since evenly distributed missed points might have a different impact on driving capacity than clustered missed points, ideally, a cluster analysis should be performed. In a preliminary analysis, we performed a grouped point analysis. We demonstrated that the "weight" of a missed point increased somewhat when there was another missed point at (optimal) 0.3 radians distance. However, the analysis was hampered by the uneven distribution of distances between points in the Esterman visual field. Moreover, the discriminative ability of the test improved only minimally.

A retrospective case-control study was conducted, consequently having no strict control over the inclusion into the "exceptional case" program or insight into the decision of the medical advisor of the CBR. We had access only to candidates who were offered an on-road driving test in the "exceptional case" program. This excludes data on the candidates who were granted a license without administering a driving test and the candidates who were denied entry in the "exceptional case" program and had their license withdrawn without administering a driving test.

Conclusion

The results of this study confirm the relation between visual field damage and impaired driving performance. When more points are seen, the likelihood of passing the on-road driving test increases. However, in our group, the Esterman visual field test shows no discriminative ability to predict driving performance on an individual level. This implies that, in our group with moderate visual field defects, the number of on-road driving tests cannot be further reduced by a more detailed definition of fail–pass criteria, based on the Esterman visual field test alone. Hence, no adjustments to policy can be made to reduce the number of tests based on our results. This study underlines the need of an accessible and reliable test that can better predict the outcome of the on-road driving test in order to regulate entry in the “exceptional case” program. Such an alternative test may, ideally, combine the advantages of the visual field test (standardized, cheap) with those of the on-road driving test (natural, dynamic stimuli, allow for free gaze movements). Up until now, such a test is not available.

References

1. Owsley C, McGwin G, Jr. Vision impairment and driving. *Survey of Ophthalmology*. 1999;43(6):535-50. doi:10.1016/s0039-6257(99)00035-1
2. Bourne R, Steinmetz JD, Flaxman S, et al. Trends in prevalence of blindness and distance and near vision impairment over 30 years: an analysis for the Global Burden of Disease Study. *The Lancet Global Health*. 2021;9(2):e130-e143.
3. Thorslund B, Strand N. Vision measurability and its impact on safe driving: a literature review. *Scandinavian Journal of Optometry and Visual Science*. 2016;9(1):1-9.
4. Huisingh C, McGwin G, Jr., Wood J, Owsley C. The driving visual field and a history of motor vehicle collision involvement in older drivers: a population-based examination. *Investigative Ophthalmology & Visual Science*. 2014;56(1):132-8. doi:10.1167/iovs.14-15194
5. Kwon M, Huisingh C, Rhodes LA, McGwin G, Jr., Wood JM, Owsley C. Association between Glaucoma and At-fault Motor Vehicle Collision Involvement among Older Drivers: A Population-based Study. *Ophthalmology*. Jan 2016;123(1):109-16. doi:10.1016/j.ophtha.2015.08.043
6. Haymes SA, Leblanc RP, Nicolela MT, Chiasson LA, Chauhan BC. Risk of falls and motor vehicle collisions in glaucoma. *Investigative Ophthalmology & Visual Science*. 2007;48(3):1149-55. doi:10.1167/iovs.06-0886
7. McGwin G, Jr., Huisingh C, Jain SG, Girkin CA, Owsley C. Binocular visual field impairment in glaucoma and at-fault motor vehicle collisions. *Journal of Glaucoma*. 2015;24(2):138-43. doi:10.1097/IJG.0b013e3182a0761c
8. McCloskey LW, Koepsell TD, Wolf ME, Buchner DM. Motor vehicle collision injuries and sensory impairments of older drivers. *Age and Ageing*. 1994;23(4):267-73. doi:10.1093/ageing/23.4.267
9. McGwin G, Jr., Mays A, Joiner W, Decarlo DK, McNeal S, Owsley C. Is glaucoma associated with motor vehicle collision involvement and driving avoidance? *Investigative Ophthalmology & Visual Science*. 2004;45(11):3934-9. doi:10.1167/iovs.04-0524
10. Yuki K, Asaoka R, Tsubota K. The relationship between central visual field damage and motor vehicle collisions in primary open-angle glaucoma patients. *PLoS One*. 2014;9(12):e115572. doi:10.1371/journal.pone.0115572
11. Okamura K, Iwase A, Matsumoto C, et al. Association between visual field impairment and involvement in motor vehicle collision among a sample of Japanese drivers. *Transportation research part F: traffic psychology and behaviour*. 2019;62:99-114.
12. Owsley C. The vision and driving challenge. *Journal of Neuro-Ophthalmology*. 2010;30(2):115-6. doi:10.1097/WNO.0b013e3181e2d045
13. Crabb DP, Smith ND, Rauscher FG, et al. Exploring eye movements in patients with glaucoma when viewing a driving scene. *PLoS One*. 2010;5(3):e9710. doi:10.1371/journal.pone.0009710
14. Kubler TC, Kasneci E, Rosenstiel W, et al. Driving with Glaucoma: Task Performance and Gaze Movements. *Optometry and Vision Science*. 2015;92(11):1037-46. doi:10.1097/OPX.0000000000000702
15. Bowers AR, Ananyev E, Mandel AJ, Goldstein RB, Peli E. Driving with hemianopia: IV. Head scanning and detection at intersections in a simulator. *Investigative Ophthalmology & Visual Science*. 2014;55(3):1540-8. doi:10.1167/iovs.13-12748
16. Wood JM, McGwin G, Jr., Elgin J, et al. On-road driving performance by persons with hemianopia and quadrantanopia. *Investigative Ophthalmology & Visual Science*. 2009;50(2):577-85. doi:10.1167/iovs.08-2506
17. de Haan GA, Melis-Dankers BJ, Brouwer WH, Bredewoud RA, Tucha O, Heutink J. Car driving performance in hemianopia: an on-road driving study. *Investigative Ophthalmology & Visual Science*. 2014;55(10):6482-9. doi:10.1167/iovs.14-14042
18. Netelenbos T. Regeling eisen geschiktheid - BWBR0011362. Accessed March, 2022, https://wetten.overheid.nl/BWBR0011362/2021-04-17
19. Esterman B. Functional scoring of the binocular field. *Ophthalmology*. 1982;89(11):1226-1234.
20. American Medical Association. Guides to the evaluation of permanent impairment *2nd ed*. 1984;Chicago, IL: American Medical Association:141-151.

21. Jorstad OK, Jonsdottir TE, Zysset S, Rowe F. A traffic perimetry test that adheres to the European visual field requirements. *Acta Ophthalmologica*. 2021;99(4):e555-e561. doi:10.1111/aos.14633
22. Nederlands Oogheelkundig Gezelschap. Werkgroep Ergoftalmologie - Keuringseisen gezichtsvermogen. Accessed March, 2022, http://www.ergoftalmologie.nl/kg/methoden_van_onderzoek.html
23. Chihuri S, Mielenz TJ, DiMaggio CJ, et al. Driving Cessation and Health Outcomes in Older Adults. *Journal of the American Geriatrics Society*. 2016;64(2):332-41. doi:10.1111/jgs.13931
24. Nyberg J, Strandberg T, Berg H-Y, Aretun Å. Welfare consequences for individuals whose driving licenses are withdrawn due to visual field loss: a Swedish example. *Journal of Transport & Health*. 2019;14
25. Nyberg J, Levin L, Larsson K, Strandberg T. Distrust of Authorities: Experiences of Outcome and Processes of People Who Had Their Driving License Withdrawn Due to Visual Field Loss. *Social Sciences*. 2021;10(2):76.
26. Silveira S, Jolly N, Heard R, Clunas NJ, Kay L. Current licensing authority standards for peripheral visual field and safe on-road senior aged automobile driving performance. *Clinical & Experimental Ophthalmology*. 2007;35(7):612-20. doi:10.1111/j.1442-9071.2007.01544.x
27. Dow J. Visual field defects may not affect safe driving. *Traffic Injury Prevention*. 2011;12(5):483-90. doi:10.1080/15389588.2011.582906
28. Racette L, Casson EJ. The impact of visual field loss on driving performance: evidence from on-road driving assessments. *Optometry and Vision Science*. 2005;82(8):668-74. doi:10.1097/01.opx.0000174719.25799.37
29. Pandit RJ, Gales K, Griffiths PG. Effectiveness of testing visual fields by confrontation. *Lancet*. 2001;358(9290):1339-40. doi:10.1016/S0140-6736(01)06448-0
30. European Parliament. Directive 2006/126/EC of the European Parliament and of the Council of 20 December 2006 on driving licences (Recast). Official Journal of the European Union;L403:18–60. Accessed March, 2022, http://eur-lex.europa.eu/LexUriServ/LexUriServ.do?uri=OJ:L:2006:403:0018:0060:EN:PDF
31. Hosmer Jr DW, Lemeshow S, Sturdivant RX. *Applied logistic regression*. vol 398. John Wiley & Sons; 2013.
32. Dickerson AE, Meuel DB, Ridenour CD, Cooper K. Assessment tools predicting fitness to drive in older adults: a systematic review. *American Journal of Occupational Therapy*. 2014;68(6):670-80. doi:10.5014/ajot.2014.011833

Supplementary Material

S1 Medical Driving License Application Process in The Netherlands

In The Netherlands, a declaration of health must be submitted when a subject applies for a driving license for the first time, is aged 75, a driver's license has been given for a limited period and an intermediate notification has been received. They must submit an official statement with questions about their general health. If the subject indicates that there is an eye disorder, restricted vision, previous eye surgery or (previous) treatment by an ophthalmologist, then a formal assessment by an ophthalmologist is mandated. The ophthalmologist assesses visual acuity and (by the confrontation method) the visual field. Also, media and fundi are examined. If there is any doubt regarding the visual field, based on the confrontation results, the medical history or the results of the ophthalmological examination, a binocular visual field test (generally Esterman) is mandatory. If there is any sign of double vision or impaired night vision then additional examinations are requested. The ophthalmologist reports the findings regarding visual acuity, visual field, double vision, night vision, cause of any impairments and if the impairments are stable or progressive in nature. Also, an advice is included regarding the validity of the license (group 1 or 2, not fit to drive, fit to drive or fit to drive for a limited period: 1, 2, 3, 5 or 10 years). It can be advised that the license is only granted after an on-road driving test is performed. The medical advisor of the CBR (a medical doctor) makes the decision about the administration of the license, the period of validity, special restrictions (e.g. daytime only) and whether or not a driving test is mandated.

S2 The On-Road Driving Test

All participants in this study underwent an on-road driving test in The Netherlands, where right-hand traffic and left-hand drive are common practice. This test is administered by an expert on practical fitness to drive of the CBR. In principle the test takes place in the participant's own vehicle on the public road. A driver training vehicle is chosen in case of (hemi)anopsia, long refrainment from driving, after a period of driving lessons due to a previous failed on-road driving test and if other vehicle adaptations are required. The duration of the test is 60 minutes with a minimal driving time of 30 minutes. There is not an obligatory fixed route for the test. However, the CBR has designed a specific protocol for on-road driving tests administered in the presence of visual field defects. This protocol includes the test must always contain a few left/right turns, different types of intersections (both

straight on and left turns), roundabouts (both ½ and ¾ rounds), roads outside urban areas (driving with higher speeds, overtaking or passing slower vehicles, driving on a winding road), highways (changing lanes, overtaking other vehicles, choosing direction independently and rounding long bends at high speed with correct position) and narrow crowded roads with bicycle traffic. The scoring system of the TRIP (Test Ride for Investigating Practical fitness to drive) is used.[1] The on-road driving test always leads to a dichotomous pass or fail outcome. However, a passed driving test can be coupled with imposing restrictions, such as mandatory vehicle adaptations, and occasionally additional advice is given on a limited duration of license renewal.

1. Tant MLM. Visual performance in homonymous hemianopia: assessment, training and driving: Groningen, The Netherlands: University Library Groningen; 2002

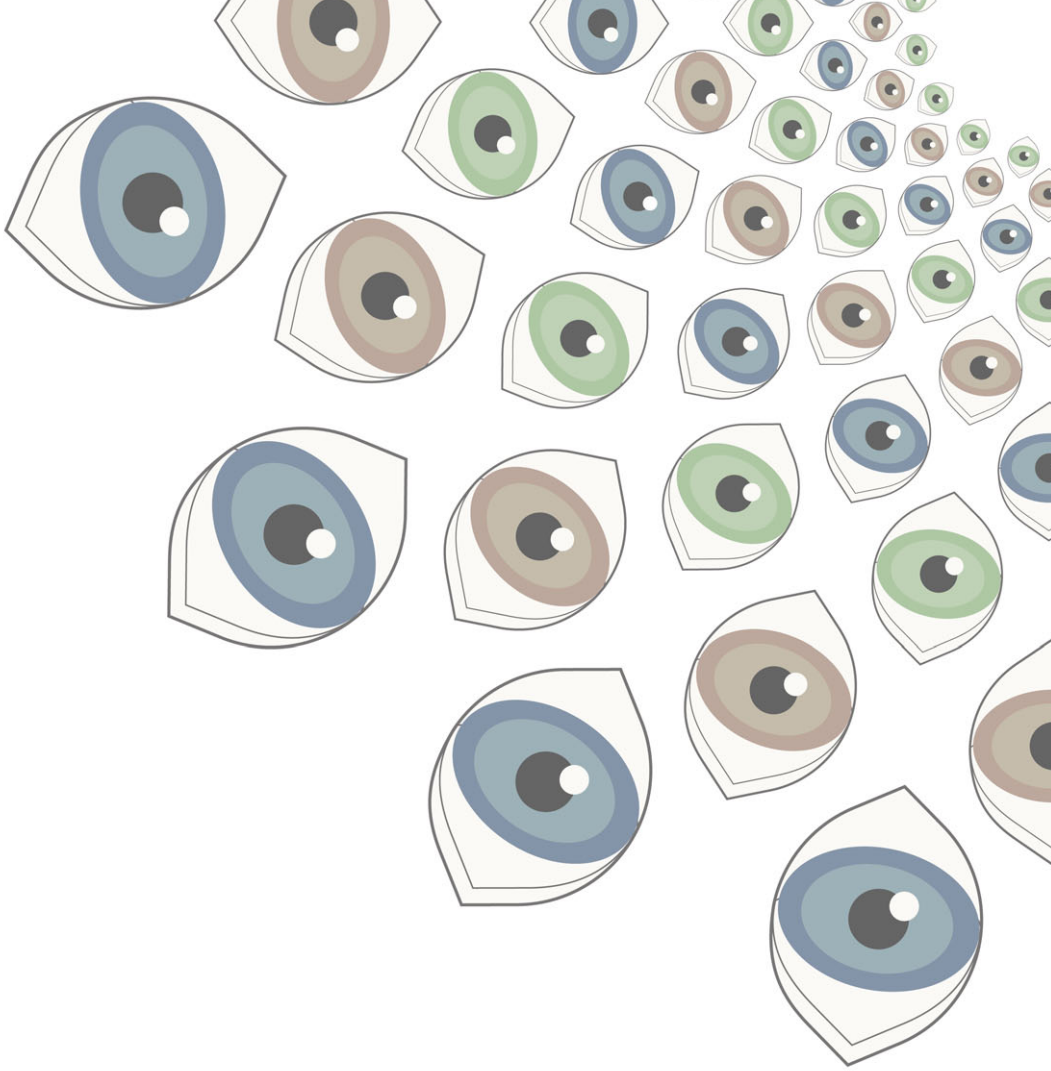

Chapter 3

A Toolkit for Wide-Screen Dynamic Area of Interest Measurements Using the Pupil Labs Core Eye Tracker

Y Faraji, JW van Rijn, RMA van Nispen, GHMB van Rens, BJM Melis-Dankers, J Koopman & LJ van Rijn

Behavior Research Methods, 2022: 1-11

Abstract

Eye tracking measurements taken while watching a wide field screen are challenging to perform. Commercially available remote eye trackers typically do not measure more than 35 degrees in eccentricity. Analysis software was developed using the Pupil Core Eye Tracking data to analyze viewing behavior under circumstances as natural as possible, on a 1.55-m-wide screen allowing free head movements. Additionally, dynamic area of interest (AOI) analyses were performed on data of participants viewing traffic scenes. A toolkit was created including software for simple allocation of dynamic AOIs (semiautomatically and manually), measurement of parameters such as dwell times and time to first entry, and overlaying gaze and AOIs on video. Participants (n =11) were asked to look at 13 dynamic AOIs in traffic scenes from appearance to disappearance in order to validate the setup and software. Different AOI margins were explored for the included objects. The median ratio between total appearance time and dwell time was about 90% for most objects when appropriate margins were chosen. This validated open-source toolkit is readily available for researchers who want to perform dynamic AOI analyses with the Pupil Core eye tracker, especially when measurements are desired on a wide screen, in various fields such as psychology, transportation, and low vision research.

Introduction

Eye tracking is growing in popularity amongst researchers from many different disciplines, including healthcare, psychology, biomedical applications, and neuroscience.[1,2] An eye tracker measures how the gaze is directed during a specific task and can give information about the allocation of visual attention as eye movements are linked to cognitive processing. Currently, many methods are based on area of interest (AOI, also known as region of interest; ROI) analyses. AOIs are defined as areas in the stimulus important to the research aim and can be used to calculate metrics such as AOI hits (when gaze coordinates lay inside an AOI) and dwell times (duration of one visit in an AOI, from entry to exit).[2] Dynamic AOIs—moving areas of interest that arise during a video or animated elements on a screen—challenge the analysis since the objects move relative to the coordinate system in which the gaze position data are recorded.[3]

Some eye trackers provide software for the analysis of dynamic AOI data, such as Tobii Pro Lab. Also, open-source options are available, such as DynAOI.[4] However, a limitation of commercially available remote and tower-mounted-based eye trackers is the restriction of head movements and a limited measurement range, typically not more than 35 degrees eccentricity. Head-mounted eye trackers that allow for free head movements and have a large measurement range are available, such as Tobii Pro glasses and Pupil Core eye trackers. However, head-mounted eye trackers provide a gaze-overlaid video and if a data file is provided, the coordinates refer to positions in the video (eye-in-head coordinates). Therefore, the use of dynamic AOI analyses becomes problematic.

Our research group aims to study compensatory viewing in traffic for persons with visual field defects in the TREYESCAN study (Traffic Eye Scanning and Compensation Analyzer). The current method of visual field testing does not properly discriminate between persons with visual field defects that are fit and unfit to drive.[5] The TREYESCAN should measure eye movements over a large field of view because the visual field is important for safe participation in traffic.[6] Defects could lay in the periphery of the visual field, subsequently underlining the need of measuring eye movements on a screen as large as possible, instead of only centrally on a small monitor. Moreover, transportation research showed that a restricted field of view of driving scenes (presented on a single screen) may lead to poorer hazard detection and less eccentric eye movements compared to a setup with the addition of side views on adjacent screens.[7,8] Therefore, we sought an accessible method for analyzing

eye movements on a screen with a wide field of view (100°) while not restricting head movements. In order to measure compensatory viewing, we are interested in conducting dynamic AOI analyses.

The Pupil Core eye tracker (Pupil Labs, Berlin), that we used in this research, can detect apriltags (QR-like markers),[9] and map the gaze onto the defined surface using Pupil Labs' Application Programming Interface (API).[10] By placing the apriltags on the bezels of the computer screen, fixed coordinates of gaze can be calculated and be used in dynamic AOI analyses, while maintaining a wide measurement area and free head movements. In essence, the mobile eye tracker is used in such a matter, that it facilitates remote eye tracking on a much wider screen, as was previously investigated in an explorative study.[11] The Pupil Core can measure up to 200 Hz per eye (120 Hz with higher resolution) and is a relatively affordable and valid option when mid-range accuracy is sufficient.[12] Pupil Labs offers open-source software, which is relatively quick to include new developments. However, current drawbacks of this software are the absence of tools for dynamic AOI allocation and analysis software.

Therefore, our aim is to develop a toolkit for the Pupil Core eye tracker, in order to perform pre-recorded gaze analyses of dynamic AOIs on a large screen with free head movements. The kit includes tools for simple allocation of dynamic AOIs (semi-automated and manually), measurement of parameters such as dwell times and time to first entry, and overlaying gaze and AOIs on video. In this paper, we present the validation results of these tools on a group of normal-sighted participants. With our software, it will be possible to quantify viewing behavior for various purposes, especially when screen-based measurements are desired on a large screen. The source code of the entire toolkit is available on GitHub *(https://github.com/treyescan/dynamic-aoi-toolkit).*

Methods

Participants

Participants were recruited using snowball sampling at Amsterdam UMC for a validation study of the toolkit. Eligibility criteria were: age above 18 years, no history of ophthalmic comorbidities, no medication use that could affect responsiveness and concentration, and no refractive correction by means of glasses or contact lenses. Participants performed an Esterman visual field test[13] and a visual acuity measurement using the Early Treatment Diabetic Retinopathy Study (ETDRS) chart.[14,15] In addition, a custom suprathreshold visual field test performed on the Humprey Field Analyser II (HFA) to screen the central 10° for visual field defects. Only

participants with a minimal binocular visual acuity of 0.0 LogMAR without refractive correction and no defects on the visual field tests were included. Participants were instructed not to wear eye makeup.

All participants provided informed consent and all procedures were approved by the Medical Ethical Committee of Amsterdam University Medical Centers—location VU University Medical Center.

Validation Task

The validation task included 13 short traffic scenes, which contained 13 dynamic AOIs varying in size, velocity, direction, and location on the screen (one object per scene). The participants were instructed to look at a certain object in each scene and track it from appearance to disappearance. Before the AOI appeared, a verbal instruction was given of the area in the scene it would appear, hence the participants already looked in that direction when the AOI appeared. The total experiment duration was 5 min. For each object, we were interested in the total dwell time and time to first entry, with the aim of validating our setup.

Videos had been recorded while driving in everyday traffic with a Sony A7III camera with a Laowa Zero-D ultra-wide field 12 mm f/2.8 lens (angle of view: 121.96°; minimal distortion). Footage was shot in 4K (3840x2160) with 25 fps. The camera was mounted centrally behind the windshield of a Toyota Prius II. A black piece of felt was put on the dashboard to prevent reflections from the dashboard surface.

Adobe Premiere Pro (Adobe Inc, San Jose, CA, USA) was used to expand and crop the video clips to 5760x1200 to fit the three screen setup (Fig. 1). The full width of the video was used. No information about the traffic scene was lost by cropping the video's height to facilitate screen fitting.

Experimental Setup and Recording Device

The validation experiment was conducted at the Amsterdam UMC, location VUmc. In a recording room, 3 HP EliteDisplay E243i 24-inch IPS LED backlit monitors with 1920x1200 resolution with thin bezels (width bezel: 0.68 cm) and a refresh rate of 60 Hz were placed in a linear formation. Nvidia Surround (Nvidia, Santa Clara, CA, USA) was used to span the video over the three screens with bezel correction. To view the video without distortion, a correction of 50 pixels was applied between two adjacent screens, thus occluding two minor portions of the video. An additional screen (Iiyama

ProLite XB2783HSU) was placed on the side, the display not visible to the participant, in order to control the validation experiment. A car seat was positioned in front of the three screens at a distance of 65 cm from eyes to the central screen's middle, in order to obtain a 100° field of view, which confines the possibility for a larger distance to the screen. The table could be altered in height to ensure the eyes were positioned in the middle of the screen (Fig. 1). Head movements were permitted in all directions.

Figure 1. TREYESCAN setup. **A**. Picture of setup. Participants are seated in front of the display monitors while wearing the Pupil Core eye tracker. **B.** Schematic overview of the set-up (view from above). The participant is located 65 cm in front of the central display monitor. The examiner is located on the right of the participant and can guide the experiment from the host monitor. On the MacBook display, stability of the signal and performance of the participant can be checked.

The participants' eye movements were recorded by a head-mounted eye-tracker (Pupil Labs Core glasses, received October 2021, Pupil Labs, Berlin, Germany). The Pupil Labs eye-tracker,[10] used in this study, has three cameras: one world camera (100° fisheye field of view, 30-Hz sampling frequency, resolution on a subset of 1280x720 pixels) to record the world from the participant's point of view, and one eye-

camera for each eye (120-Hz sampling frequency, resolution on a subset of 400x400 pixels). Pupil Labs capture v3.3.0 was used for the recordings. The experiment was conducted using two computers: Acer Nitro (N50-610 I9426-JK with NVIDIA GeForce RTX 2060 video card and Intel Core i5 processor) for stimulus presentation and an Apple MacBook Pro with M1 chip (as recommended by Pupil Labs) for recording of eye movements. All experiments were performed under the same lighting conditions (~ 250 Lux). The luminance differs for the central screen (1–210 cd/m2) and the peripheral screens (1.5–150 cd/m2), measured from the position of a participant.

Before each validation task, a nine-point screen calibration routine was used on the three-screen setup as provided by Pupil Labs (personal correspondence). Similarly, the calibration was validated by a routine with 12 points of different positions. The Pupil Labs software then generates a value for the accuracy and precision. The validation routine was repeated after the task, to get insight in changes in accuracy and precision throughout the task, such as slippage of the glasses.[16]

Methods of Data Analysis

Pupil Labs Player v3.3.0 was used to export the measurements. The analysis script was written in Python 3.8.3[17] using NumPy,[18] Pandas,[19] OpenCV,[20] and SciPy.[21] For visualization, Matplotlib was used.[22]

Surface Definition

The Surface Tracker plugin by Pupil Labs[10] was used to define the surface area of the display with apriltags.[9] Because of the wide screen, the surface was divided in nine Pupil Labs surfaces (Fig. 2). We found that with more and narrower surfaces the gaze coordinates became more accurate. Twenty-two apriltags were placed within the video (width of 80 pixels). The corner apriltags were enlarged for better detection at greater angles (width of 160 pixels), as seen in Fig. 2. A Python routine is included for this purpose in the toolkit. The surface detection was not constantly optimal due to the small size of the apriltags and the backlight of the screens, hence 18 additional apriltags printed on paper (width marker of 4 cm, total width including white border of 6 cm) were placed on the top and bottom row of the screen's bezels in order to enhance the detection quality of the surfaces (Fig. 1). A dummy surface was defined, merely registering the screen's apriltags, in order to benchmark the start and end of the task. In between each scene, an additional unique apriltag was placed in order to monitor the time synchronization of the task and obtain an indication of possible

latencies. The nine surface gaze files were pooled to one gaze file (Fig. 3a) and the coordinate system was transformed so that the screen's middle was (0,0).

Figure 2. Indication of the surface distribution.

Preprocessing the Gaze Data

A median noise reduction function was used as a lowpass filter on the eye movement data to smooth out noise (Fig. 3a), while preserving the features of the sampled data.[23] We chose a median noise reduction algorithm, because compared to a moving average algorithm, the data is less smoothed even though the most prominent noise is removed, less 'false' gaze coordinates are created and the amplitude of the velocity peaks is not reduced as severely.[24] A window size of three samples was chosen for one-sample spike reduction.[25]

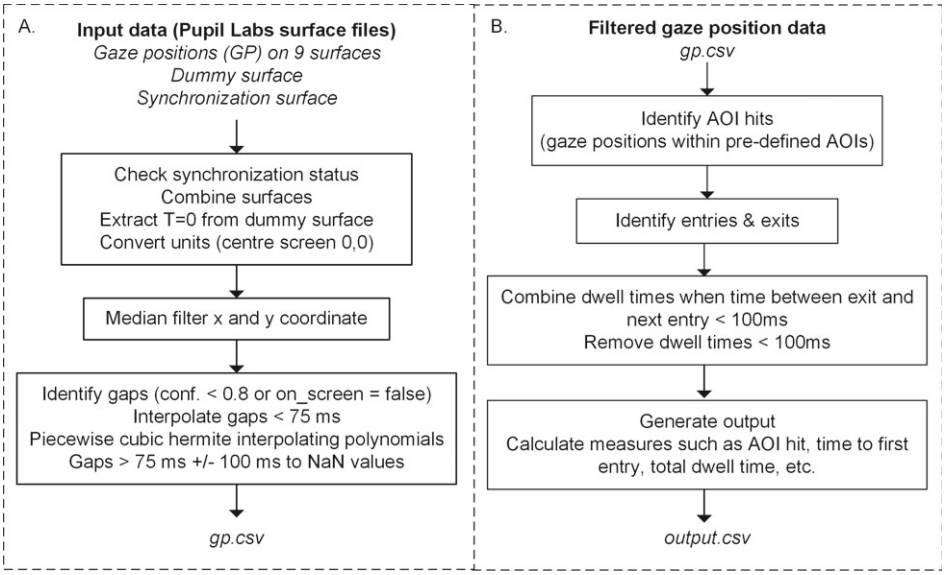

Figure 3. Flowcharts of steps in data processing. **A.** Pre-processing of the gaze data. **B.** Gaze and AOI matching process.

Pupil Labs provides a quality assessment of the pupil detection for every sample, as a "confidence" value between 0.0 (pupil could not be detected), and 1.0 (pupil was detected with very high certainty). A Boolean variable (on_screen) is also provided by Pupil Player which indicates if the gaze was plotted within the surface areas. In our software, samples with a confidence level below 0.8 (e.g., because of blinks) and samples outside the monitor's surface were treated as gaps in the data (Fig. 3a). This threshold is also used by Pupil Labs when determining valid gap samples for the calibration procedure. If the gap duration was below 75 ms, the gaze coordinates were filled in using linear interpolation.[24,26] Longer gaps were kept in the data frame and labeled as Not a Number (NaN) values. We regarded the samples ± 100 ms around a gap as additional gap samples, where the pupil of the eye may be partially occluded.[27]

The Pupil Core eye tracker has two eye camera's that each measure with a sampling rate of 120 Hz in antiphase. The Pupil Labs Fusion algorithm combines these signals to a sampling rate of 240 Hz. However, as it does not provide a constant sampling rate, we used piecewise cubic Hermite interpolating polynomials to obtain samples at a sampling rate of 240 Hz.[12]

AOI Allocation

In order to determine if a participant viewed an AOI, the coordinates of the bounds of these AOIs must be obtained. We decided to determine all AOIs by the use of rectangles, as this was the most accessible shape for the AOIs in traffic scenes.

Two programs, written in Python, were used to draw rectangles around the 13 dynamic AOIs in the traffic scenes. AOI_tracking.py tracks the object semi-automatically by using an OpenCV algorithm, which compares to consecutive frames and redraws the AOI on the next frame. It also corrects the size of the rectangle according to the size of the AOI, as objects that move away or towards the camera vary in size considerably from beginning until the end. We noticed this program works well, except in some instances, e.g., when an object covers a large part of the scene. Hence, we also created another script that interpolates the bounding boxes between two boxes drawn, AOI_selection.py. This program also contains an option to draw AOIs entirely manually frame by frame. Both scripts generate a bounding box with x and y values for each object on the relevant frame number, an object type label and allow for additional custom labels. The coordinates of the AOI bounding boxes are also transformed to the coordinate system with (0,0) as the screen's center.

Matching Gaze and AOI Data

A frame-by-frame method was used to match the gaze data with the AOI data (Fig. 3b). We computed the corresponding frame number for each eye tracker sample, since the eye tracker samples were retrieved with 240 Hz (120 Hz for each eye camera) and the AOI data was based on footage with 25 fps. For each gaze sample, we checked if the corresponding frame number lay within the boundaries of the AOI box.

A variable margin (in degrees of visual angle) can be added around every AOI box in order to compensate for eye tracking inaccuracy.[2,28] Because of the large angle of view (100°) these margins, in screen coordinates, become larger at the peripheral parts of the screen. This is calculated frame-by-frame, by determining the distance in pixels for the left and right side of the AOI separately for a given degree, as these can be significantly different due to the location and size of the AOI on the screen. For the top and bottom, both margins are calculated using the center y-coordinate of the AOI. It is recommended to add a margin around AOIs of 1° to 1.5° of visual angle, and when accuracy is low, increase margin size to ensure inclusion of all fixations on an AOI. However, larger AOI margins increase the risk of attributing fixations that do not belong to an object.[2,28] Therefore, for the results of the validation task we experimented with different values for the margins to give insight in the effects on parameters such as dwell time percentages.

The entries and exits within an AOI were extracted and the dwell times between each entry and exit were calculated. We assumed the time between an exit and a new entry should not be shorter than 100 ms, because this would likely be due to precision errors than of the participant's gaze deliberately exiting and entering the object. If this time was indeed shorter than 100 ms, the time between the exit and new entry was pooled with the previous dwell time, thus combining the two visits. If a dwell time remained shorter than 100 ms, the dwell was not included in the total dwell time measure. The sum of dwell times provides the total dwell time within an AOI. We decided on 100 ms as a threshold for these variables, since Engmann, et al.[29] found that 96.1% of the fixations in their study lasted longer than 100 ms. Also, Salvucci and Goldberg[30] report that fixations typically have a duration of at least 100 ms. For a dwell time to be relevant it needs to consist of at least one fixation otherwise no cognitive processes could have taken place. Thus, 100 ms was considered a safe cut-off. However, the values of these variables can be altered in the toolkit according to the experiment's requirements.

Time to first entry is computed by extracting the time between the objects first appearance and the first entry. The dwell time percentage is calculated between

the total appearance time of an object and the total dwell time to explore what percentage of time the object was looked at when it was in view.

Overlay Gaze and AOIs in Video Footage

We developed three tools for overlaying the gaze over the video for visualization of included AOIs and gaze data. The tool overlay_aois.py overlays the drawn AOI bounding boxes with margins, overlay_single_participant.py overlays all AOI boxes with the gaze data of one participant and overlay_multiple_participants.py overlays all AOI boxes with the gaze data of all participants. For the overlay tools discriminative colors were used from the color alphabet.[31]

Statistical Analysis

The statistical analyses were performed with IBM SPSS Statistics for Windows, Version 28.0 (SPSS, Armonk, NY, USA) and our analysis software programmed in Python. Graphs were made in GraphPad for Windows, Version 9.0 (GraphPad Software, San Diego, CA, USA).

Results

Eleven participants (median age 27, range 25–59, 5 female) were included to perform the validation task. The participant and measurement characteristics are shown in Table 1. Accuracy and precision, as provided by Pupil Labs and obtained during the validation procedures before and after the task, did not change significantly during the task of 5 min.

Table 1. Participant and measurement characteristics

	***n* = 11**
Age (year) median [range]	27 [25-59]
Number of female participants (N)	5
Binocular visual acuity (logMAR) mean ± SD	-0.13 ± 0.091
Esterman visual field abnormalities	0
Prescription eyeglasses/contact lenses	0
Accuracy before task (°) mean ± SD	2.05 ± 0.43
Precision before task (°) mean ± SD	0.10 ± 0.017
Accuracy after task (°) mean ± SD	2.12 ± 0.69
Precision after task (°) mean ± SD	0.098 ± 0.020

When pre-processing the gaze data, samples with a confidence value below 0.8 were set to NaN values. Before interpolation, this was 3.59% (median, IQR [1.87–11.08])

of total samples. 2.14% (median, IQR [1.44–3.88]) of total samples were marked as samples outside the monitor's surface and were also set to NAN. Some samples had both a poor confidence and were not on screen, hence after this step, a total of 5.20% (median, IQR [2.75–13.56]) of samples were set to NaN values. Subsequently, the length of the gaps was determined and gaps that were shorter than 75 ms were interpolated. After this interpolation, 3.89% (median, IQR [2.56–7.98]) of samples remained a NaN value. When extending the gaps with ± 100 ms, 7.05% (median, IQR [5.01–14.16]) of samples were set to NaN values. These samples were consequently considered as gap samples in the analyses.

As can be seen in Table 2, objects of various sizes, location, direction, and velocity were included in the validation task. An object can have a large range of sizes, as the objects become larger when nearing the camera, e.g., Road Sign 1, which starts as a small object and becomes a large object at the side of the screen when the car passes it. We included objects that move from one side of the screen to the other, and objects that appear in the center of the screen and disappear from the sides, which is the case for oncoming traffic, traffic lights, road signs etc. Only Car 2 starts in the middle and ends in the middle. Van 1 stands out as an object with a short and rapid appearance.

Table 2. Traffic Scenes and AOI characteristics

	Duration of Scene (s)	Duration of AOI visibility (s)	Width AOI (pixels; median (min – max))	Height AOI (pixels; median (min – max))	Average velocity of AOI (°/s)
Car 1	17.6	10.5	865 (150 – 2350)	275 (75 – 725)	-7.2
Car 2	69.4	69.2	168 (48 – 544)	144 (52 – 284)	-0.02
Cyclist 1	23.2	9.8	160 (70 – 525)	200 (125 – 455)	9.7
Cyclist 2	17.3	9.8	215 (85 – 660)	390 (140 – 660)	8.6
Cyclist 3	11.6	4.6	160 (60 – 590)	165 (90 – 540)	-11.6
Cyclist 4	13.2	10.3	52 (40 – 1020)	120 (76 – 1168)	4.6
Pedestrian 1	31.6	25.5	195 (70 – 455)	210 (75 – 330)	-2.0
Road Sign 1	10.8	6.4	60 (40 – 892)	68 (36 – 424)	6.9
Road Sign 2	11.2	6.8	44 (24 – 185)	42 (28 – 245)	-7.1
Scooter 1	23.2	9.8	104 (24 – 185)	160 (24 – 185)	-9.0
Scooter 2	9.3	5.4	36 (28 – 1116)	72 (44 – 920)	-8.1
Traffic light 1	12.6	11.8	32 (20 – 340)	60 (40 – 410)	3.7
Van 1	11.6	1.7	1790 (160 – 2110)	730 (395 – 760)	56.5

Width of screen: 5760 pixels. Height of screen: 1200 pixels. Duration of Scene: the duration of the entire scene in which the AOI is included. Duration of AOI visibility: the time during which the AOI is visible. The average velocity is calculated by dividing the trajectory (middle of start point till middle of end point) in degrees by duration of AOI visibility (negative numbers represent objects that move from the right to the left side of the screen).

Our toolkit was applied on the gaze data for different sizes of AOI margins. Figure 4 presents the percentage between total appearance time and calculated dwell time for each object. It shows that adding a margin, considerably increases the calculated dwell time percentage. After 1.5° the measures only improve slightly and most dwell percentages lay around 90%. This margin seems the most acceptable margin, as it is large enough to reduce inaccurate hits, but is at the same time the smallest margin possible to decrease possible overlap with other AOIs in the scene. In the supplementary material S1 (Video Van1) and S2 (Video Scooter1) two objects of the task can be seen with the gaze data and AOIs with margins of 1.5°. Also, the raw data table that supports Fig. 4 is included in S3.

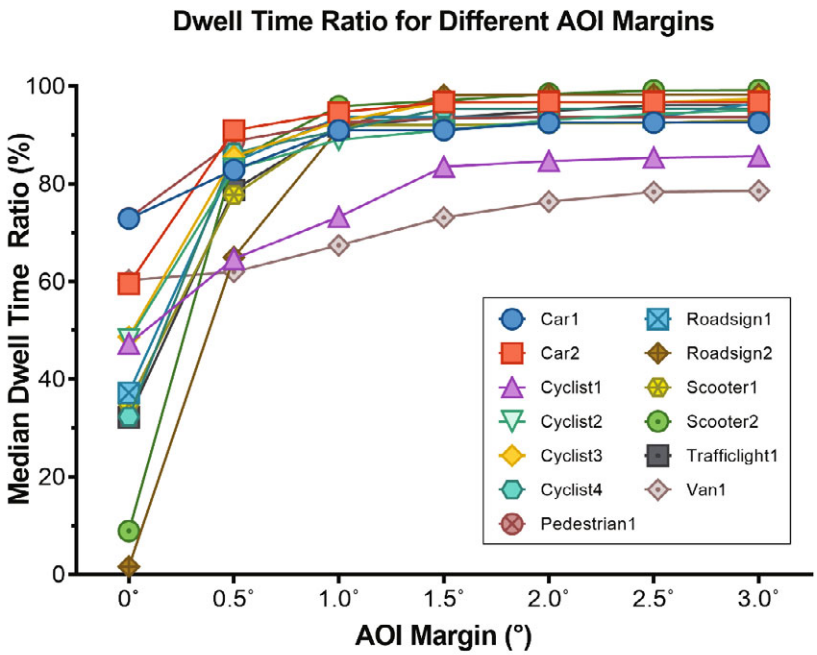

Figure 4. Median dwell time percentage for different AOI margins. Each symbol denotes the median dwell time percentage for 1 AOI.

Figure 5 gives insight in the distribution of calculated dwell time percentages for each participant. It can be seen that when a margin of 1.5° is chosen, most calculated dwell time percentages of the participants are above 80% and median dwell time percentages are around 90%. Especially Van 1 and Cyclist 1 show a wide distribution of dwell time percentages.

The median time to first entry measure was close to zero and below 50 ms for most objects, when a margin of 1.5° is chosen. However, the last exit time was often significantly earlier than the disappearance time for the objects that disappear at the sides of the screen, which is the case for most objects.

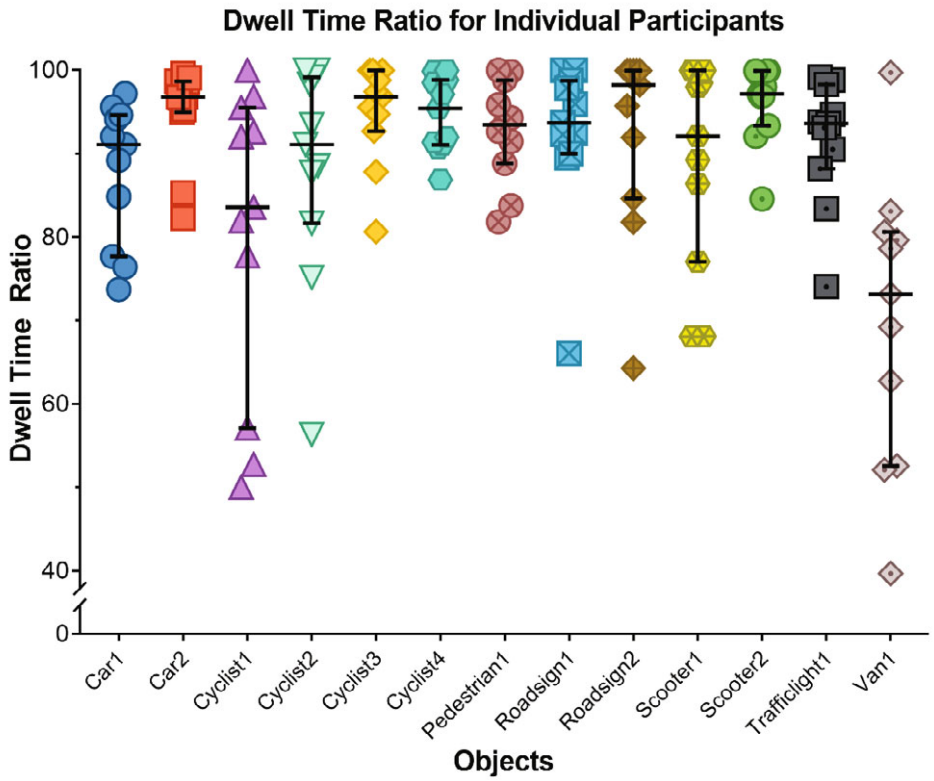

Figure 5. Dot plot of the dwell time percentage (%) for each object for AOI margin 1.5°. Each dot represents one participant. The median and interquartile range are also illustrated.

Feasibility

The question is why we did not obtain dwell time percentages of (close to) 100% for all participants when viewing the AOIs, since participants were instructed to track them from appearance to disappearance. Multiple factors could contribute to our results.

Gap samples (during blinks) were excluded from the dataset. When an AOI is viewed for an extended period of time such as Car 2, it is inevitable that the participant will blink multiple times, which has an effect on the measured dwell time.

Furthermore, when analyzing the results of our toolkit we assumed that participants had followed the objects accordingly and that discrepancies were due to eye tracker or toolkit inaccuracies. However, we noticed that especially fast moving objects, such as Van1 (see S1 – Video Van1) are not properly followed by all participants. In some instances, a participant did not immediately look at an object after it appeared (although instructed otherwise).

When looking at the gaze data of the validation task it is clear that the accuracy gets poorer towards the sides of the screen at larger angles, between 40 and 50° (see S2 – Video Scooter1). It is well known in eye-tracking research that accuracy is best in the middle and poorest in the corners of the screen.[2] We aimed to correct for this by adding a larger margin towards the sides of the screen as determined by the position of the object on the screen, but this was not enough for some cases.

Furthermore, when the participant looks at the side of the screen, due to the inaccuracy at larger angles, data samples are labeled as “not looking on the screen” and hence considered as missing samples in the dataset. This is visible in the Video Van1 (see S1) where the gaze points of multiple participants are not visible because the gaze points fall outside of the screens edge due to the inaccuracy. We assume that this aspect was the biggest issue for the lower dwell time percentage, since most objects disappear from the sides of the screen. We expect this not to be a disturbing issue when using this method on a natural viewing task, because then participants will not be instructed to follow an object from appearance to disappearance, and generally will not be looking at the edges of the screen.

Discussion

In this paper, we present a toolkit for analyzing dynamic AOI analyses on a large screen without the restriction of head movements. The results of our validation task show promising results for the functionality of the toolkit using the Pupil Core eye tracker. For most followed objects (11/13) the calculated median dwell time percentages are around 90%.

When using video stimuli in eye tracker research, synchronization between stimulus presentation and recording software is critical.[2] As we presented the stimuli and the recording software on different computers, the probability of latencies decreases, because the processor and hard disk do not have to perform the demanding operations simultaneously. However, the probability of latency remains, because

video players typically run slightly faster or slower than the recording of data samples, and as a result the data sample resulting from a participant looking at a particular frame in the video can be stored earlier or later in the data file. Moreover, the beginning of the recordings is determined by the presentation of the apriltags. Since the scene camera records in 30 fps, a delay of 33 ms could occur after the onset of the video. In order to get an indication of the synchronization status in our setup, we placed an apriltag between every scene of the validation task. We found a discrepancy of 0 to 62.5 ms between the expected appearance of the apriltag and the actual eye-tracking data. When also considering the inherent delay of 10 ms of the Pupil Labs' cameras,[12] we find this value acceptable for our research aim.

In some eye-tracking studies, researchers use fixation measures instead of dwell times measures for AOIs analyses. In this toolkit, we decided to use dwell time measures for the dynamic areas of interest analysis. Susac, et al.[32] concluded that it is adequate to report only one of these measures. In addition, Vansteenkiste, et al.[33] found a high correlation when comparing a fixation-by-fixation analysis to a frame-by-frame method when analyzing dwell time percentages. This indicates that both methods work well. A frame-by-frame method was chosen for our toolkit to check for robustness without adding another subjective variable. However, the fixation algorithm provided by Pupil Labs can also be used with our detection software.

In this toolkit we offer two tools for the allocation of AOIs. Recently, Bonikowski, et al.[34] also presented open-source software for determining dynamic AOI using object tracking. They offer a neat application with integrated control panels. A benefit of our toolkit is the possibility of margin addition and the incorporation of the software that matches gaze with AOIs.

A limitation of our validation study is the inclusion of individuals without glasses or contact lenses. We wanted to test our toolkit in the most ideal situation. Hence, no conclusions can be drawn about the functionality of the Pupil Core eye tracker in combination with our toolkit when using refractive correction. The AOIs were in all cases defined as rectangles, while AOIs such as round traffic signs and cyclists, do not fill the rectangle shape entirely. However, this was the most accessible shape for most objects in traffic situations. Moreover, the results are based on a small sample of 11 participants, who watched scenes for 5 min, which may not represent the accuracy and precision during a longer task. The analysis of dynamic AOIs remains complex. Since objects move relative to the coordinate system in which the gaze

position data is recorded, it is difficult to make any definite statements relating to the size of the AOIs.

When considering all the challenges that arise with this type of measurement methods and analyses, it can be concluded that our toolkit performs acceptably for the research aim. To the best of our knowledge, this is the first toolkit that uses the Pupil Core eye tracker and apriltags for dwell time measures in dynamic areas of interest on a large screen. As well as providing various tools that are necessary for analysis and visualization purposes.

Conclusion

This validated open-source toolkit is ready to use for researchers who want to perform dynamic AOI analyses with the Pupil Core eye tracker, especially when measurements are desired on a wide screen. We provide tools for simple allocation of dynamic AOIs (semi-automatically and manually), measurement of parameters such as dwell times and time to first entry, and overlaying gaze and AOIs on video. With our software, it is possible to quantify viewing behavior for various purposes. In further research, our aim is to investigate compensatory viewing strategies in traffic, but our setup is also readily available for eye tracking studies in other fields, such as psychology, transportation, and low vision research.

References

1. Carter BT, Luke SG. Best practices in eye tracking research. *International Journal of Psychophysiology*. 2020;155:49-62. doi:10.1016/j.ijpsycho.2020.05.010
2. Holmqvist K, Andersson R. *Eye tracking: A comprehensive guide to methods, paradigms and measures*. Lund Eye-Tracking Research Institute. 2017.
3. Hessels RS, Benjamins JS, Cornelissen THW, Hooge ITC. A Validation of Automatically-Generated Areas-of-Interest in Videos of a Face for Eye-Tracking Research. *Frontiers in Psychology*. 2018;9:1367. doi:10.3389/fpsyg.2018.01367
4. Papenmeier F, Huff M. DynAOI: A tool for matching eye-movement data with dynamic areas of interest in animations and movies. *Behavior Research Methods*. Feb 2010;42(1):179-87. doi:10.3758/BRM.42.1.179
5. Faraji Y, Tan-Burghouwt MT, Bredewoud RA, van Nispen RMA, van Rijn LJR. Predictive Value of the Esterman Visual Field Test on the Outcome of the On-Road Driving Test. *Translational Vision Science & Technology*. 2022;11(3):20. doi:10.1167/tvst.11.3.20
6. Owsley C, McGwin G, Jr. Vision impairment and driving. *Survey of Ophthalmology*. 1999;43(6):535-50. doi:10.1016/s0039-6257(99)00035-1
7. Alberti CF, Shahar A, Crundall D. Are experienced drivers more likely than novice drivers to benefit from driving simulations with a wide field of view? *Transportation Research Part F: Traffic Psychology and Behaviour*. 2014;27:124-132.
8. Shahar A, Alberti CF, Clarke D, Crundall D. Hazard perception as a function of target location and the field of view. *Accident Analysis and Prevention*. 2010;42(6):1577-84. doi:10.1016/j.aap.2010.03.016
9. Wang J, Olson E. AprilTag 2: Efficient and robust fiducial detection. *2016 IEEE/RSJ International Conference on Intelligent Robots and Systems (IROS)*. 2016:4193-4198.
10. Kassner M, Patera W, Bulling A. Pupil: An open source platform for pervasive eye tracking and mobile gaze-based interaction. *Proceedings of the 2014 ACM international joint conference on pervasive and ubiquitous computing: Adjunct publication*. 2014:1151-1160.
11. Haase H, Overvliet KE, Romeijn N, Koopman J. *How People with a Visual Field Defect Scan their Environment: An Eye-Tracking Study*. 2019. Accessed April, 2022. https://studenttheses.uu.nl/handle/20.500.12932/33317
12. Ehinger BV, Gross K, Ibs I, Konig P. A new comprehensive eye-tracking test battery concurrently evaluating the Pupil Labs glasses and the EyeLink 1000. *PeerJ*. 2019;7:e7086. doi:10.7717/peerj.7086
13. Esterman B. Functional scoring of the binocular field. *Ophthalmology*. 1982;89(11):1226-1234.
14. Ferris III FL, Kassoff A, Bresnick GH, Bailey I. New visual acuity charts for clinical research. *American journal of ophthalmology*. 1982;94(1):91-96.
15. Yu HJ, Kaiser PK, Zamora D, et al. Visual Acuity Variability: Comparing Discrepancies between Snellen and ETDRS Measurements among Subjects Entering Prospective Trials. *Ophthalmology Retina*. 2021;5(3):224-233. doi:10.1016/j.oret.2020.04.011
16. Niehorster DC, Santini T, Hessels RS, Hooge ITC, Kasneci E, Nystrom M. The impact of slippage on the data quality of head-worn eye trackers. *Behavior Research Methods*. 2020;52(3):1140-1160. doi:10.3758/s13428-019-01307-0
17. van Rossum G. Python tutorial. Centrum voor Wiskunde en Informatica (CWI), Amsterdam; 1995.
18. Harris CR, Millman KJ, van der Walt SJ, et al. Array programming with NumPy. *Nature*. 2020;585(7825):357-362.
19. McKinney W. Data structures for statistical computing in python. *Proceedings of the 9th Python in Science Conference*. 2010;445:51-56.
20. Bradski G. The OpenCV Library. *Dr Dobb's Journal: Software Tools for the Professional Programmer*. 2000;25(11):120-123.

21. Virtanen P, Gommers R, Oliphant TE, et al. SciPy 1.0: Fundamental algorithms for scientific computing in Python. *Nature methods*. 2020;17(3):261-272.
22. Hunter JD. Matplotlib: A 2D graphics environment. *Computing in Science & Engineering*. 2007;9(03):90-95.
23. Juhola M. Median filtering is appropriate to signals of saccadic eye movements. *Computers in Biology and Medicine*. 1991;21(1-2):43-9. doi:10.1016/0010-4825(91)90034-7
24. Olsen A. The Tobii I-VT fixation filter. *Tobii Technology*. 2012;21:4-19.
25. Larsson L, Nystrom M, Ardo H, Astrom K, Stridh M. Smooth pursuit detection in binocular eye-tracking data with automatic video-based performance evaluation. *Journal of Vision*. 2016;16(15):20. doi:10.1167/16.15.20
26. Komogortsev OV, Gobert DV, Jayarathna S, Gowda SM. Standardization of automated analyses of oculomotor fixation and saccadic behaviors. *IEEE Transactions on Biomedical Engineering*. 2010;57(11):2635-2645.
27. Costela FM, Otero-Millan J, McCamy MB, et al. Fixational eye movement correction of blink-induced gaze position errors. *PLoS One*. 2014;9(10):e110889. doi:10.1371/journal.pone.0110889
28. Orquin JL, Ashby NJ, Clarke AD. Areas of interest as a signal detection problem in behavioral eye-tracking research. *Journal of Behavioral Decision Making*. 2016;29(2-3):103-115.
29. Engmann S, t Hart BM, Sieren T, Onat S, Konig P, Einhauser W. Saliency on a natural scene background: effects of color and luminance contrast add linearly. *Attention, Perception, & Psychophysics*. 2009;71(6):1337-52. doi:10.3758/APP.71.6.1337
30. Salvucci DD, Goldberg JH. Identifying fixations and saccades in eye-tracking protocols. *Proceedings of the 2000 symposium on Eye tracking research & applications*. 2000:71-78.
31. Green-Armytage P. A colour alphabet and the limits of colour coding. *Journal of the International Colour Association*. 2010;5
32. Susac A, Bubic A, Planinic M, Movre M, Palmovic M. Role of diagrams in problem solving: An evaluation of eye-tracking parameters as a measure of visual attention. *Physical Review Physics Education Research*. 2019;15(1):013101.
33. Vansteenkiste P, Cardon G, Philippaerts R, Lenoir M. Measuring dwell time percentage from head-mounted eye-tracking data--comparison of a frame-by-frame and a fixation-by-fixation analysis. *Ergonomics*. 2015;58(5):712-21. doi:10.1080/00140139.2014.990524
34. Bonikowski L, Gruszczyński D, Matulewski J. Open-source software for determining the dynamic areas of interest for eye tracking data analysis. *Procedia Computer Science*. 2021;192:2568-2575.

Supplementary Video 1 and 2

Supplementary Table S3

Table S3. Calculated dwell time percentage (%) for different AOI margins (median (IQR))

	0°	0.5°	1.0°	1.5°	2.0°	2.5°	3.0°
Car1	72.9 (63.0-88.9)	82.9 (73.9-91.3)	91.0 (77.7-94.0)	91.1 (77.7-94.6)	92.6 (77.9-95.6)	92.6 (78.8-95.6)	92.6 (79.8-95.6)
Car2	59.5 (39.5-75.8)	91.0 (70.0-97.4)	94.7 (89.7-98.5)	96.8 (94.9-98.7)	96.8 (95.0-98.7)	96.9 (95.1-98.7)	96.9 (95.1-98.7)
Cyclist1	47.3 (25.4-57.6)	64.7 (38.2-87.8)	73.3 (49.0-93.5)	83.6 (57.1-95.5)	84.7 (61.0-96.0)	85.4 (66.5-96.0)	85.7 (79.4-96.0)
Cyclist2	48.1 (35.2-75.3)	83.1 (61.3-91.7)	89.1 (76.1-97.2)	91.1 (81.6-99.1)	93.0 (82.5-100.0)	94.4 (82.5-100.0)	95.2 (82.5-100.0)
Cyclist3	48.7 (31.5-76.4)	85.7 (73.6-92.7)	92.9 (87.8-96.8)	96.8 (92.7-100.0)	96.8 (92.7-100.0)	96.8 (94.4-100.0)	97.4 (94.7-100.0)
Cyclist4	32.3 (18.8-58.5)	86.5 (47.1-92.7)	91.0 (82.9-98.8)	95.4 (91.0-98.8)	95.4 (91.5-99.2)	95.5 (92.0-99.4)	95.5 (92.0-99.4)
Pedestrian1	73.0 (44.2-82.6)	88.8 (77.7-97.4)	92.6 (83.8-98.3)	93.4 (88.8-98.8)	93.7 (88.8-99.8)	93.7 (88.8-99.8)	93.7 (88.8-99.8)
Roadsign1	37.3 (19.2-54.9)	84.5 (73.1-87.2)	93.7 (87.3-98.7)	93.7 (90.0-98.7)	93.7 (91.5-98.7)	93.7 (91.5-98.7)	96.6 (92.8-99.2)
Roadsign2	1.7 (0.1-7.1)	65.0 (26.8-85.1)	91.4 (80.3-97.1)	98.2 (84.6-99.9)	98.4 (84.7-99.9)	98.4 (87.6-99.9)	98.4 (89.6-99.9)
Scooter1	35.1 (23.5-42.9)	77.8 (44.8-97.1)	92.1 (71.7-99.1)	92.1 (77.0-100.0)	92.4 (85.9-100.0)	92.5 (87.7-100.0)	93.0 (87.8-100.0)
Scooter2	9.0 (2.9-20.5)	84.8 (70.3-93.8)	95.9 (89.0-99.2)	97.2 (93.4-99.9)	98.5 (96.0-99.9)	99.2 (97.6-99.9)	99.2 (97.6-99.9)
Trafficlight1	32.2 (9.0-41.6)	78.8 (68.2-90.5)	91.8 (82.6-96.2)	93.6 (88.2-98.3)	94.9 (88.2-98.3)	96.2 (88.2-98.3)	96.2 (88.2-98.6)
Van1	60.3 (51.8-80.6)	62.0 (52.1-80.6)	67.5 (52.1-80.6)	73.2 (52.6-80.6)	76.4 (53.6-80.6)	78.4 (54.1-81.6)	78.6 (54.1-83.1)

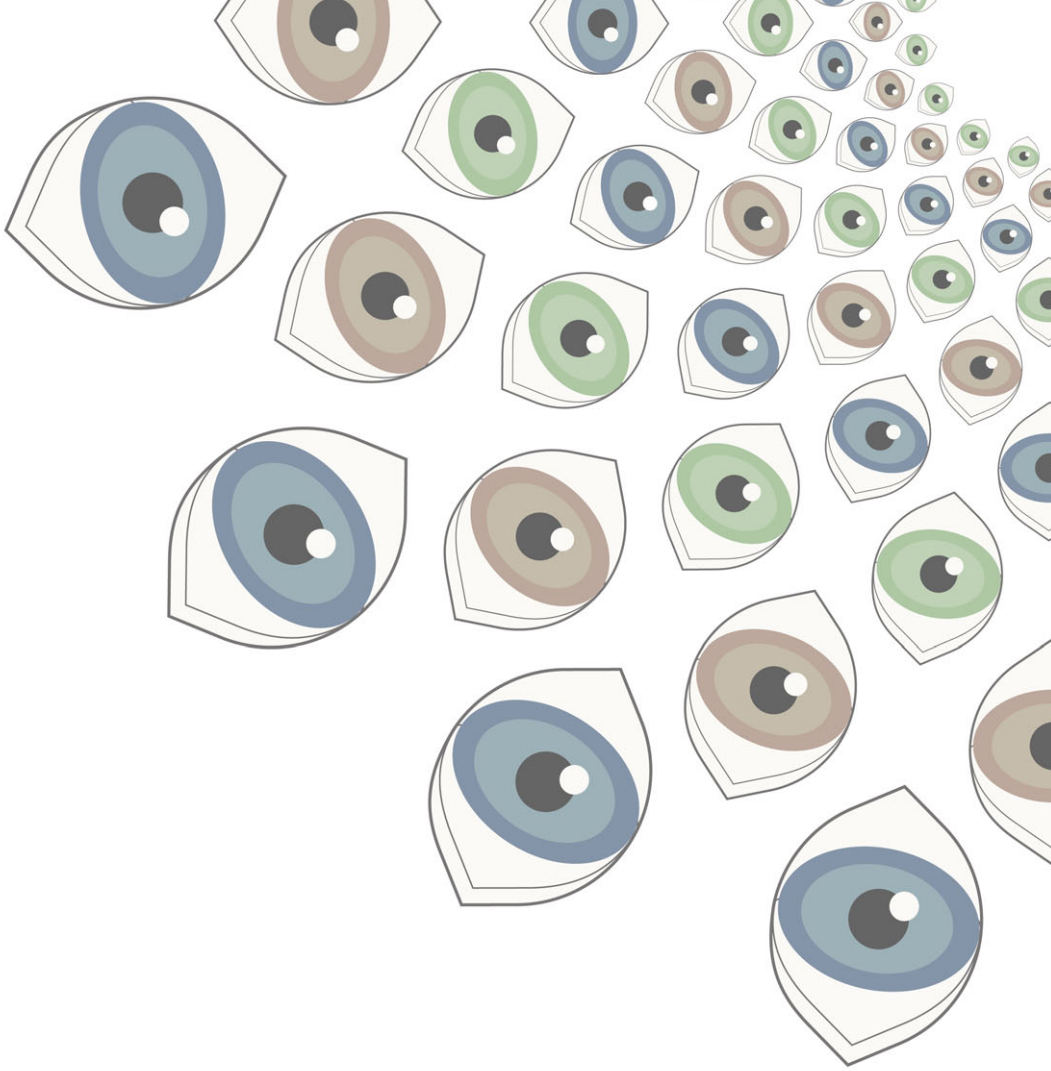

Chapter 4

TREYESCAN: Configuration of an Eye Tracking Test for the Measurement of Compensatory Eye Movements in Patients with Visual Field Defects

Y Faraji, JW van Rijn, RMA van Nispen, GHMB van Rens, BJM Melis-Dankers, J Koopman & LJ van Rijn

Scientific Reports, 2023; 13:20479

Abstract

The Traffic Eye Scanning and Compensation Analyzer (TREYESCAN) is introduced as an innovative eye tracking test designed to measure compensatory eye movements in individuals with visual field defects. The primary objective of the test is to quantitatively assess and analyze the compensatory eye movements employed by patients with visual field defects while viewing videos of various traffic scenes from the viewpoint of a driver of a passenger car. The filming process involved capturing a wide range of driving conditions and hazards, aiming to replicate real-world scenarios. Specific dynamic areas of interest within these scenes were selected and assessed by a panel of experts on medical and practical fitness to drive. Pilot measurements were conducted on a sample of 20 normally-sighted individuals during two different measurement sessions. The results provide valuable insights into how individuals without visual impairment view the dynamic scenes presented in the test. Moving forward, the TREYESCAN will be used in a case–control study involving glaucoma patients and control subjects, with the goal of further investigating and understanding the mechanisms employed by individuals with glaucoma to compensate for their visual field defects.

Introduction

Primary open-angle glaucoma (POAG) is the leading cause of irreversible blindness in the world,[1] characterized by progressive damage to the optic nerve and consequent visual field loss.[2] The impact of this condition significantly affects the daily lives and independence of those affected.[3,4] Driving and mobility, in particular, are crucial aspects that contribute to an individual's quality of life and sense of autonomy.[5] The current method of static visual field testing does not properly discriminate between persons with visual field defects that are fit and unfit to drive.[6] Merely testing visual field defects does not reflect the impairment of those affected since defects may be compensated for, such as by head and eye movements.

While previous studies have explored compensatory eye movements in persons with glaucoma during on-road driving,[7,8] driving simulator tests,[9,10] and hazard perception tests,[11,12] a knowledge gap remains regarding the mechanisms by which these patients use head and eye movements to compensate for their visual field defects. This is particularly relevant in the context of dynamic areas of interest (AOIs) within traffic scenes, which refer to specific regions of a stimulus that are relevant for the research objective. AOIs are utilized to measure various metrics such as AOI hits, which occur when gaze coordinates fall within an AOI.[13] The analysis of dynamic AOIs, which refer to moving regions of interest that emerge during video presentations or animated elements on a screen, presents a challenge due to the movement of these objects relative to the coordinate system in which the gaze position data is recorded.[14] Existing research has primarily focused on fixations and saccades, without exploring the relevance of viewing AOIs. Investigating AOI hits, entry times and dwell times can improve the analysis of compensatory eye movements. For instance, establishing a correlation between the frequency of saccades and AOI hits, could shed light on the quality of compensatory eye movements in persons with visual field loss. Exploring these compensatory mechanisms is of importance, as they play a crucial role in helping individuals with visual field defects in overcoming visual limitations and maintaining functional performance in visually demanding situations, like driving.

To bridge this research gap, we have developed an innovative eye tracking test, the TREYESCAN (Traffic Eye Scanning and Compensation Analyzer), with the objective of measuring compensatory eye movements in patients with visual field defects. The TREYESCAN measures eye movements over a wide field of view (100°), recognizing the vital role played by the visual field in safe traffic participation.[15] Given that visual field defects may reside in the periphery, it is apparent that eye movements need

to be assessed on a large screen, rather than solely focusing on a small centrally located monitor, covering approximately 30º. Additionally, transportation research has highlighted that a restricted field of view of driving scenes (presented on a single monitor) can lead to poorer hazard detection and less eccentric eye movements compared to setups involving additional side views on adjacent monitors.[16,17] Consequently, we developed an accessible method for analyzing eye movements on a screen with a wide field of view (100°), while accommodating unrestricted head and eye movements.

This study introduces the methodology employed in the development of the TREYESCAN. We provide insights into the process of traffic scene selection and identification of areas of interest within the videos. We carefully curated a diverse range of traffic scenarios, encompassing various driving conditions and potential hazards. Additionally, we investigate the results obtained from pilot measurements conducted on a group of normally sighted individuals. By examining the gaze behavior and eye movements of individuals with normal vision, we gain a baseline understanding of how individuals without visual field defects interact visually with the dynamic scenes presented in our test.

Methods

Experiment Setup, Recording Device and Analysis Software

The present study employed an experimental setup and methodology that we described in a previously published work.[18] The experiment took place at Amsterdam University Medical Centers (UMC), location VU University Medical Center (VUmc), and utilized three 24-inch HP EliteDisplay E243i monitors with a resolution of 1920 × 1200 pixels and a pixel density of 94.34 ppi. Participants sat in a car seat positioned 65 cm away from the screens to achieve a 100° field of view, while the table could be adjusted in height to ensure that the eyes were centered on the middle of the screen (Fig. 1). Head movements were permitted in all directions during the experiment.

The participants' eye movements were recorded by a head-mounted eye tracking device (Pupil Labs Core glasses, received October 2021, Pupil Labs, Berlin, Germany).[19] The Surface Tracker plugin by Pupil Labs was used to define the surface area of the display with apriltags, which are QR-like markers.[20] This allows the gaze to be mapped on the screen surface, thus obtaining screen-based gaze coordinates with a head-mounted eye tracker.

Figure 1. TREYESCAN setup.[18] **A**. Picture of setup. Participants are seated in front of the display monitors while wearing the Pupil Core eye tracker. The individual depicted in the image is not a study participant and has provided consent for the publication of the image. **B.** Schematic overview of the set-up (view from above). The participant is located 65 cm in front of the central display monitor. The examiner is located on the right of the participant and can guide the experiment from the host monitor. On the MacBook display stability of the signal and performance of the participant could be monitored.

The data were exported using Pupil Labs Player v3.3.0, and dynamic area of interest analyses were performed using the TREYESCAN Toolkit software,[18,21] written in Python 3.8.3[22] using NumPy,[23] Pandas,[24] OpenCV,[25] Matplotlib,[26] and SciPy.[27]

Traffic Scenes

Two different driving routes, each with an approximate duration of 30 min, were collaboratively designed with the CBR (Dutch driving test organization), the central office for driver's license administration in The Netherlands. These routes were specifically selected in the city of Amsterdam, characterized by its urban environment with narrow streets, thereby presenting complex and challenging traffic scenarios. Each route was driven five times.

Video footage was captured using a Sony A7III camera equipped with a Laowa Zero-D ultra-wide field 12 mm f/2.8 lens (angle of view: 121.96°; minimal distortion) from within a moving Toyota Prius II vehicle. The camera was mounted centrally behind the windshield, and a black piece of felt was placed on the dashboard to prevent reflections (Fig. 2A). The footage was captured in 4 K resolution (3840 × 2160) at 25 frames per second. The video clips were subsequently expanded and cropped to a resolution of 5760 × 1200 using Adobe Premiere Pro (Adobe Inc, San Jose, CA, USA) to fit the three-screen setup (Fig. 2B).

The video content was analyzed to identify relevant traffic scenarios, that require the driver's attention, while also ensuring that objects were included from diverse directions in the peripheral visual field. To minimize memory recollection effects, for each traffic scene, a duplicate scene was chosen that contained the same part of the route driven, but with different objects. Finally, a total of 42 traffic scenes were selected and compiled into 6 videos of approximately 8 min each.

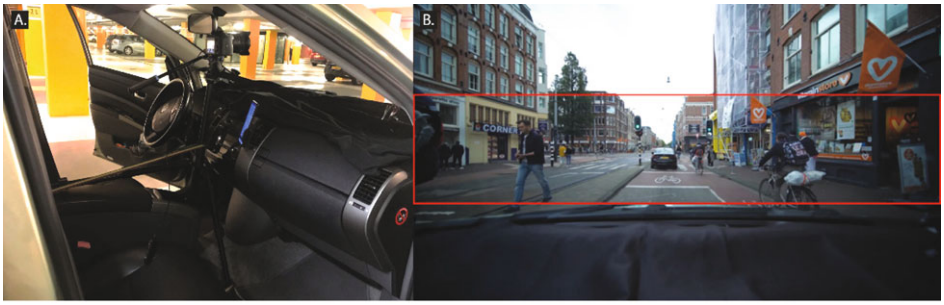

Figure 2. Recording and editing of traffic scenes. **A**. The car and camera setup. **B.** Indication of crop to 5760 × 1200. The full width of the video was used. No information about the traffic scene was lost by cropping the video's height to facilitate screen fitting.

AOIs

In order to determine which objects were relevant to the analysis, a panel of 10 raters comprising 5 experts on practical fitness to drive of the CBR and 5 experienced drivers with knowledge of conducting traffic-related research and/or patient assessment (co-authors RvN, GvR, BM, JK, and LvR), were presented with the 6 videos. The panel had 42.5 (median, IQR [34.0–43.8]) years of driving experience. A web application was developed to enable raters to individually indicate dynamic AOIs in the video by mouse clicks (the source code for this application is available as open-source code on Github[28]: https://github.com/treyescan/marking-aois). The application included options to view

in different speed settings, play/pause and rewind the videos. The raters had to choose between two categories, Must-Be-Seen and May-Be-Seen objects. The former included objects that necessitate active or passive consideration by the driver, such as reducing speed, changing lanes and delaying acceleration, while the latter included objects that are relevant to be seen by a driver but do not require a change in driving behavior, such as pedestrians on the sidewalk and oncoming traffic in the other lane.

Figure 3 presents a heatmap of the distribution of all mouse clicks of the 10 raters for the 6 videos. Notably, most clicks were made in the central part of the screen. The results of the 10 raters were manually coded for each scene in the six videos by observing the videos with an overlay of circle animations representing the location of the clicks. An object was included as a relevant AOI if it was rated by 5 or more raters. If an object was chosen by 4 raters, a panel reviewed its inclusion. The majority of raters determined whether an object was Must-Be-Seen or May-Be-Seen. Traffic lights were included in all cases. A new AOI was incorporated when there was a change in the color of the traffic lights or when the brake lights of a car were activated.

The Dynamic allocation of AOIs was performed using tools that were previously described in our published work.[18] These tools enabled us to determine the location of each AOI for every frame of the video, tracking them from their initial appearance to their disappearance. The TREYESCAN software allows for the addition of margins around the areas of interests, in order to compensate for the inaccuracy of the eye tracker. A margin size of 2.5° was chosen for the analysis.

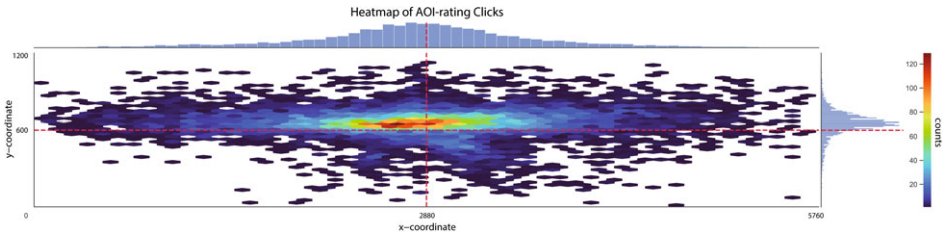

Figure 3. Heatmap of the distribution of all mouse clicks made by the 10 raters for the 6 videos. Dimensions of heatmap represent the dimensions of the video screen. Histograms of distributions of amount of clicks are shown for the x- and y-axis.

Measurements in Normal-Sighted Individuals

The recruitment of normally-sighted participants was done through snowball sampling. Eligibility criteria required participants to have no history of ophthalmic comorbidities and at least 5 years of driving experience. The participants performed

an Esterman visual field test[29] and a visual acuity measurement using the ETDRS chart.[30] Additionally, a customized central visual field test was programmed using the Humphrey Field Analyzer II (HFA). The test employed a three-zone strategy, with an age-corrected test mode according to HFA routines, a III white stimulus, 80 points, and a point spacing of 2°. Its purpose was to screen the central 10° binocularly for any potential visual field defects, as the Esterman visual field test does not measure this area. Only participants with a minimal visual acuity of 0.0 LogMAR (20/20 Snellen or 1.0 decimal notation) and no defects on the visual field tests were included in the study. Participants with multifocal prescription glasses were excluded.

During the experiment, the participants' eye movements were recorded while they viewed the six videos with traffic scenarios. Following the viewing of three videos, a scheduled intermission was provided, allowing participants to take a break. During this intermission, participants were asked if they had any feedback on the setup, videos, or their experience during the test. The researcher conducting the experiment documented any feedback provided verbally. After all videos had been viewed, the same question was asked to ascertain if participants had supplementary insights or comments contributing to their previously offered feedback. To isolate the visual aspect of the task, the videos were presented without accompanying traffic sounds. The participants were instructed to imagine themselves as the driver of the vehicle and to press a button whenever they identified an object that required action, such as reducing speed or changing lanes. This instruction was given to avoid the interference caused by providing a verbal commentary during concurrent hazard perception tasks.[31] Before each video, a nine-point screen calibration was conducted, followed by a 12-point validation routine, which both extended across the entire screen.[18] The Pupil Labs software then generates a value for the accuracy and precision of the calibration. During the calibration process, we set a target accuracy threshold of less than 2.5°, in line with the specifications provided in the Pupil Labs documentation, which indicates that 3D Gaze Mapping should achieve an accuracy range of 1.5° to 2.5°. When the initial calibration did not meet this accuracy requirement, two additional calibration attempts were performed. After the third calibration, the accuracy value obtained was accepted, also when it exceeded 2.5°.

Following a four-week interval, the participants underwent a second viewing of the videos in a different order to gather data from two separate instances. A randomization tool was employed to determine the viewing order, which could be presented as either 123–456 or 456–123. During the second measurement session,

the participant was presented with the opposite viewing order from their initial session. The use of this time interval, coupled with the inclusion of duplicate scenes, was intended to reduce potential recall bias.

All procedures involved in collecting and analyzing data from human subjects were conducted in accordance with the ethical standards of the 1964 Declaration of Helsinki and its subsequent amendments. The experimental protocol was officially approved by the Medical Ethical Committee of Amsterdam UMC, location VUmc (METC Number: 2020.475). All participants provided informed consent prior to participation. The individual depicted in Fig. 1A was not a study participant and has provided informed consent for the publication of the image in an online open access publication.

Determining the Contents of TREYESCAN

The included participants viewed 6 videos of approximately 8 min on two measurement sessions. For the next study stage, a case–control study with glaucoma patients, the objective is to create a test consisting of the most effective scenes. To determine which videos should be included in the final test, a stepwise approach was used, based on the feedback of the included participants and the traffic scene characteristics.

Determining the Relevant AOIs to Include in TREYESCAN

The data obtained from this pilot study will be used to determine the most relevant AOIs for inclusion in the subsequent phase of analysis in the case–control study. We hypothesize that the included normally sighted participants with considerable driving experience, have a good understanding of where their visual focus should lie within the traffic scenes. Consequently, it would be inappropriate to evaluate the patient population in later stages using AOIs that are not looked at by normally sighted individuals. To address this, we propose that an AOI should be included if it has been viewed, arbitrarily, by at least half of the participants.

On the other hand, when conducting AOI analyses in eye tracking, it is important to consider entry time — the duration from the onset of the stimulus until the AOI is first viewed.[13] We observed that certain AOIs do not require a deliberate saccade movement to be immediately “hit”, due to a (close to) central location or added margins. Consequently, it would be unfair to compare entry times for objects in the case–control study that are consistently and falsely “hit” by most participants in this

pilot study. To address this issue, we decided to exclude AOIs that start in the central 10º of the screen. Our findings indicate that AOIs originating within the central 10º are predominantly objects in the oncoming lane, which start at a small size and therefore obtaining large margins. Consequently, these AOIs do not capture deliberate gaze behavior since they are immediately and falsely "hit" when looking at the road ahead.

Similarly, we have also encountered other objects starting within the central screen of the setup that exhibit similar characteristics. For the object appearing between the central 10º and 30º, we have introduced an additional variable, namely entry time. We identified AOIs with a short entry time, taking into account previous research indicating that a natural saccade latency of 120–150 ms occurs with everyday stimuli and environments. Hence, we set a threshold of 120 ms for the median entry time of all participants, enabling us to select only deliberate saccades to these AOIs.[13,32,33] The use of median entry time was necessary due to the skewed distribution of entry times. If an object appeared within the central 10º to 30º and had an entry time shorter than 120 ms it would be marked for exclusion in that measurement session (T1 or T2).

In summary, the exclusion of an AOI was determined based on the following criteria for each for each measurement session separately: (1) if it was observed by less than half of the participants, (2) if its appearance was within the central 10º, and (3) if its appearance was within the central 10°–30° and the median entry time was shorter than 120 ms. If any of these criteria were met, the AOI was considered for exclusion in that particular measurement session. Only when an AOI satisfied the exclusion criteria in both measurement sessions, it was generally marked for exclusion.

Results

Participant Characteristics

A total of twenty participants, with a median age of 34.0 years (IQR [26.0–56.0]), were included in the study. These individuals viewed the six videos with traffic scenes on two measurement sessions separated by a four-week interval. Logistical constraints prevented one participant from participating in the second measurement session.

Table 1 presents the participant characteristics and measurement details. All participants had a minimum of five years of driving experience, showing a wide range of experience, distance traveled, and frequency of days driven per month. The randomization process ensured an equal distribution of the viewing order among

participants. None of the participants had any visual impairments, and none self-reported the use of medication that could affect responsiveness and concentration.

Figure 4 displays the accuracy and precision measurements derived from the calibration and validation process. The majority of these values lay within the accuracy range specified by Pupil Labs, which is 1.5°–2.5°.

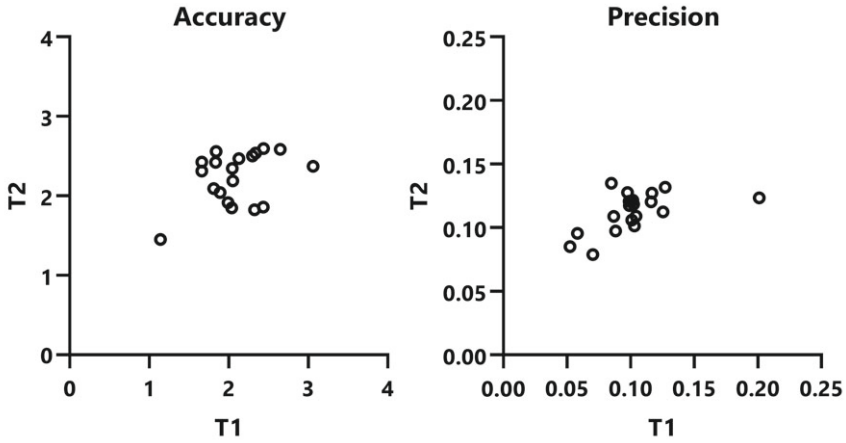

Figure 4. Scatterplots of mean accuracy and precision values as provided by the Pupil Labs validation routine. These measurements were taken prior to the presentation of each video, and the mean values were derived from the six accuracy and precision measurements conducted during a single measurement session.

Table 1. Participant characteristics and measurement details

	***n* = 20**
Age (year) median [IQR]	34.0 [26.0 to 56.0]
Number of female participants (N)	14
Binocular visual acuity (logMAR) median [IQR]	-0.1 [-0.1 to -0.03]
Esterman visual field abnormalities (N)	0
Prescription eyeglasses (N)	1
Contact lenses (N)	1
Education (years) median [IQR]	16.0 [15.0 to 16.0]
Driving experience (years) median [IQR]	15.0 [7.1 to 36.3]
Distance driven per month (km) median [IQR]	200.0 [100.0 to 837.5]
Days driven per month (days) median [IQR]	10.0 [3.3 to 20.0]
Accident involvement	
- Number of accidents with injury	1
- Number of accidents without injury	2
Video order randomization, first measurement:	
- 123 – 456	9
- 456 - 123	11

Table 2. Ratios of time spent in a region to total video length (mean ± SD)

	All measurements (*n* = 234)	T1 measurements (*n* = 120)	T2 measurements (*n* = 114)
Central 10°*	0.376 ± 0.105	0.378 ± 0.101	0.373 ± 0.109
Central 20°*	0.565 ± 0.116	0.573 ± 0.107	0.557 ± 0.125
Central 30°*	0.675 ± 0.111	0.683 ± 0.099	0.667 ± 0.122
Entire screen	0.851 ± 0.106	0.856 ± 0.086	0.846 ± 0.123
Left side	0.462 ± 0.093	0.474 ± 0.086	0.449 ± 0.098
Right side	0.389 ± 0.072	0.381 ± 0.066	0.398 ± 0.076
Top half	0.223 ± 0.153	0.212 ± 0.156	0.235 ± 0.150
Bottom half	0.628 ± 0.170	0.644 ± 0.175	0.611 ± 0.162

*Diameter is 10, 20 or 30 degrees.

Screen Regions

Table 2 presents the ratios of time spent in different regions of the total screen (three monitors together) to the total video length. Approximately 85% of the total time (0.851 ± 0.106) was dedicated to observing the entire screen, since gaps due to blinking and instances when participants looked away from the screen were not considered as valid gap samples; 85% is considered a reliable outcome for valid gaze samples.[13]

Furthermore, over 50% of the observation time was focused on the central 20° region of the screen (0.565 ± 0.116). This pattern was consistent across both the T1 and T2 measurement sessions. Additionally, participants tended to spend more time on the left side and the bottom half of the screen. The similarity observed between the T1 and T2 measurements indicates a valid reproducibility of the time spent in specific regions.

Qualitative Participant Experience

Following the experiment, participants were asked to provide feedback regarding their experience with the tasks. Participants complimented the realism of the traffic scenes, the setup, and the clarity of the task. Several participants reported experiencing feelings of dizziness or nausea during the tasks, particularly at scenes with unexpected fast turns or when moving over speed bumps. The symptoms of simulator sickness did not prevent participants to finish watching all videos within a single measurement session. Another limitation that participants highlighted was the absence of side- and rearview mirrors, especially when objects came into view from behind the vehicle, resulting in a startled sensation. Additionally, participants reported challenges in estimating the speed and direction of the vehicle, due to the

absence of provided information during the tasks and their role as passive observers rather than actively driving. Furthermore, participants expressed that the duration of the task, which involved watching six videos of eight minutes, was quite tiring.

Qualitative Filtering

Based on the participants' feedback and their reported experiences, we made the decision to select the most suitable scenes for the final TREYESCAN tasks (two videos of approximately eight minutes). The selection process took into account both participant feedback and specific characteristics of the scenes. The scenes were chosen in the following order, as described in Fig. 5.

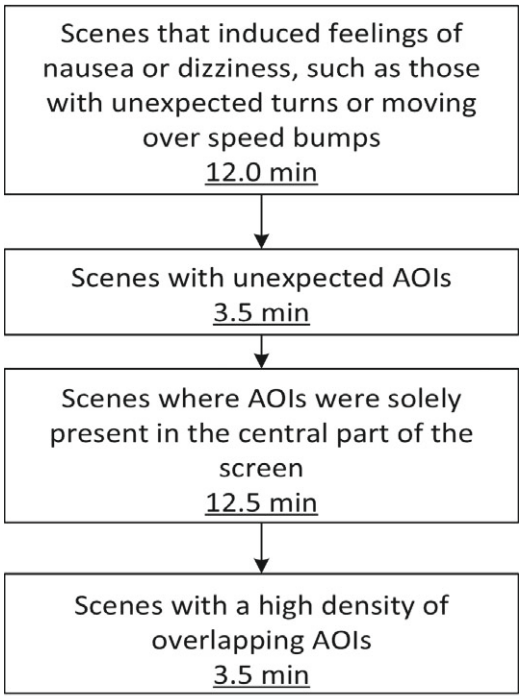

Figure 5. Excluded (parts of) Scenes with Duration of Removal. (1) Parts of scenes with turns and speed bumps were entirely removed. In cases where only the initial or final segment of a scene featured a turn, that specific portion was removed, while the remainder of the scene was retained for subsequent analysis. (2) Scenes or portions were excluded if they included objects entering the view from behind the vehicle. Such instances could provoke a startled sensation among participants, as these objects were not anticipated through the use of side mirrors. (3) After implementing the above-mentioned exclusion steps, certain scenes no longer contained any peripheral AOIs and were confined solely to the central region of the screen. These scenes were subsequently removed from the analysis due to the limited potential for measuring compensatory eye movements. (4) Certain scenes exhibited a high density of relevant AOIs intersecting with one another. To simplify the subsequent AOI analysis, these scenes or parts of scenes were excluded.

AOI Selection

Subsequently, the AOIs within the scenes that remained in the TREYESCAN were further analyzed. The first column in Table 3 displays the distribution of the 325 AOIs across different categories. Out of these, 165 of these AOIs were classified as Must-Be-Seen objects, while 160 were categorized as May-Be-Seen objects.

Figure 6 illustrates the median entry time and the number of participants who did not view an AOI for all cyclists objects during the T1 and T2 measurements, as an example. Notably, median entry times for each object are similar for the T1 and T2 measurement sessions, indicating consistent results.

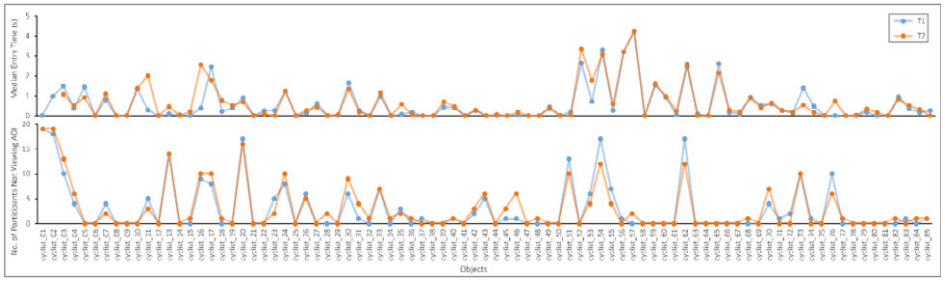

Figure 6. A. Graph representing the median time to first entry for the T1 (Blue) and T2 (Orange) measurements for all the cyclist objects. **B.** Graph representing the number of participants not viewing an AOI for all the cyclists for the T1 and T2 measurements.

The remaining AOIs were analyzed based on the number of participants who viewed them, their location on the screen, and the entry time, as described in the methods section. Table 3 provides an overview of the exclusion process and portrays the number of AOIs that would be excluded based on each criterion. Notably, while several car AOIs are excluded, a higher proportion of cyclist and pedestrian AOIs remain in the analysis. By applying these exclusion criteria, a total of 124 AOIs out of the initially marked 325 AOIs would remain in the analysis in further phases. Among these 124 remaining AOIs, 64 are categorized as Must-Be-Seen objects and 60 as May-Be-Seen objects.

Table 3. Selection of AOIs

	AOIs before selection	AOI <10°	*n* < 10		AOI 10°-30° & ET <120ms		Excluded AOIs after selection		
			T1	T2	T1	T2	T1	T2	T1 & T2
Ambulance[a]	1	0	0	0	1	1	1	1	1
Barricade	1	1	0	0	0	0	1	1	1
Bus	2	1	0	0	0	0	1	1	1
Car	69	43	3	4	10	8	56	55	54
Cyclist	85	28	7	7	14	10	48	45	42
Motorcycle	16	6	0	0	3	4	9	10	9
Pedestrian	85	33	7	5	20	14	57	52	49
Police[a]	2	1	0	0	0	0	1	1	1
Sign	6	3	0	0	1	0	4	3	3
Traffic light	37	25	1	0	3	5	28	30	27
Tram	4	1	0	0	1	2	2	3	2
Truck	4	2	0	0	0	0	2	2	2
Van	13	8	0	0	3	2	11	10	9
Total AOIs	325	152	18	16	56	46	221	214	201

[a] Ambulance and police vehicles did not have emergency vehicle signals activated.
AOI < 10°: AOIs that start within central 10°. N < 10: AOIs that have been viewed by less than 10 participants. AOI 10°–30° & ET < 120 ms: AOIs that start within central 10° to 30° and median entry time is < 120 ms.

Video Examples

In the supplementary material S1 (Video Cyclist_6), S2 (Video Cyclist_7), and S3 (Video Cyclist_54), three videos of the task are provided with the gaze data and AOIs with margins of 2.5°. Video S1_Cyclist_6 serves as an example of an AOI that was excluded based on a short median entry time. Due to the margins and central appearance of the AOI, the entry time was marked as 0 for many participants (median entry time T1: 0 s, median entry time T2: 0 s). Video S2_Cyclist_7 is an illustrative example of a relevant AOI since the median entry time accurately reflects a deliberate gaze movement towards it (median entry time T1: 0.795 s, median entry time T2: 1.09). Lastly, video S3_Cyclist_54, represents an AOI located on the far right of the video with minimal participant's gaze towards it (T1: 3 participants, T2: 7 participants). Consequently, it may be justifiable to exclude the marked AOIs in the analysis of the case–control study involving glaucoma patients.

Discussion

The development of the TREYESCAN may initiate a step forward in understanding compensatory eye movements in glaucoma patients during real-world tasks like driving. By employing a wide field of view and incorporating dynamic areas of interest within traffic scenes, we expect that our eye tracking test might address the limitations of traditional visual field testing methods and might provide valuable insights into the visual exploration and hazard perception abilities of individuals with visual field defects. To improve the test, we utilized data obtained from normally sighted individuals to select the most suitable scenes and AOIs for the final version of the TREYESCAN, which will be employed in a case–control study involving glaucoma patients.

Based on participant feedback, scenes featuring rapid turns and high speed bumps were excluded from the TREYESCAN, due to reports of dizziness or a nauseous feeling. However, none of the participants had to discontinue the measurements due to simulator sickness. In a study conducted by Keshavarz, et al.[34], it was found that older adults (age 65+) experienced more simulator sickness than younger adults (age 18–39). It should be noted that the population in our study was relatively young (median age 34.0 years (IQR [26.0–56.0])). In a subsequent phase of the research, which will involve a group of glaucoma patients and age-matched control subjects, it is expected that the participants will be older than this initial group. Therefore, attention must be given to the experiences of this older group concerning simulator-induced sickness.

In our sample, it was observed that participants directed their gaze towards the central 20° of the screen for more than 50% of the total viewing time (0.565 ± 0.116). This remained consistent across both measurement sessions, indicating the absence of a learning effect. A similar finding was reported in a study conducted by Deng, et al.[35], where they found that drivers predominantly focused their attention on the end of the road in front of the vehicle when viewing traffic images. Similarly, Underwood, et al.[36] found that both novice and experienced drivers predominantly fixated on the road far ahead and mid ahead while driving a car. Furthermore, our results revealed that participants allocated more viewing time to the left side of the screen (0.462 ± 0.093) compared to the right side (0.389 ± 0.072), and this pattern also remained consistent across both measurement sessions. As can be seen in Fig. 1, the scenes have been recorded in the center of the front windshield, but as we realized in a later

stadium: unfortunately slightly skewed to the left. This was the case for one of the two routes driven, of which most scenes were included in the 2 final videos. Figure 3 also shows that more AOIs were selected on the left side of the center of the screen. Consequently, resulting in an increased gaze allocation towards the left side of the screen, when focusing on the road ahead. This is a limitation of our traffic scenes that should be taken into consideration when interpreting future results of the case–control study.

In addition, we examined the relevant AOIs that would be suitable for incorporation into the TREYESCAN analysis for the subsequent phase of the case–control study. Prior research by Smith and Mital[37], has demonstrated that initial saccades tend to prioritize fixation on the central region of the screen, regions characterized by high motion and people. It is important to acknowledge that this default gaze pattern may have influenced the participants' visual attention towards the AOIs in our study. It will be interesting to compare the findings in this study with the outcomes derived from the glaucoma patients in the subsequent phase of our research.

The TREYESCAN test demonstrates several strengths that contribute to its utility in assessing compensatory eye movements in individuals with visual field defects, such as glaucoma. By capturing the complexity of realworld driving situations, the test may provide a means to explore how these individuals visually interact with dynamic traffic scenes. The inclusion of a wide field of view and unrestricted head movements addresses visual field defects. This enables participants to utilize their remaining visual field effectively and to explore the traffic scenes naturally. Moreover, the collaboration with experts of practical driving ability and experienced drivers in the development of the test enhances its validity and real-world relevance. Additionally, the pilot measurements conducted with normally sighted individuals establish a valuable baseline, providing a selection for relevant scenes and AOIs, and a reference point for future studies involving glaucoma patients and control subjects.

However, several limitations should be considered. Firstly, simulator sickness experienced by some participants during the test poses a potential challenge that needs to be further investigated in future studies. The absence of side mirrors, rearview mirror and dashboard in the experimental setup may limit the assessment of visual scanning behavior during driving, which may not completely capture the strategies employed by individuals with visual field defects in real-world scenarios. Additionally, the assessment of potential hazards may be influenced by challenges

in accurately estimating vehicle speed and direction, arising from the passive role of observing rather than actively driving.

Moving forward, the TREYESCAN will be applied in a case–control study including glaucoma patients and controls. By comparing the eye movements and gaze patterns of these two groups, we aim to study the compensatory mechanisms employed by individuals with glaucoma. The valuable insights obtained from individuals without a visual impairment in this study, have significantly contributed to refining the test by identifying the most effective scenes and AOIs. Furthermore, these insights have established a baseline understanding of the test's functionality and performance.

Conclusion

This study presents the development and methodology of our novel eye tracking test, the TREYESCAN. We provide insights into the process of traffic scene selection and the identification of AOIs within these dynamic traffic scenarios by an expert rater panel. Pilot measurements conducted on normally sighted individuals have provided valuable insights into the setup's performance and serve as a baseline for understanding gaze behavior and eye movements in the dynamic scenes presented. These results contributed to the selection of relevant AOIs to include in the test. Looking ahead, this research project aims to contribute to a better understanding of how individuals with visual field defects utilize compensatory eye movements to overcome visual limitations, enabling them to maintain functional performance in visually demanding situations such as driving.

References

1. Flaxman SR, Bourne RRA, Resnikoff S, et al. Global causes of blindness and distance vision impairment 1990-2020: a systematic review and meta-analysis. *Lancet Global Health*. 2017;5(12):e1221-e1234. doi:10.1016/S2214-109X(17)30393-5
2. Jonas JB, Aung T, Bourne RR, Bron AM, Ritch R, Panda-Jonas S. Glaucoma. *Lancet*. 2017;390(10108):2183-2193. doi:10.1016/S0140-6736(17)31469-1
3. McKean-Cowdin R, Varma R, Wu J, Hays RD, Azen SP. Severity of visual field loss and health-related quality of life. *American Journal of Ophthalmology*. 2007;143(6):1013-23. doi:10.1016/j.ajo.2007.02.022
4. Freeman EE, Munoz B, West SK, Jampel HD, Friedman DS. Glaucoma and quality of life: the Salisbury Eye Evaluation. *Ophthalmology*. 2008;115(2):233-8. doi:10.1016/j.ophtha.2007.04.050
5. Ramulu P. Glaucoma and disability: which tasks are affected, and at what stage of disease? *Current Opinion in Ophthalmology*. 2009;20(2):92-8. doi:10.1097/ICU.0b013e32832401a9
6. Faraji Y, Tan-Burghouwt MT, Bredewoud RA, van Nispen RMA, van Rijn LJR. Predictive Value of the Esterman Visual Field Test on the Outcome of the On-Road Driving Test. *Translational Vision Science & Technology*. 2022;11(3):20. doi:10.1167/tvst.11.3.20
7. Kasneci E, Sippel K, Aehling K, et al. Driving with binocular visual field loss? A study on a supervised on-road parcours with simultaneous eye and head tracking. *PLoS One*. 2014;9(2):e87470. doi:10.1371/journal.pone.0087470
8. Lee SS, Black AA, Wood JM. Scanning Behavior and Daytime Driving Performance of Older Adults With Glaucoma. *Journal of Glaucoma*. 2018;27(6):558-565. doi:10.1097/IJG.0000000000000962
9. Kubler TC, Kasneci E, Rosenstiel W, et al. Driving with Glaucoma: Task Performance and Gaze Movements. *Optometry and Vision Science*. 2015;92(11):1037-46. doi:10.1097/OPX.0000000000000702
10. Prado Vega R, van Leeuwen PM, Rendon Velez E, Lemij HG, de Winter JC. Obstacle avoidance, visual detection performance, and eye-scanning behavior of glaucoma patients in a driving simulator: a preliminary study. *PLoS One*. 2013;8(10):e77294. doi:10.1371/journal.pone.0077294
11. Lee SS, Black AA, Wood JM. Effect of glaucoma on eye movement patterns and laboratory-based hazard detection ability. *PLoS One*. 2017;12(6):e0178876. doi:10.1371/journal.pone.0178876
12. Crabb DP, Smith ND, Rauscher FG, et al. Exploring eye movements in patients with glaucoma when viewing a driving scene. *PLoS One*. 2010;5(3):e9710. doi:10.1371/journal.pone.0009710
13. Holmqvist K, Andersson R. Eye tracking: A comprehensive guide to methods, paradigms and measures. *Lund, Sweden: Lund Eye-Tracking Research Institute*. 2017;
14. Hessels RS, Benjamins JS, Cornelissen THW, Hooge ITC. A Validation of Automatically-Generated Areas-of-Interest in Videos of a Face for Eye-Tracking Research. *Frontiers in Psychology*. 2018;9:1367. doi:10.3389/fpsyg.2018.01367
15. Owsley C, McGwin G, Jr. Vision impairment and driving. *Survey of Ophthalmology*. 1999;43(6):535-50. doi:10.1016/s0039-6257(99)00035-1
16. Alberti CF, Shahar A, Crundall D. Are experienced drivers more likely than novice drivers to benefit from driving simulations with a wide field of view? *Transportation Research Part F: Traffic Psychology and Behaviour*. 2014;27:124-132.
17. Shahar A, Alberti CF, Clarke D, Crundall D. Hazard perception as a function of target location and the field of view. *Accident Analysis & Prevention*. 2010;42(6):1577-84. doi:10.1016/j.aap.2010.03.016
18. Faraji Y, van Rijn JW, van Nispen RMA, et al. A toolkit for wide-screen dynamic area of interest measurements using the Pupil Labs Core Eye Tracker. *Behavior Research Methods*. 2022;doi:10.3758/s13428-022-01991-5
19. Kassner M, Patera W, Bulling A. Pupil: an open source platform for pervasive eye tracking and mobile gaze-based interaction. *Proceedings of the 2014 ACM international joint conference on pervasive and ubiquitous computing: Adjunct publication*. 2014:1151-1160.
20. Wang J, Olson E. AprilTag 2: Efficient and robust fiducial detection. *2016 IEEE/RSJ International Conference on Intelligent Robots and Systems (IROS)*. 2016:4193-4198.
21. Faraji Y, van Rijn JW. Dynamic AOI Toolkit v1.1.0. Computer software. 2023;doi:https://doi.org/10.5281/zenodo.8029272
22. van Rossum G. Python tutorial. Centrum voor Wiskunde en Informatica (CWI), Amsterdam; 1995.
23. Harris CR, Millman KJ, van der Walt SJ, et al. Array programming with NumPy. *Nature*. 2020;585(7825):357-362.

24. McKinney W. Data structures for statistical computing in python. *Proceedings of the 9th Python in Science Conference*. 2010;445:51-56.
25. Bradski G. The OpenCV Library. *Dr Dobb's Journal: Software Tools for the Professional Programmer*. 2000;25(11):120-123.
26. Hunter JD. Matplotlib: A 2D graphics environment. *Computing in Science & Engineering*. 2007;9(03):90-95.
27. Virtanen P, Gommers R, Oliphant TE, et al. SciPy 1.0: Fundamental algorithms for scientific computing in Python. *Nature methods*. 2020;17(3):261-272.
28. Faraji Y, van Rijn JW. Marking AOIs v1.0.0. Computer software. 2022;doi:https://doi.org/10.5281/zenodo.7022592
29. Esterman B. Functional scoring of the binocular field. *Ophthalmology*. 1982;89(11):1226-1234.
30. Yu HJ, Kaiser PK, Zamora D, et al. Visual Acuity Variability: Comparing Discrepancies between Snellen and ETDRS Measurements among Subjects Entering Prospective Trials. *Ophthalmology Retina*. 2021;5(3):224-233. doi:10.1016/j.oret.2020.04.011
31. Young AH, Crundall D, Chapman P. Commentary driver training: Effects of commentary exposure, practice and production on hazard perception and eye movements. *Accident Analysis & Prevention*. 2017;101:1-10. doi:10.1016/j.aap.2017.01.007
32. Trottier L, Pratt J. Visual processing of targets can reduce saccadic latencies. *Vision Research*. 2005;45(11):1349-54. doi:10.1016/j.visres.2004.12.007
33. White BJ, Stritzke M, Gegenfurtner KR. Saccadic facilitation in natural backgrounds. *Current Biology*. 2008;18(2):124-8. doi:10.1016/j.cub.2007.12.027
34. Keshavarz B, Ramkhalawansingh R, Haycock B, Shahab S, Campos J. Comparing simulator sickness in younger and older adults during simulated driving under different multisensory conditions. *Transportation research part F: traffic psychology and behaviour*. 2018;54:47-62.
35. Deng T, Yang K, Li Y, Yan H. Where does the driver look? Top-down-based saliency detection in a traffic driving environment. *IEEE Transactions on Intelligent Transportation Systems*. 2016;17(7):2051-2062.
36. Underwood G, Chapman P, Brocklehurst N, Underwood J, Crundall D. Visual attention while driving: sequences of eye fixations made by experienced and novice drivers. *Ergonomics*. 2003;46(6):629-46. doi:10.1080/0014013031000090116
37. Smith TJ, Mital PK. Attentional synchrony and the influence of viewing task on gaze behavior in static and dynamic scenes. *Journal of Vision*. 2013;13(8)doi:10.1167/13.8.16

Supplementary Video 1, 2 and 3

Every colored dot represents the gaze of one participant in the first measurement session. Labels with participant id are presented next to the dots. Must-Be-Seen AOIs are depicted as pink/red and May-Be-Seen as light blue/dark blue. Margins of 2.5 degrees are depicted around the AOIs as red or dark blue.

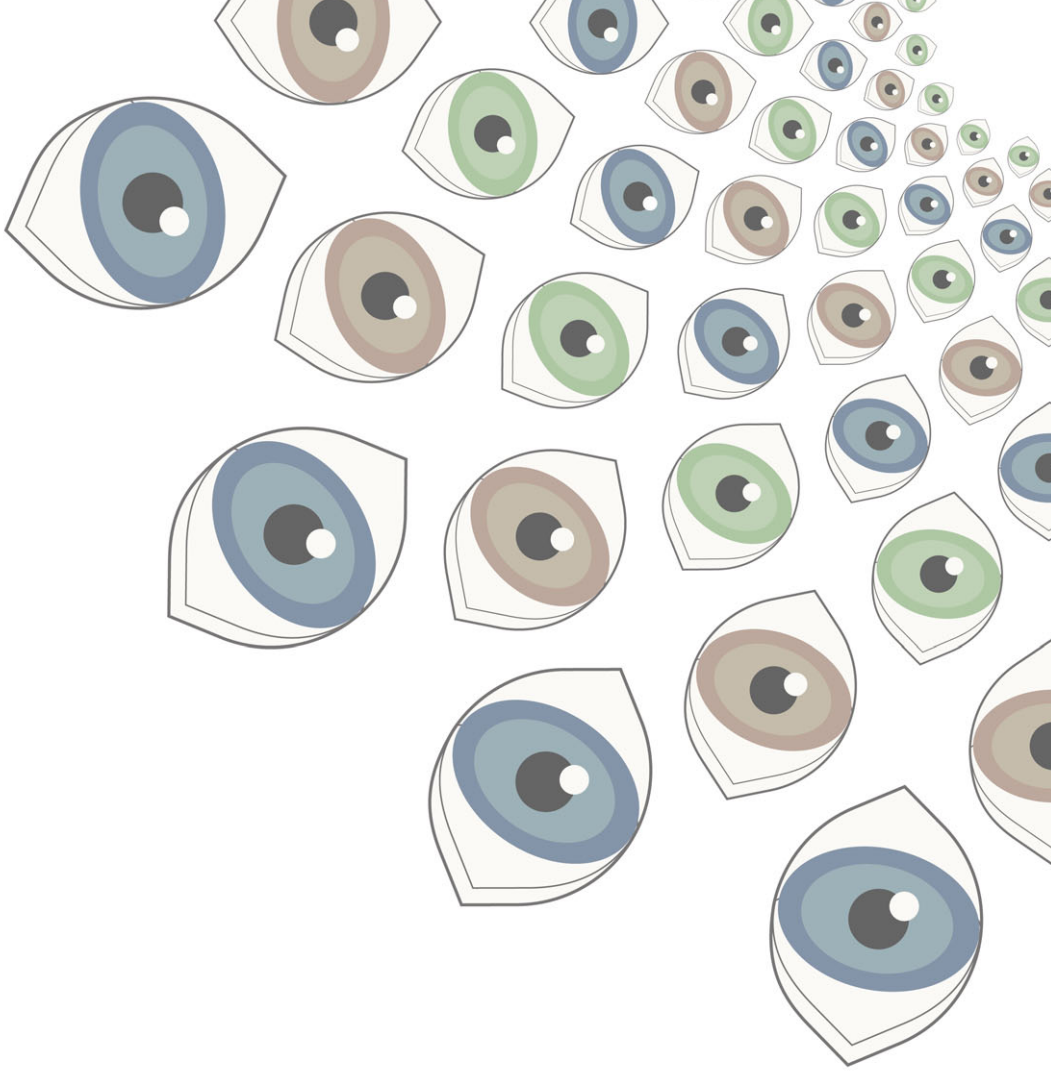

Chapter 5

Traffic Scene Perception Utilizing TREYESCAN: A Comparative Study between Glaucoma Patients and Normally-Sighted Individuals

Y Faraji, JW van Rijn, RMA van Nispen, GHMB van Rens, BJM Melis-Dankers, J Koopman & LJ van Rijn

Manuscript under review

[redacted]

[redacted]

[redacted]

[redacted]

[redacted]

5

[redacted]

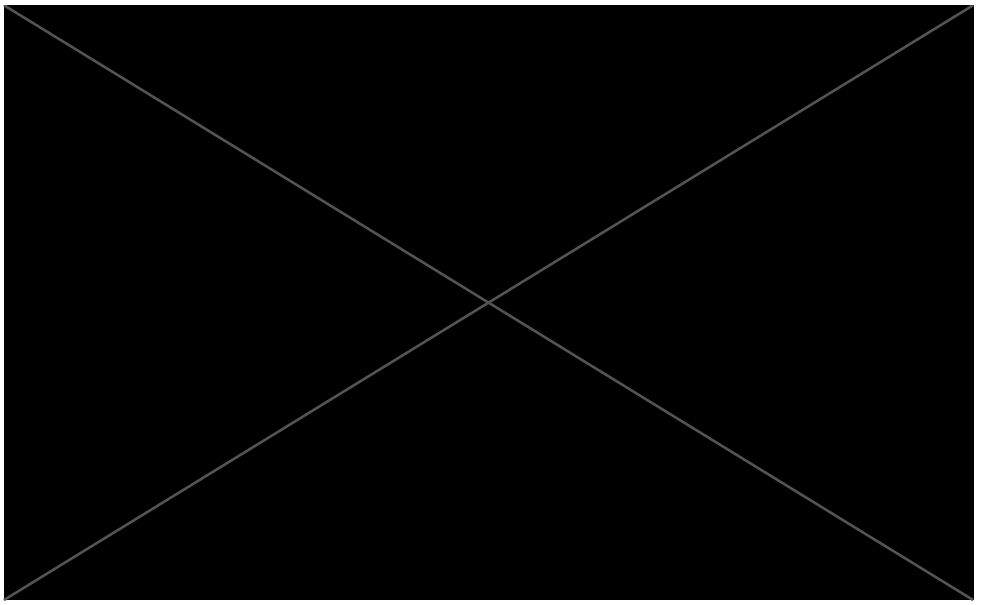

[redacted]

[redacted]

[redacted]

[redacted]

[redacted]

[redacted]

[redacted]

[redacted]

[redacted]

[redacted]

[redacted]

[redacted]

[redacted]

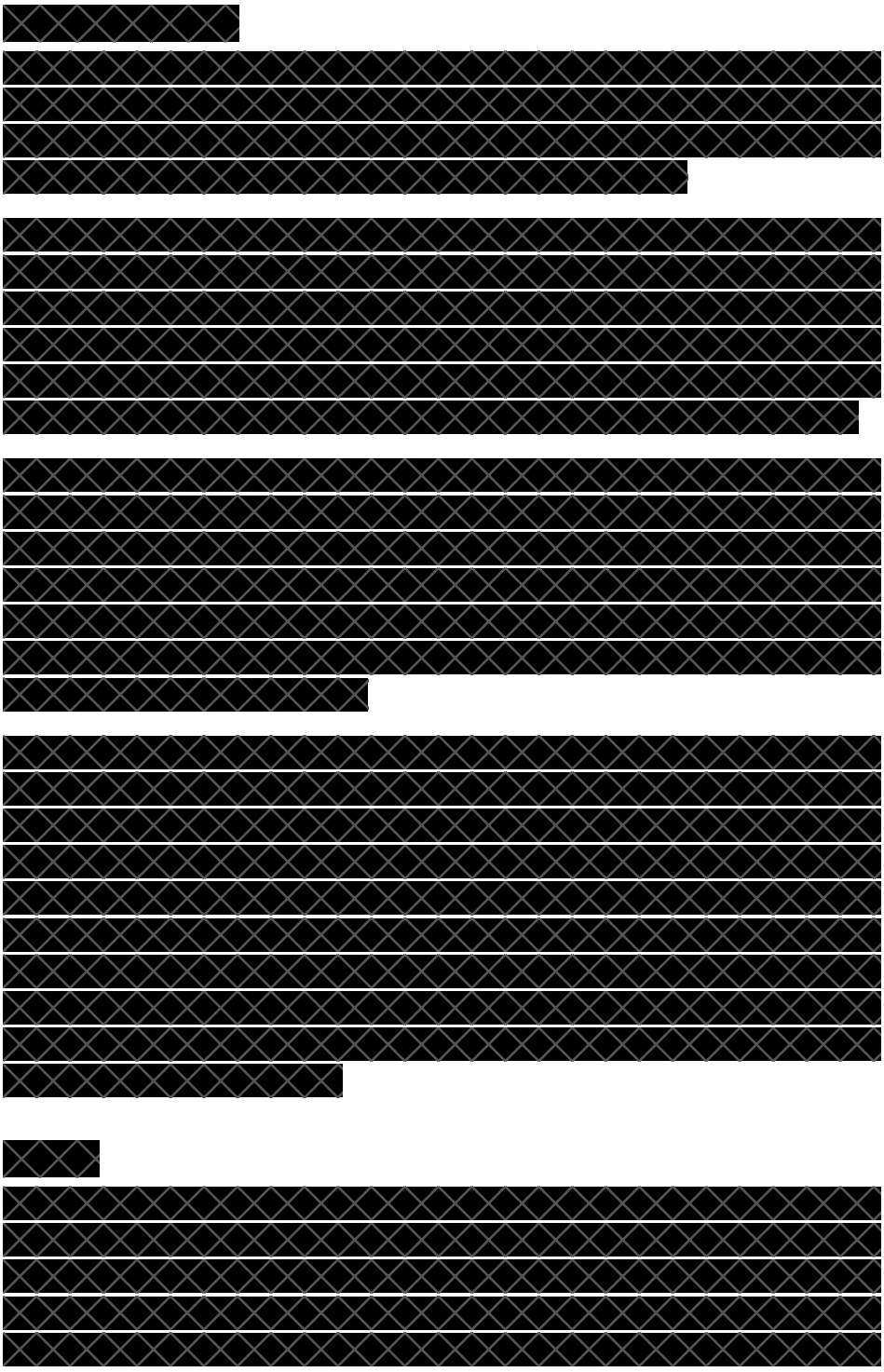

[redacted]

[redacted]

[redacted]

[redacted]

[redacted]

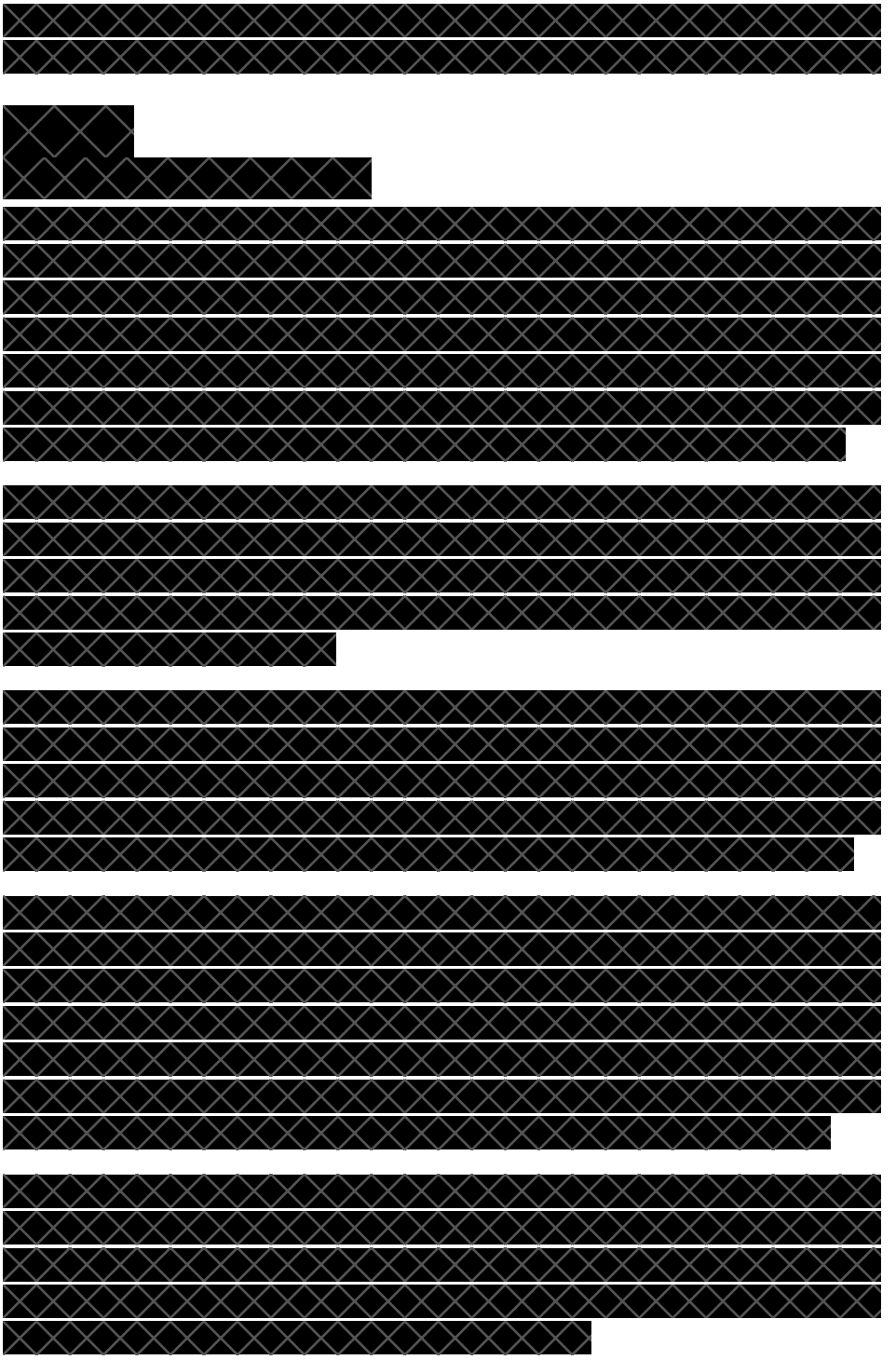

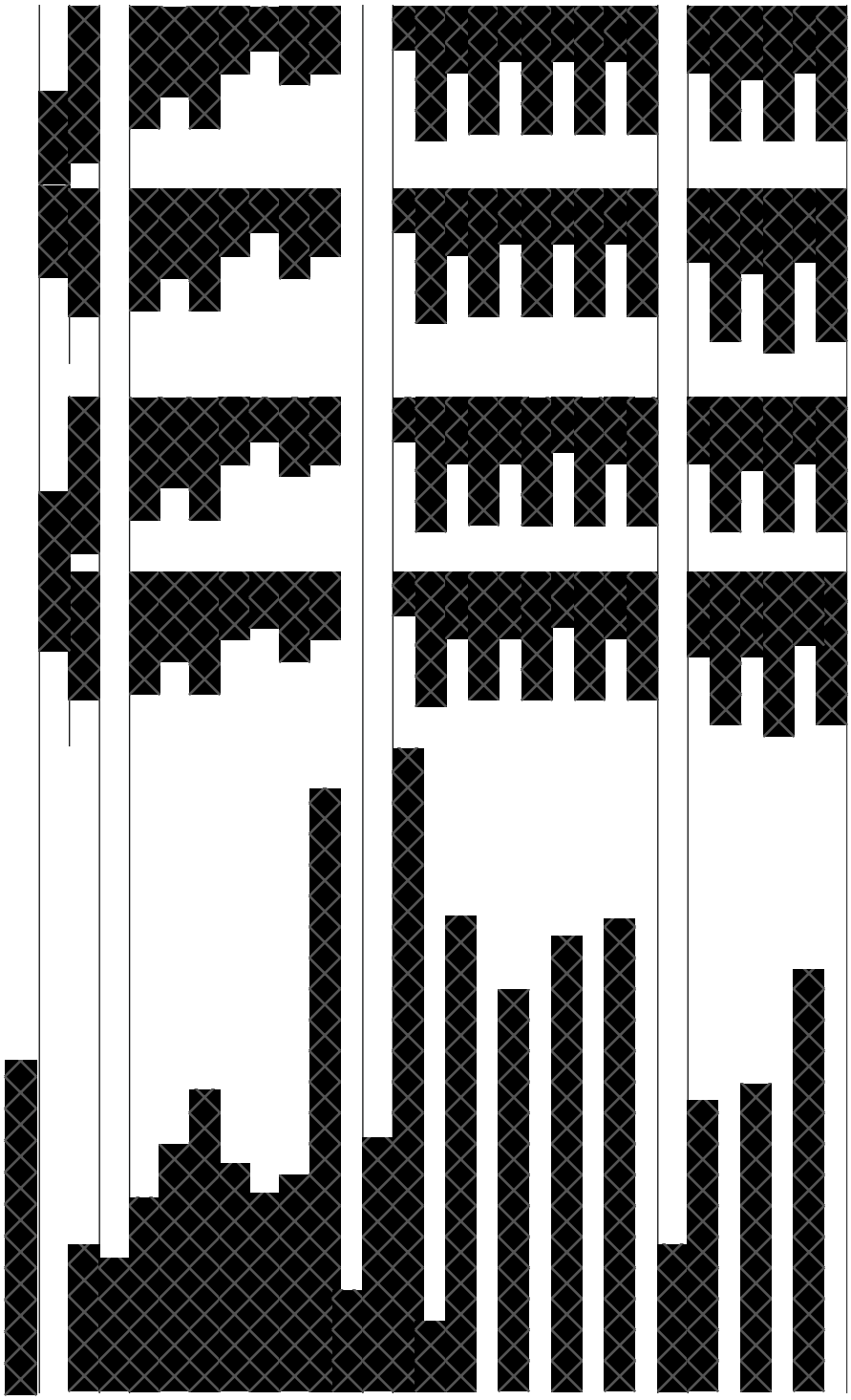

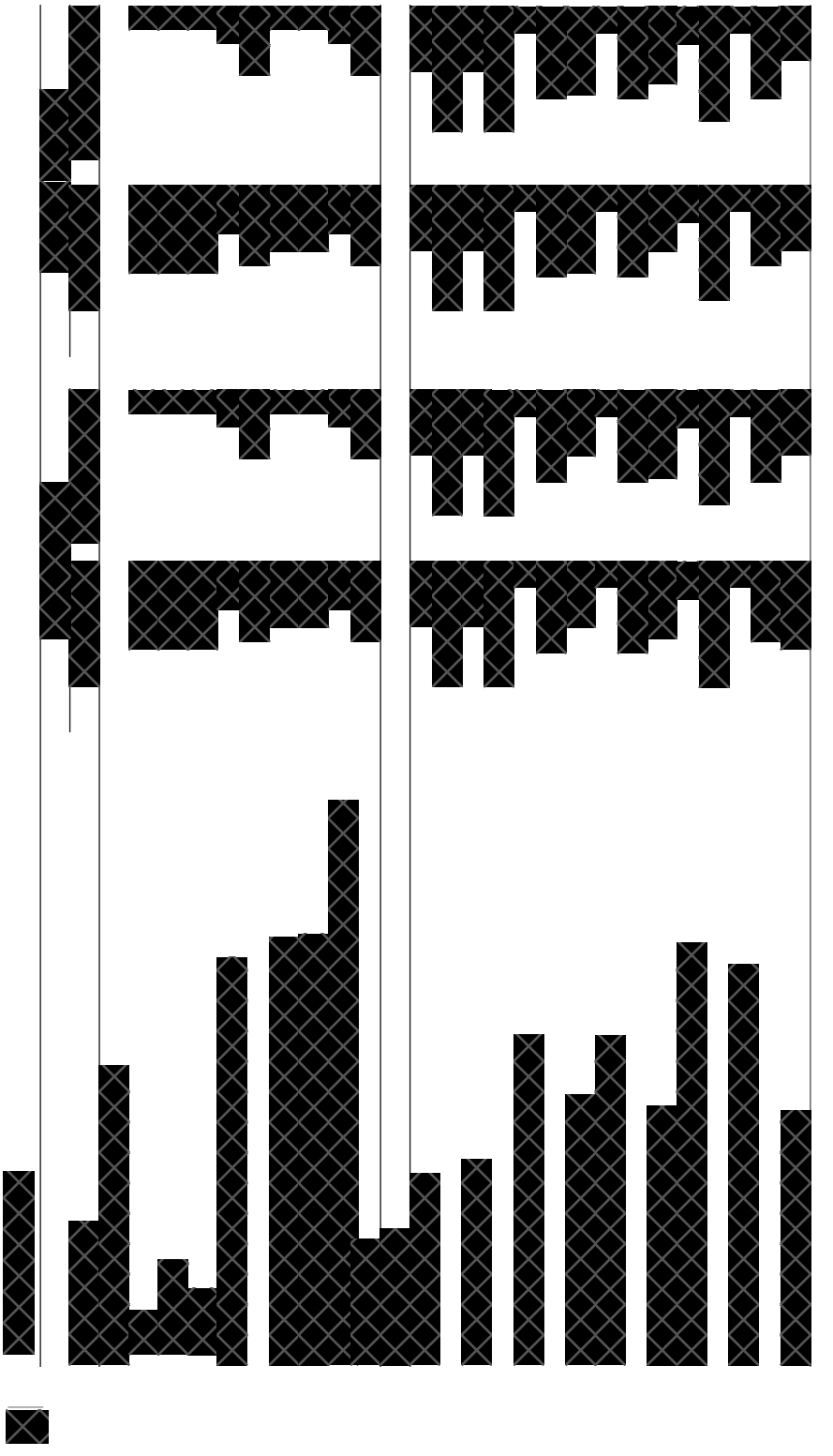

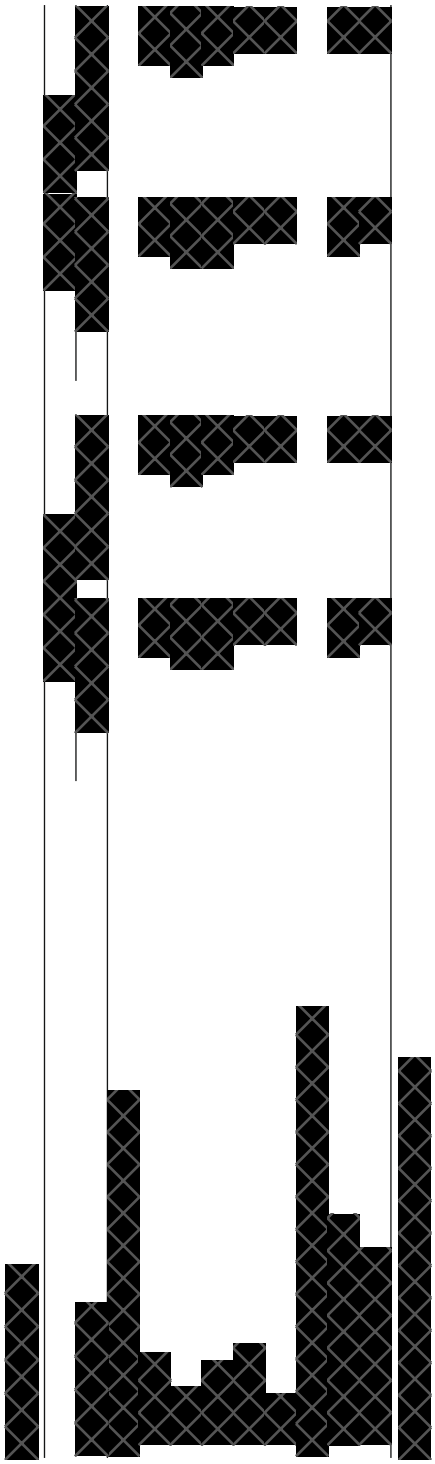

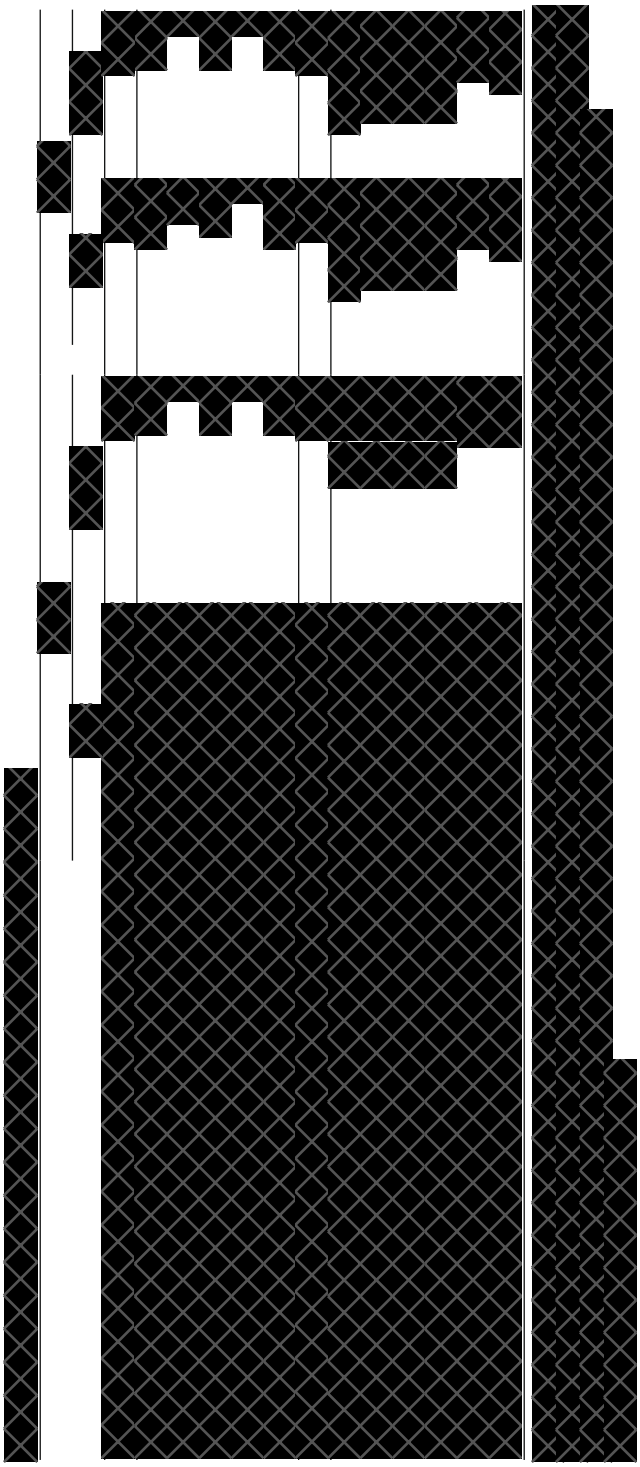

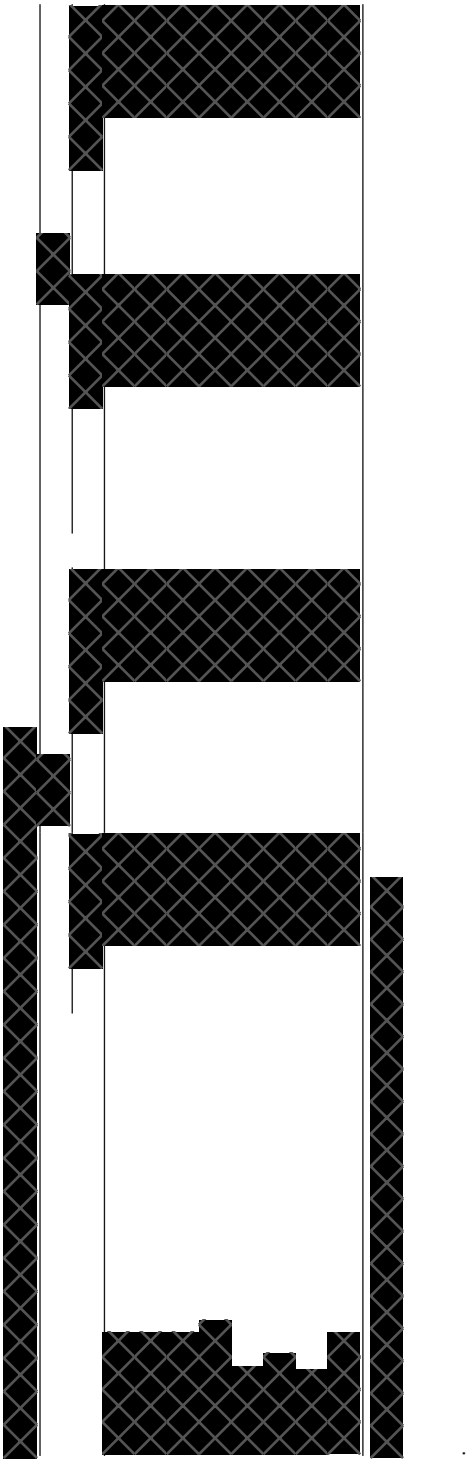

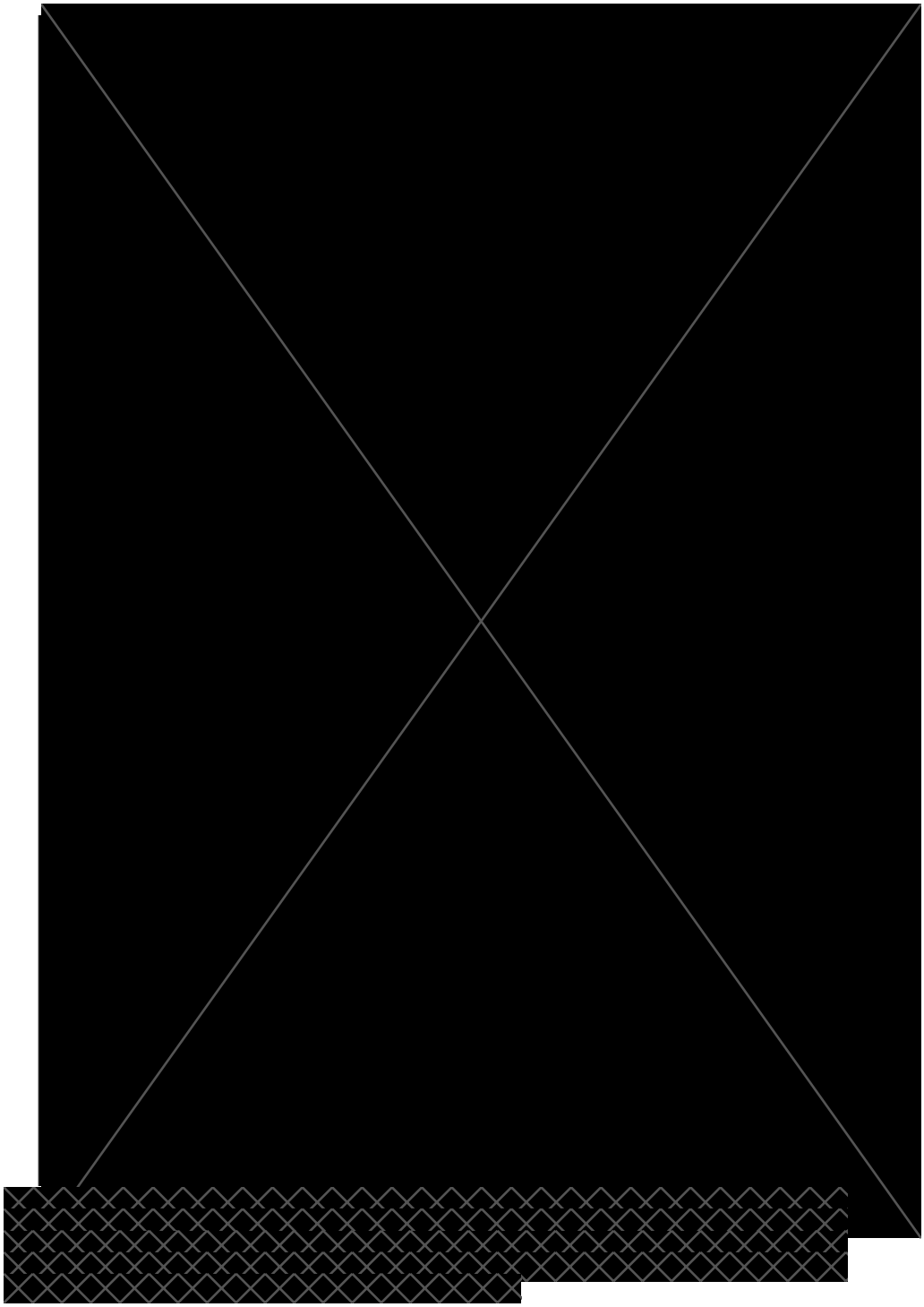

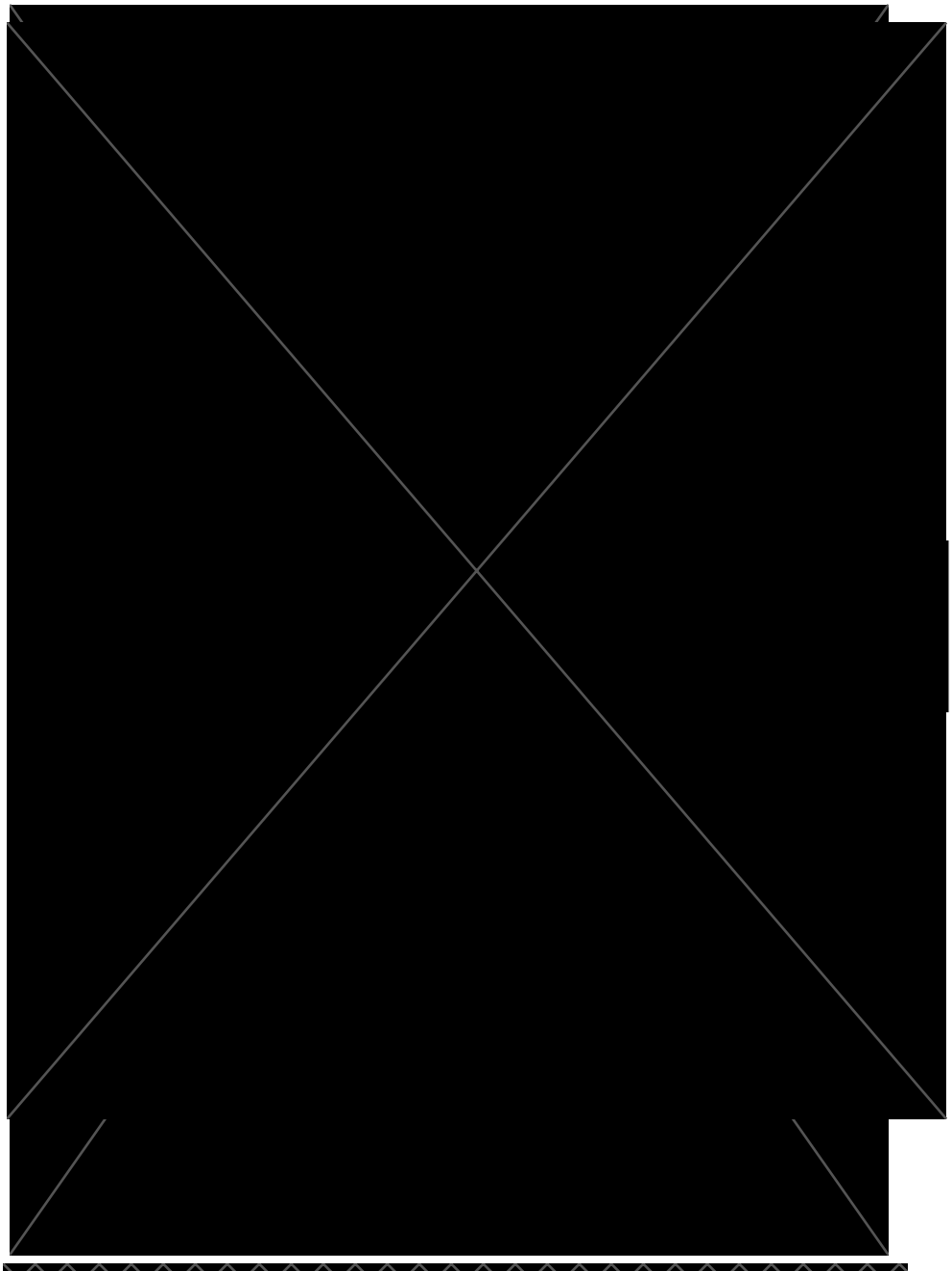

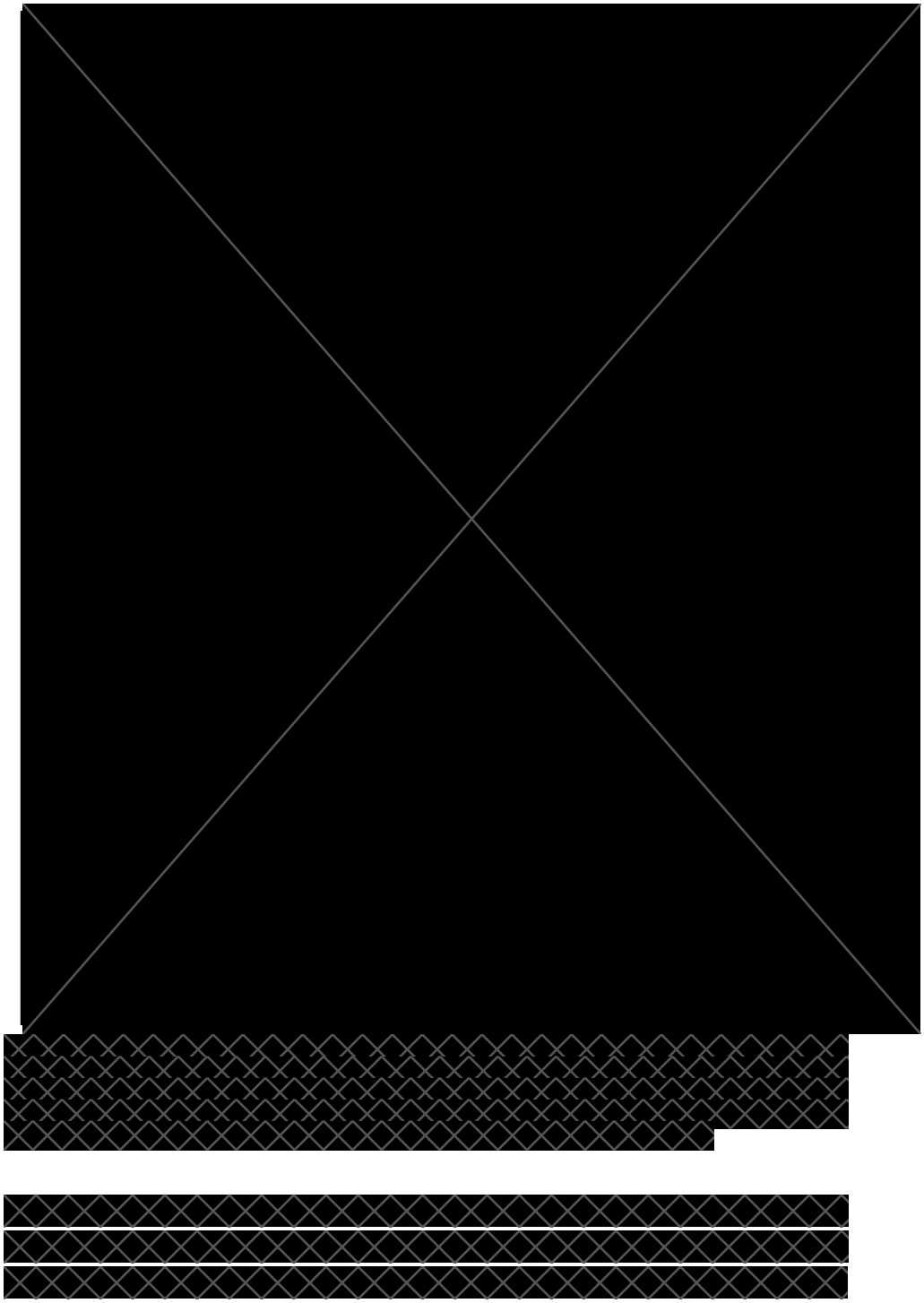

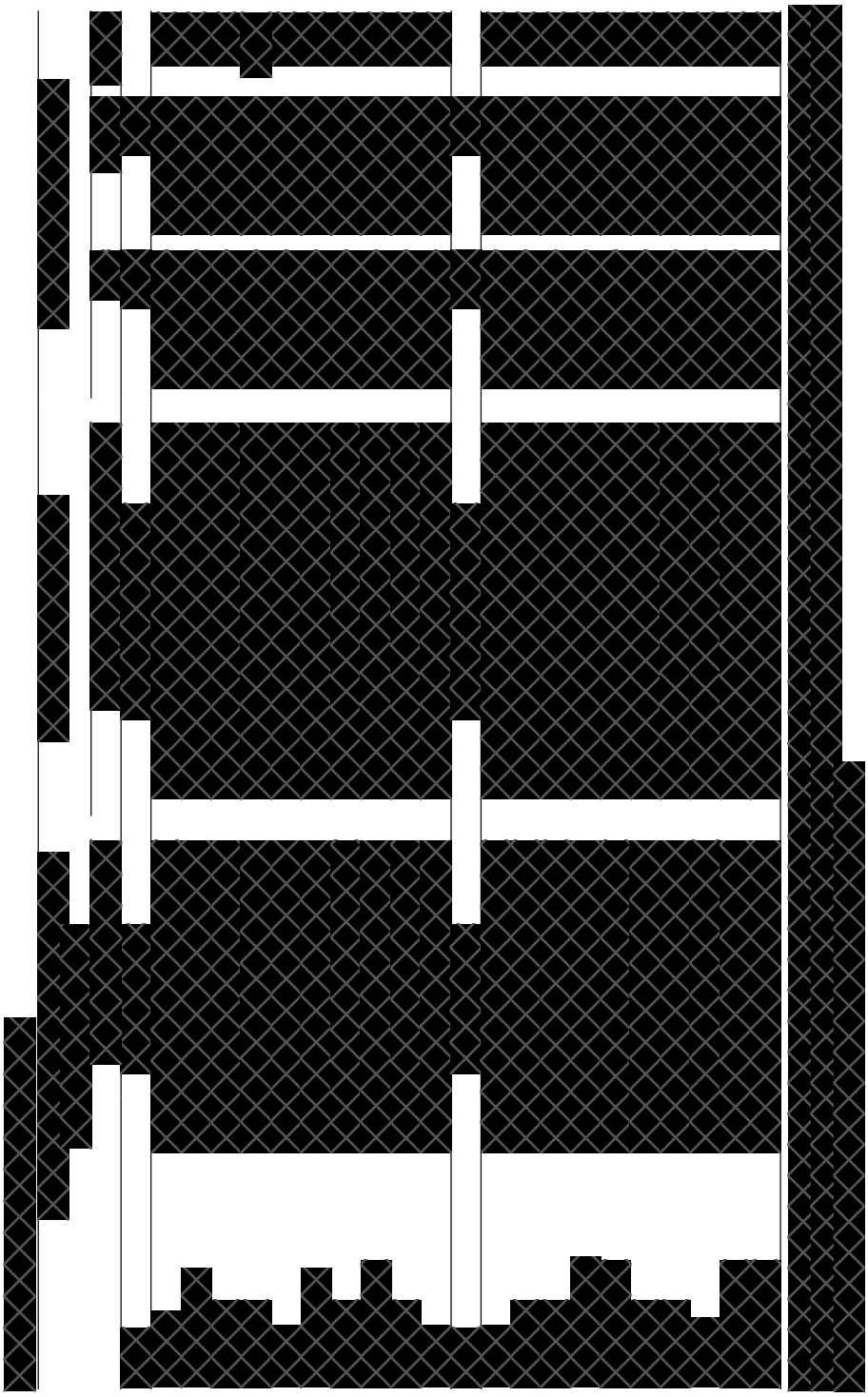

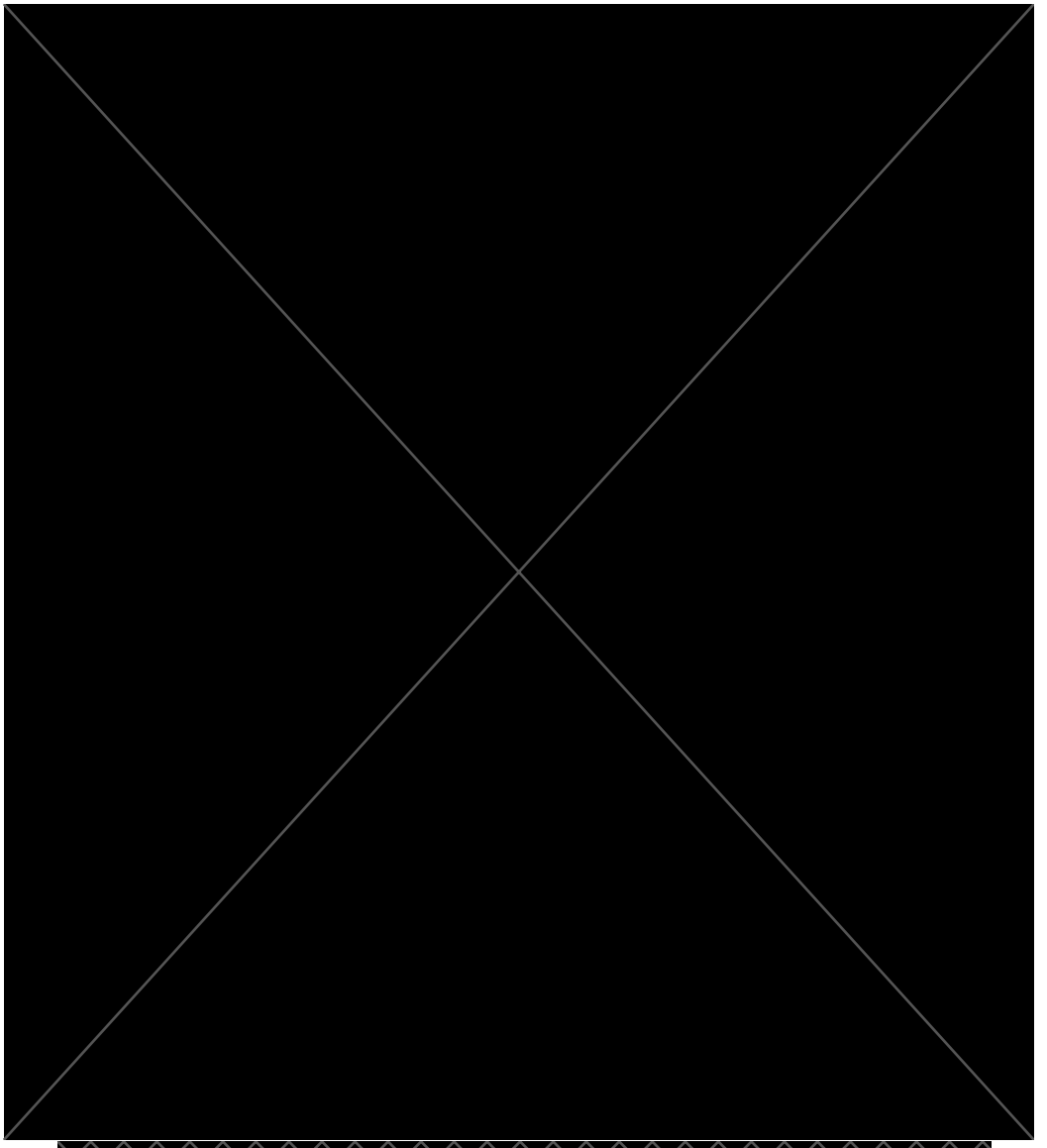

[redacted]

[redacted]

[redacted]

[redacted]

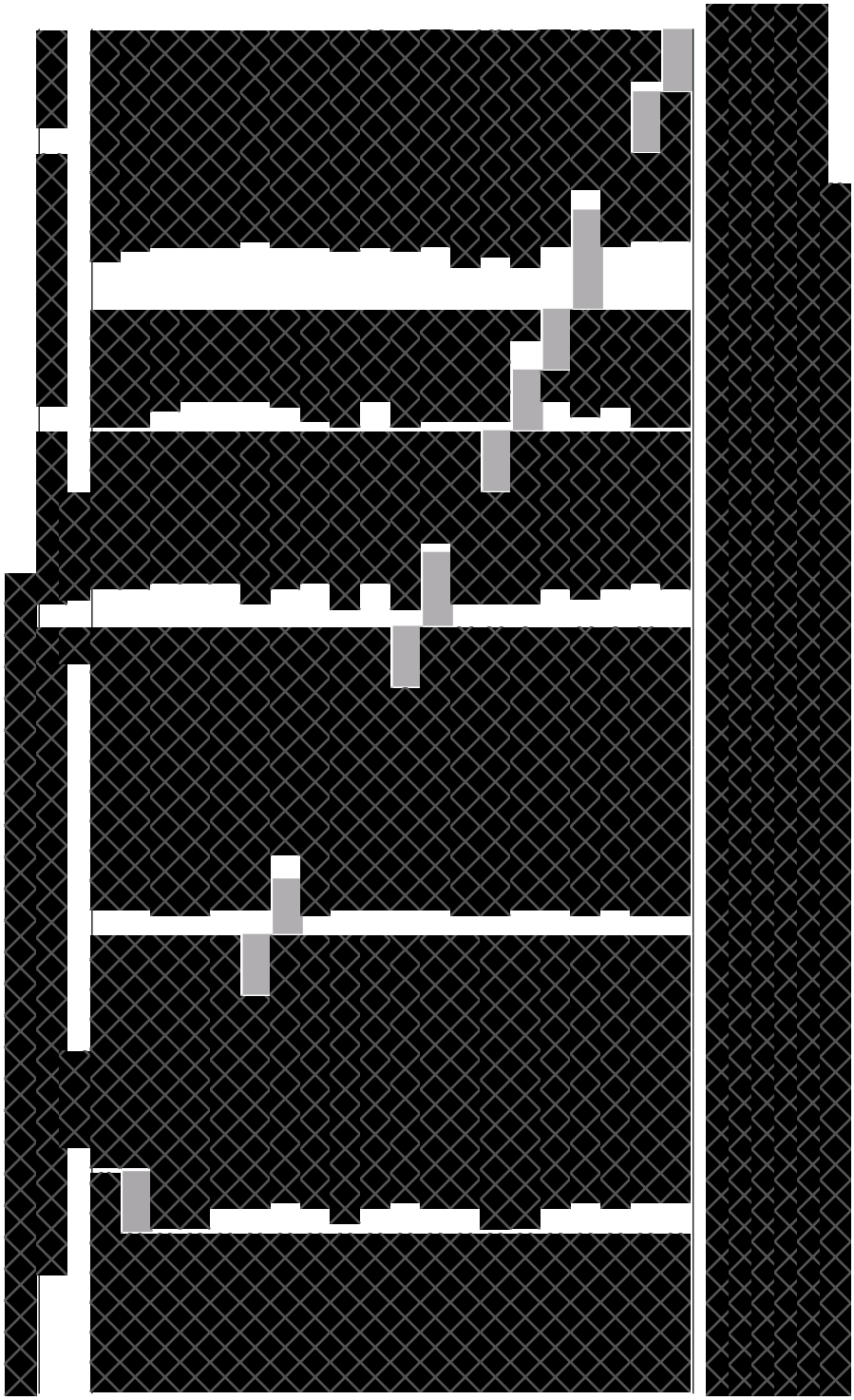

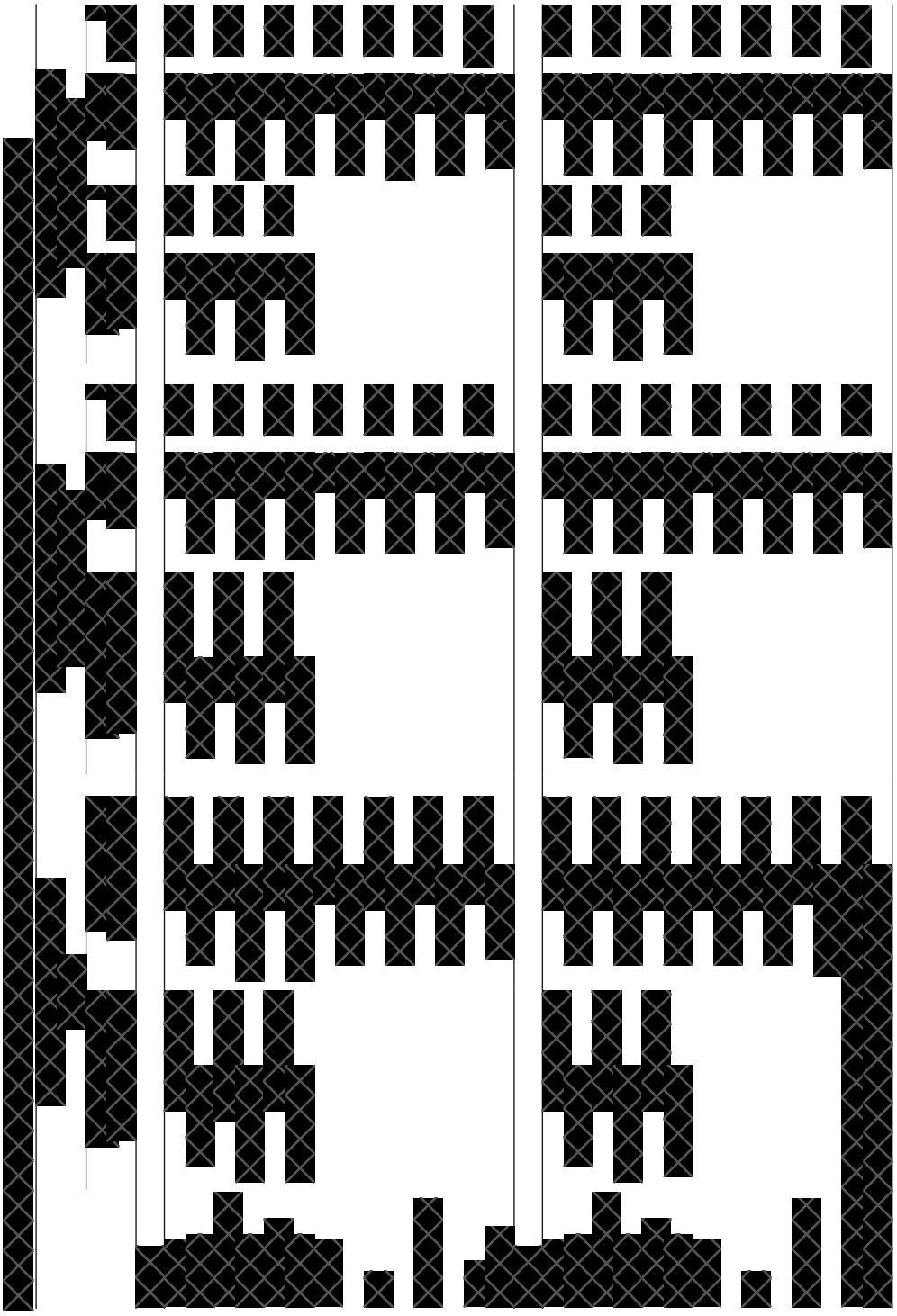

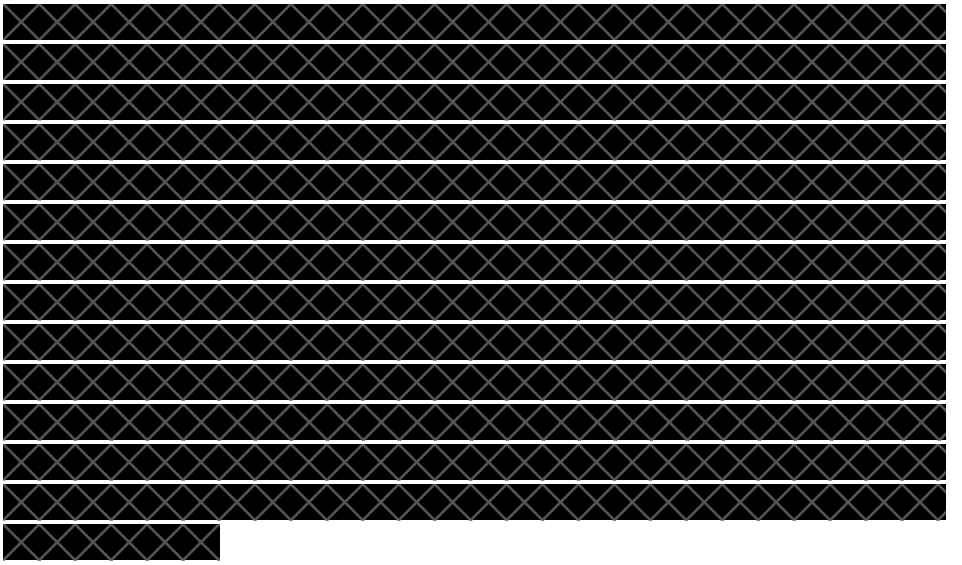

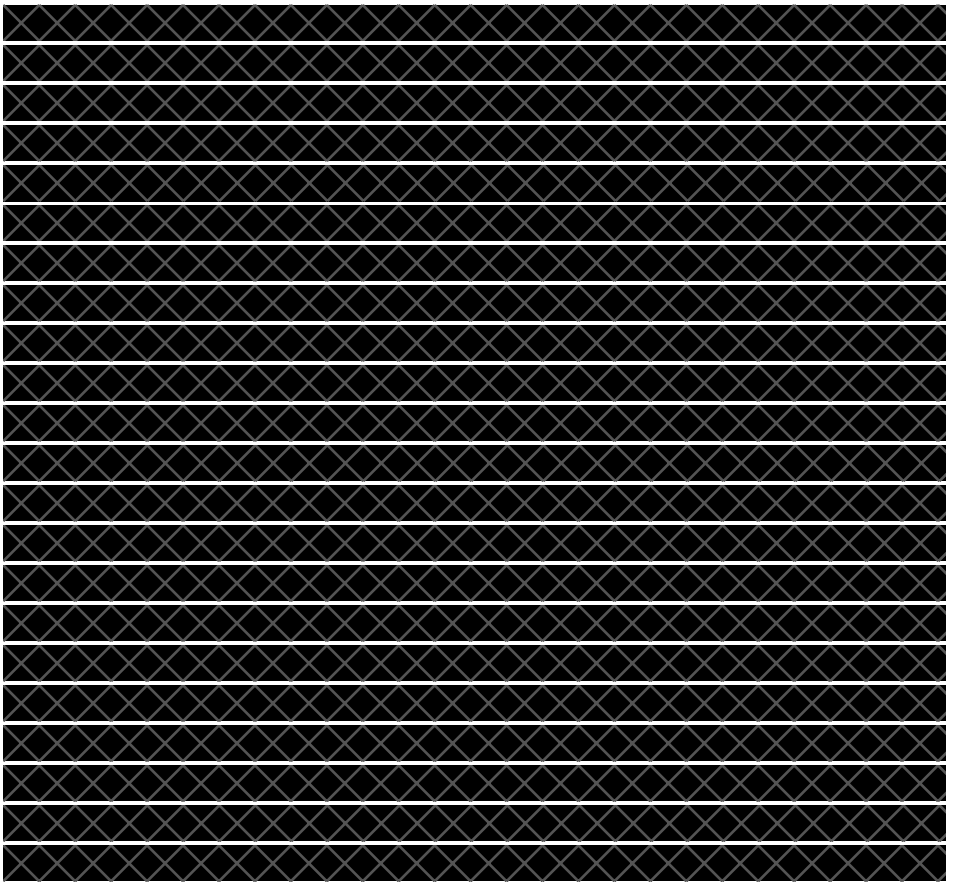

[redacted]

[redacted]

[redacted]

[redacted]

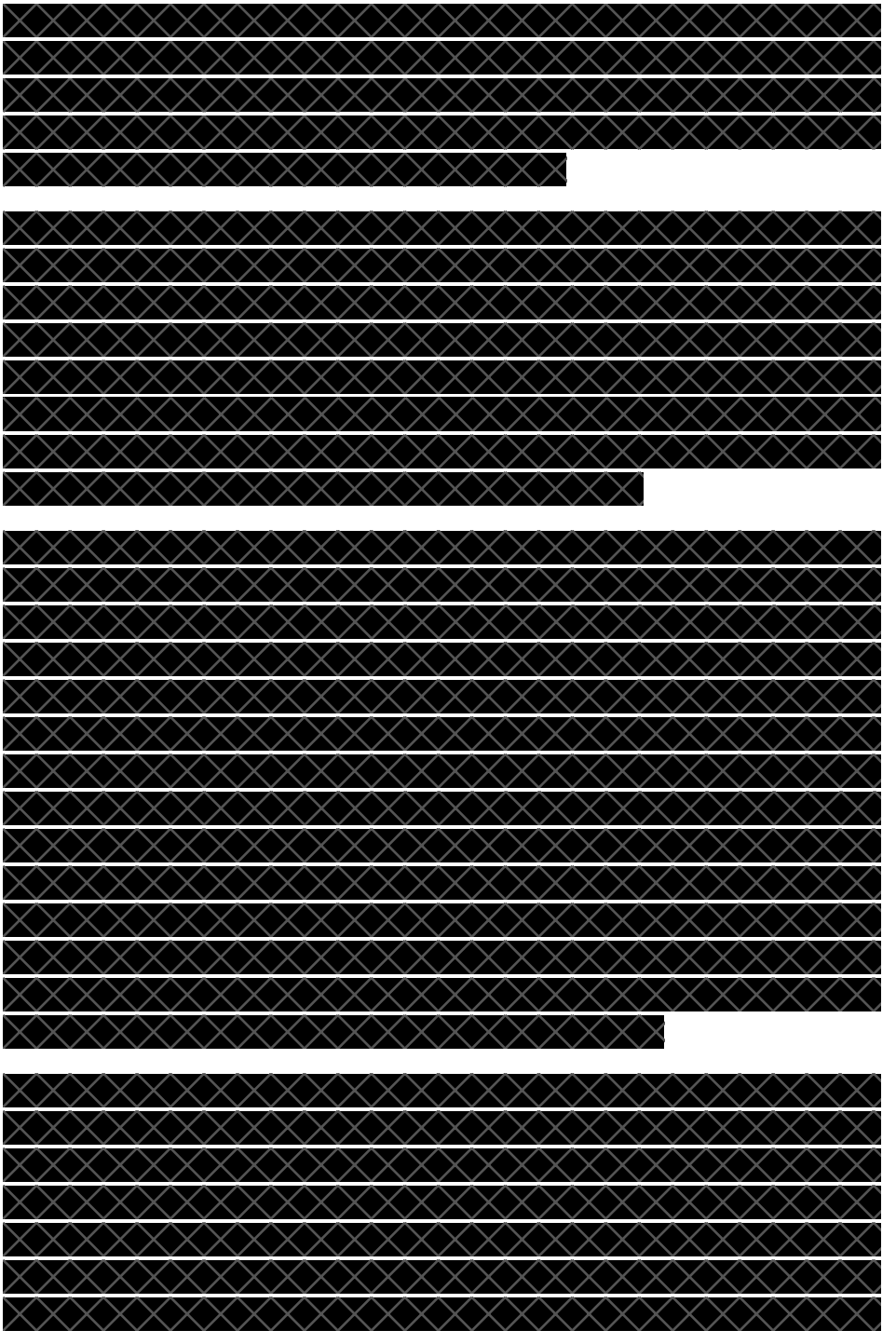

[redacted]

[redacted]

[redacted]

[redacted]

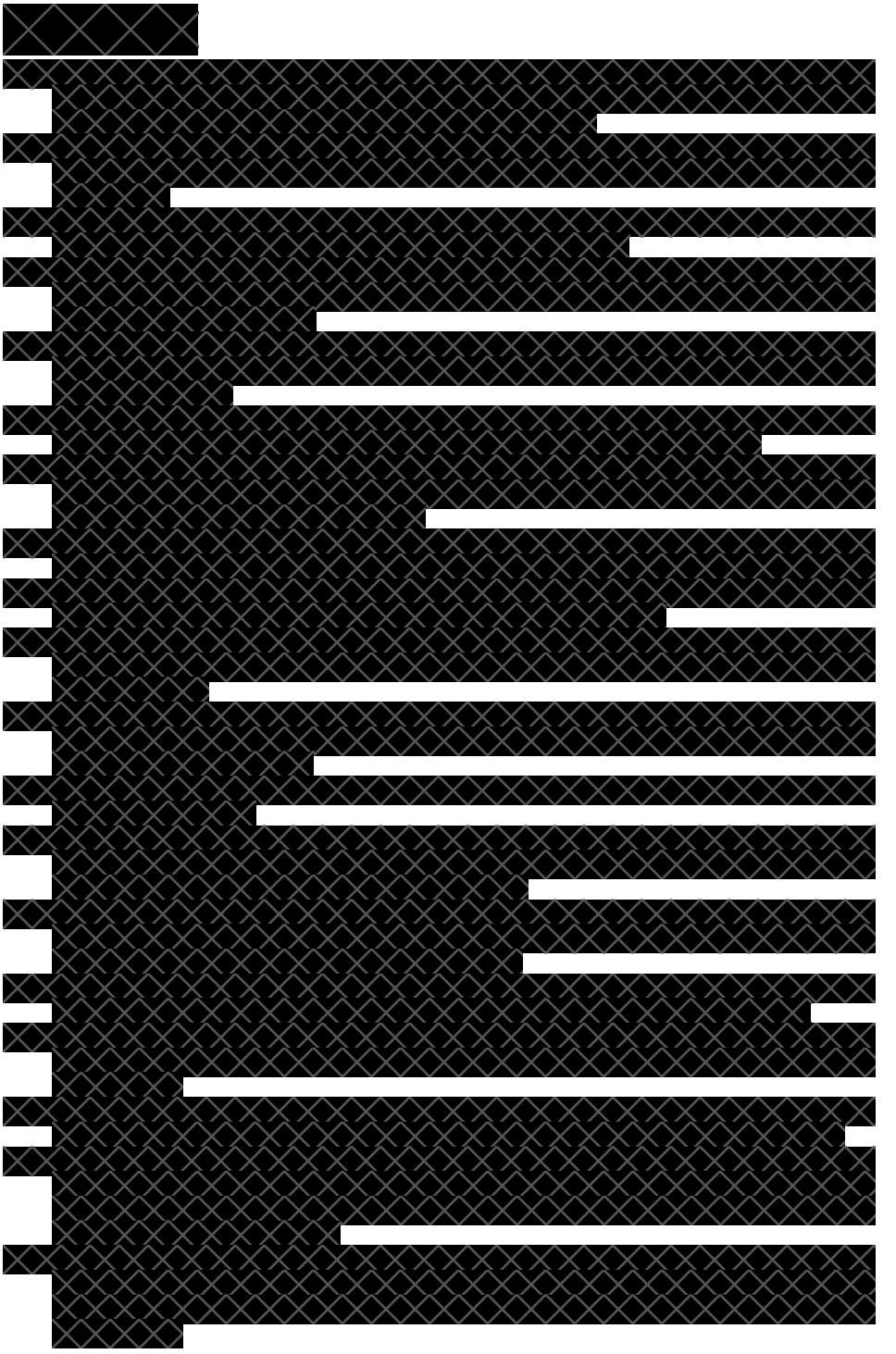

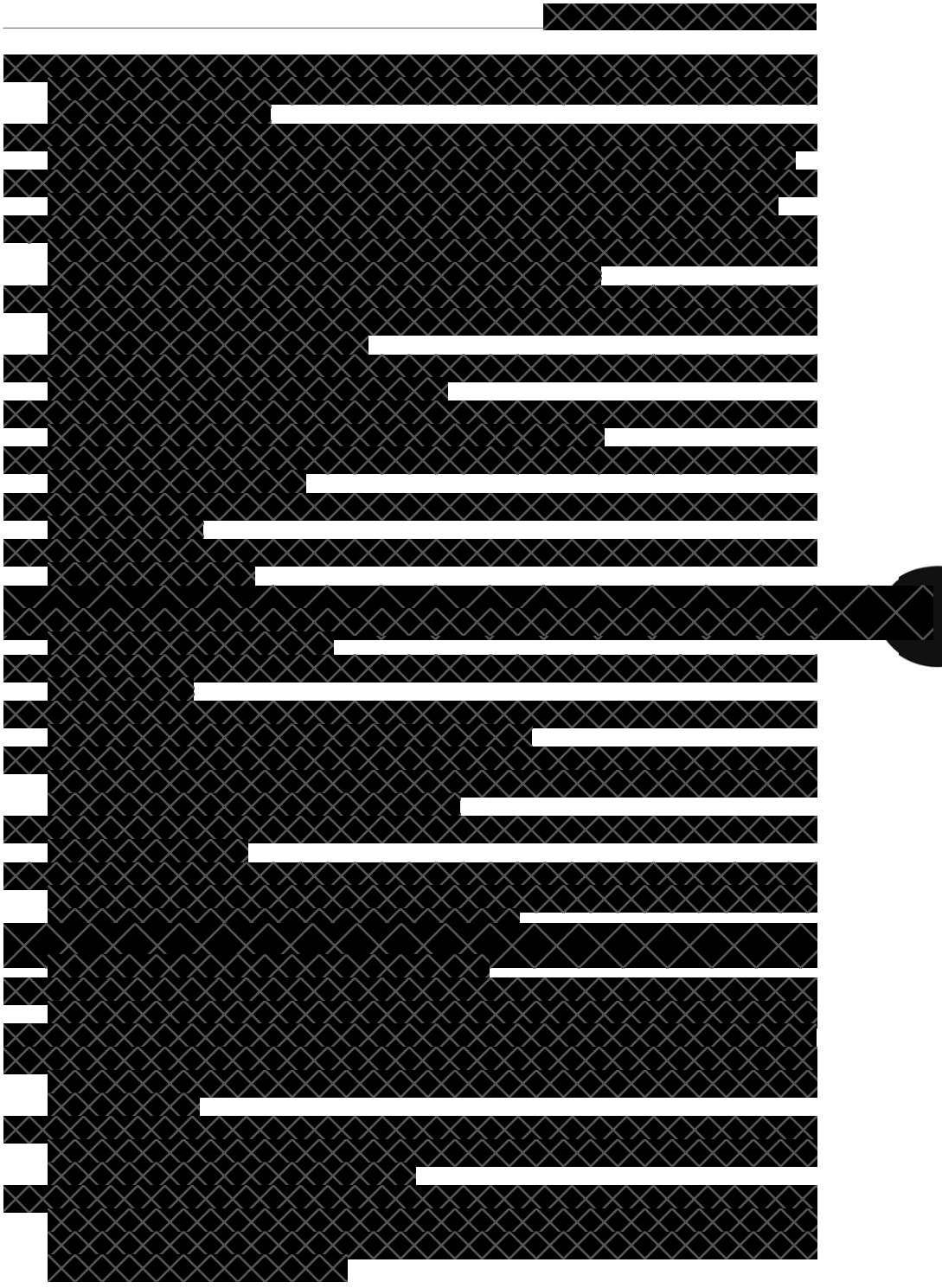

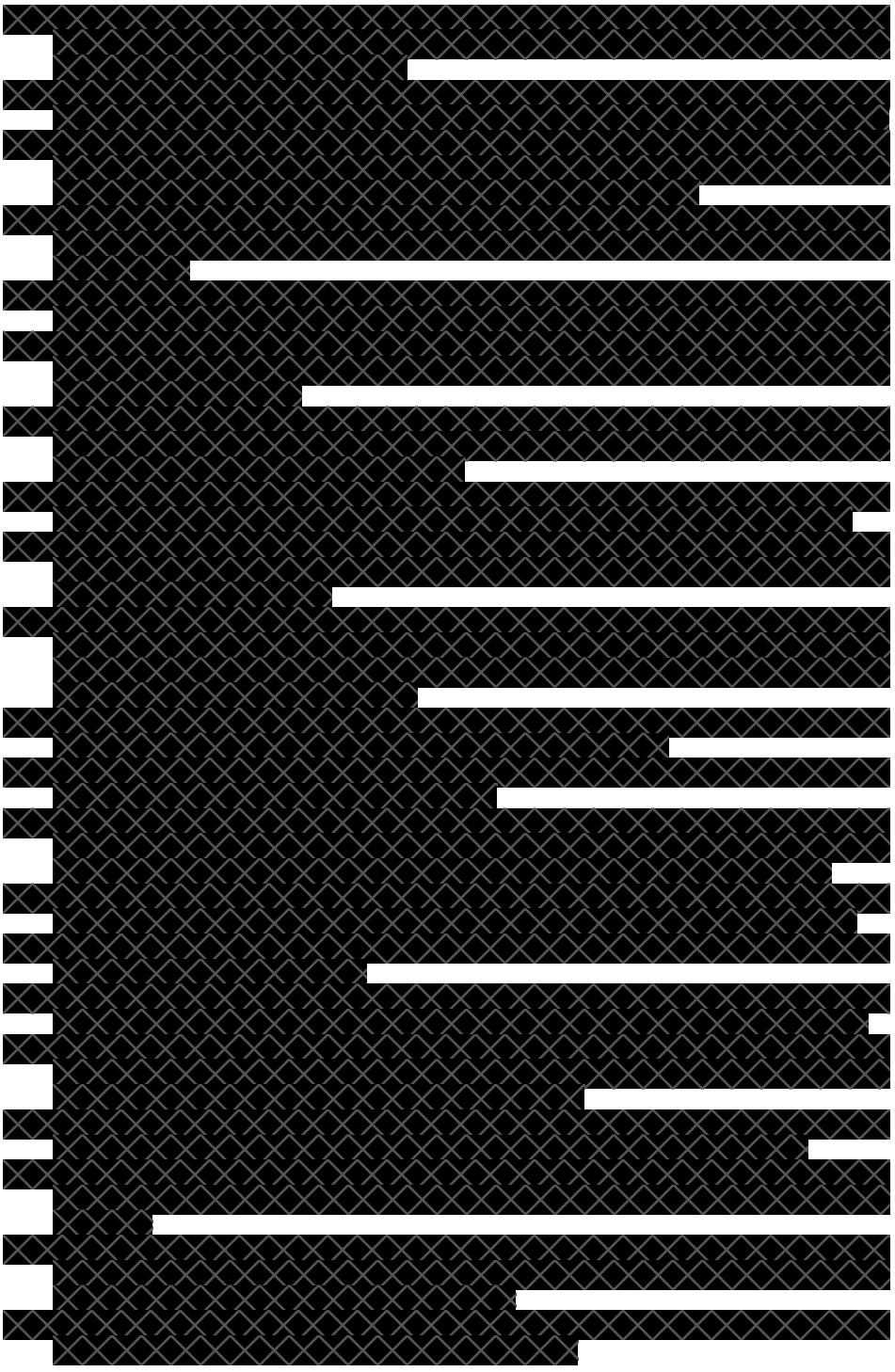

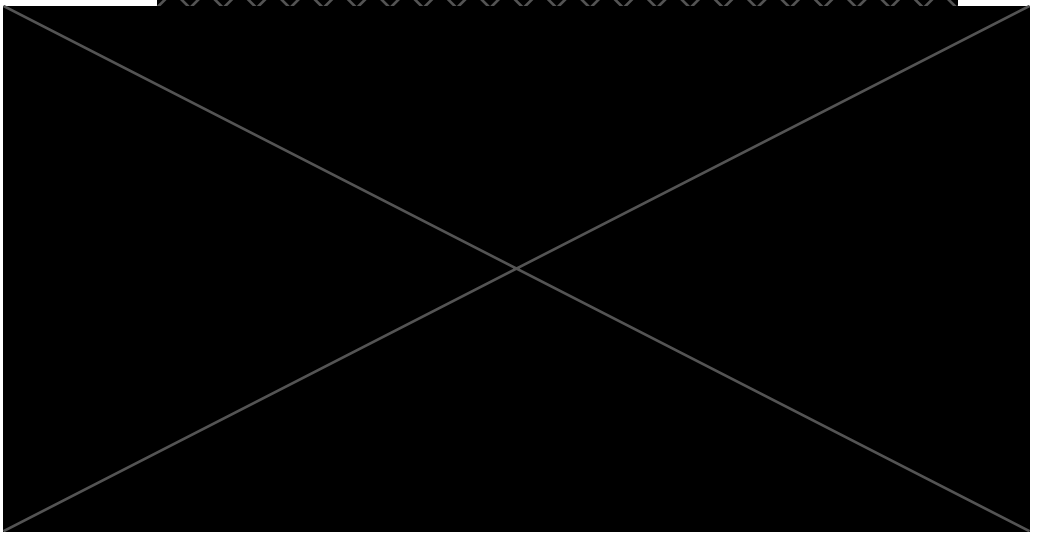

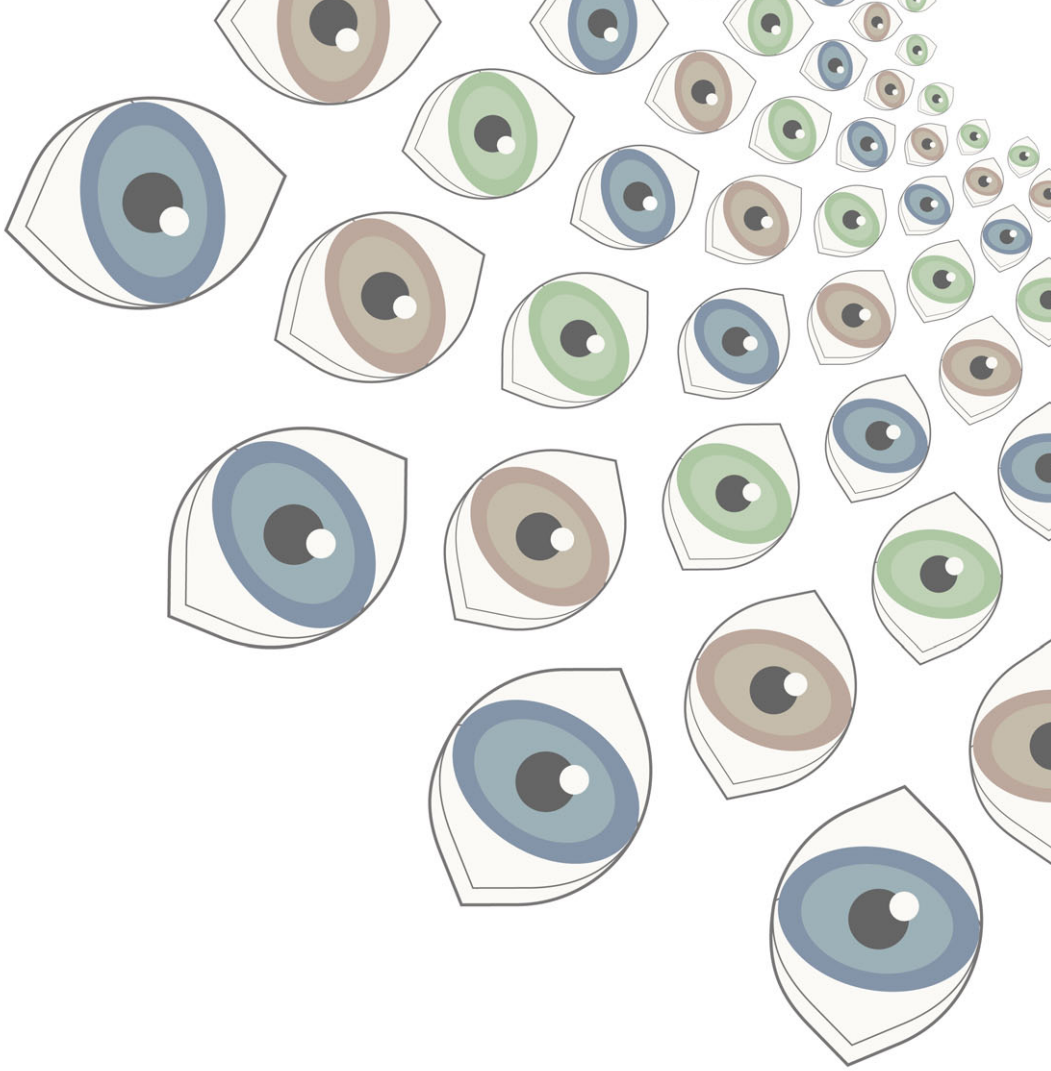

Chapter 6

Summary, General Discussion and Conclusion

The project presented in this thesis centers around the development of TREYESCAN: Traffic Eye Scanning and Compensation Analyzer. A test designed to quantitatively assess compensatory viewing abilities on a wide screen in individuals with visual field loss, which allows for unrestricted head and eye movements. Establishing vision standards for determining fitness to drive is challenging, considering the negative consequences of driving cessation on mobility, independence, and quality of life.[1] The impact of peripheral visual field loss on driving performance is established, but the precise level of loss incompatible with safe driving remains uncertain, as compensation abilities vary widely between individuals and increased scanning is reported to aid adaptation.[2] Given the relatively weak evidence supporting current vision standards, there is a need to explore whether compensatory eye movements enable individuals with varying levels of visual field loss to effectively perceive their surroundings while driving. The aim is to distinguish between effective and ineffective compensatory scanning in individuals with visual field loss, focusing solely on this skill without measuring additional abilities associated with driving. Therefore, TREYESCAN can offer advantages over static visual field testing, since eye and head movements are permitted for compensation of visual field loss.

Chapter 1 provided a general introduction on glaucoma, the primary cause of visual field loss in the elderly population[3] and the leading cause of irreversible blindness worldwide.[4] Primary open-angle glaucoma (POAG) represents a significant public health concern with a global prevalence of 2.4% in the population over 40 years old, impacting 68.56 million individuals in 2021.[5] The chapter discussed the impact on the optic nerve and the visual field,[6] and the importance of timely detection and intervention.[7] The phenomenon of unawareness of visual field loss in glaucoma patients,[8] compensatory eye movements,[9,10] and the challenges of driving with visual field defects were also explored.[2] Presently, the Esterman visual field test,[11] a suprathreshold binocular test, serves as the standard for assessing the visual field in glaucoma patients undergoing driving evaluations in the Netherlands. In **chapter 2**, an analysis of data from the CBR (Dutch driving test organization) was conducted to determine the predictive value of the Esterman visual field test on the outcome of on-road driving tests. Subsequently, the TREYESCAN was developed, with detailed accounts of the developmental stages presented in **chapters 3 and 4**. **Chapter 3** covered the validation and development of the setup and open-source software of the TREYESCAN. **Chapter 4** outlined procedures involved in traffic scene recording, as well as pilot measurements in normally-sighted individuals for the selection of suitable scenes and Areas of Interest (AOIs). **Chapter 5** presented the TREYESCAN

case-control study results, involving glaucoma patients at various stages of disease progression and control participants. The relationship between visual field loss and compensatory eye movements was explored.

This chapter includes a summary of this thesis' main findings, leading to a subsequent general discussion and conclusion.

Main Findings

Predictive Value Esterman Visual Field

In **chapter 2** the relationship between the Esterman visual field test and on-road driving performance was explored with data obtained from the CBR.[12] A retrospective chart review was performed for driver's license applicants who, based on their visual field, performed an on-road driving test. Cases (*n* = 101) with a failed on-road driving test were matched with 101 controls who had passed the test. The Esterman visual field was divided in regions, and the count of missed points within each region was determined. The analyses revealed a significant correlation between the number of missed points in most regions of the visual field and the increased odds of failing the on-road driving test. This underlines the importance of the visual field for driving performance. We found that the center may be more important than the periphery and that the left side may be more important than the right side. This could be attributed to the practice of right-hand traffic and left-hand drive in The Netherlands. On the other hand, in our group, the Esterman visual field test showed no discriminative ability to predict driving performance on an individual level, emphasizing the discrepancy between laboratory visual field testing and practical on-road assessments. This may be attributed to the static nature of the Esterman test, which requires the patient to fixate and fails to measure the dynamic viewing skills essential for traffic situations. This study highlights the need for an accessible and reliable alternative test that can improve the prediction of on-road driving test outcomes. Ideally, such a test would combine the standardized and cost-effective nature of the visual field test with the naturalistic and dynamic stimuli characteristics of the on-road driving test, allowing for unrestricted head and eye movements.

Toolkit for Dynamic AOIs

Chapter 3 introduced the TREYESCAN setup and a novel open-source toolkit designed for the analysis of dynamic AOIs on wide screens, using the Pupil Core eye tracker.[13] The objective to measure eye movements on a wide screen with unrestricted head

movements, posed a challenge due to the limitations of commercially available eye trackers in head movement restriction and a limited measurement range. Moreover, conducting dynamic AOI analyses requires obtaining screen-based coordinates of the eye tracking signal, which is challenging with head-mounted eye trackers. The integration of the Pupil Core head-mounted eye tracker with apriltags (QR-like markers) on the surface area, addressed these challenges by facilitating mapping of the gaze onto the screens displaying the video recordings, therefore enabling a wide measurement area and unrestricted head movements. Essentially, the head-mounted eye tracker is utilized to facilitate remote eye tracking on wider screens. The presented toolkit offers essential tools for the allocation of dynamic AOIs, incorporating both semi-automatic and manual methods. It also facilitates the measurement of AOI parameters such as dwell times and entry times. Additionally, the toolkit provides visualization tools that enable the overlay of gaze and AOIs onto the video recordings. The functionality of the toolkit was validated through measurements involving 11 participants without a visual impairment, and showed promising results. Given the inherent challenges in dynamic AOI measurement analyses, our validated toolkit can be used by researchers using the Pupil Core eye tracker across various research fields, particularly in study designs necessitating wide-screen measurements.

Configuration of TREYESCAN

Chapter 4 described a pilot study aimed at selecting scenes and suitable AOIs for the final version of the TREYESCAN test.[14] Traffic scenes were recorded in Amsterdam with a wide field lens positioned centrally behind the windshield of a driving car. Two routes were collaboratively designed with the CBR, each driven five times. Subsequently, interesting traffic scenarios were identified and compiled into six videos of approximately 8 minutes. A panel of raters, comprising CBR experts on practical fitness to drive and experienced drivers, assessed these videos. The raters categorized AOIs into Must-Be-Seen (requiring active or passive consideration) and May-Be-Seen objects (relevant to be seen but not requiring a change in driving behavior). The location of selected dynamic AOIs was tracked in every frame using tools from the dynamic AOI toolkit. To improve scene and AOI selection for TREYESCAN, the six videos were presented to 20 normally-sighted individuals across two measurement sessions, with simultaneous eye tracking. Participant feedback led to the exclusion of scenes featuring rapid turns and high speed bumps due to reported dizziness or nausea. Additionally, scenes where an AOI suddenly appeared from behind the vehicle were excluded, considering a potential startled reaction from participants and the absence of side

mirror information. Scenes with exclusively central screen AOIs and a large number of overlapping AOIs, were also removed. Eye tracking data within the remaining traffic scenes were analyzed in relation to the allocated AOIs using the toolkit's software. The AOI exclusion criteria were based on the appearance location, the median entry time, and the total amount of participants viewing an AOI. AOIs which met the exclusion criteria in both measurement sessions were marked for removal.

Case-Control Study

Chapter 5 presented the results of the case-control study conducted to investigate AOI viewing and saccadic activity in glaucoma patients with varying degrees of visual field loss compared to control participants using the TREYESCAN. In addition to the two TREYESCAN tasks, demographic information, visual function measures, visual field tests, and questionnaire data were collected from 50 glaucoma patients and 26 control participants. The Integrated Visual Field (IVF) was calculated and used to categorize glaucoma patients in the categories "Mild", "Moderate", and "Severe". For the analysis, the TREYESCAN toolkit was used,[15] and an adaptation of the REMoDNaV event classification algorithm (the adaptation accounts for wide viewing angles).[16] Due to specific criteria not all eye tracking measures of the glaucoma patients and control participants were useable, which lead to the inclusion of 40 glaucoma patients and 23 control participants for Task 1 and 37 glaucoma patients and 23 control participants for Task 2. The results revealed that control participants exhibited increased AOI viewing and saccadic activity compared to glaucoma patients. A significant difference was observed in the entry times for Must-Be-Seen objects, with controls demonstrating faster viewing. However, glaucoma patients with severe visual field loss did not perform significantly worse than glaucoma patients with mild visual field loss, and there was considerable overlap and variability in the results of the glaucoma patients. Linear regression models indicated an association between total saccades and the number of observed objects, suggesting that glaucoma patients might enhance object detection through increased saccadic movements. The results emphasize the importance of considering compensatory viewing strategies in patients with glaucomatous visual field loss and underline the potential of compensatory vision training.

Methodological Considerations

Traffic Scene Recordings

For the TREYESCAN, it was essential to acquire authentic traffic scene videos. Our test incorporates real-world traffic scenarios, rather than relying on artificial animations

or staging specific situations. The traffic scenes were recorded in Amsterdam, a city within The Netherlands characterized by a high volume of road users, including pedestrians, cyclists, and trams that are frequently positioned in the central part of the road. Suitable driving routes were collaboratively determined with the CBR. This approach, facilitated the capture of diverse and interesting traffic scenarios without the necessity of artificially staging situations. It should be acknowledged, however, that this urban representation does not capture the range of the traffic conditions present throughout the entirety of the Netherlands, particularly the rural areas. Moreover, some participants conducting the test might be inexperienced with driving in urban areas. We made the decision to use urban recorded scenes that present interesting AOIs for the TREYESCAN, because we believe rural areas with less AOIs in the scenes would not challenge the measurement of compensatory viewing skills.

The recording procedure involved a tripod-mounted camera securely fixated to the vehicle with tension straps to minimize the impact of vibrations. An ultra-wide field lens ensured the recording of a wide field of view without introducing a disruptive fish-eye effect on the video's peripheral parts. Numerous participants praised the test for its realistic quality, emphasizing an immersive experience due to the wide field of view. Based on our current knowledge, we would consider the use of a gimbal for future traffic scene recordings, which is a gyroscopic device designed for video capture without undesirable camera vibrations or shakes. The gimbal could be suspended from the headliner of the car, precisely positioned at the center of the scene, thereby rectifying the leftward skew in the current TREYESCAN videos.[14] Nevertheless, it is important to note that the current scenes, recorded without the use of a gimbal, retain their usability, because they demonstrate an acceptable level of stability. Moreover, significant time and effort were invested in post-processing these scenes, underscoring the need for careful consideration before deciding to rerecord them.

A decision was made to exclusively show front-view video footage, as the addition of extra videos at the sides or top of the screen, mimicking side and rearview mirrors,[17] would create artificial rather than realistic additions. The same consideration was made for the addition of a dashboard animation,[18,19] which would not test the same scanning towards the dashboard as in a real car, especially because the participants are not controlling the vehicle themselves. However, the absence of side mirrors, rearview mirror and dashboard in the experimental setup may have limited the assessment of visual scanning behavior during driving, which may not completely

capture the strategies employed by individuals with visual field defects in real-world scenarios. On the other hand, the primary objective of TREYESCAN is to identify individuals with visual field loss who effectively and ineffectively scan a scene, and this goals is achieved without the inclusion of additional elements like dashboard and mirrors.

Furthermore, the recorded scenes were deliberately restricted to daytime settings with favorable weather conditions, excluding precipitation and fog. A hypothesis was made that scenes recorded under low-light or unfavorable weather conditions would present reduced contrast conditions, which may not mimic real-world driving conditions under similar circumstances. However, it is important to acknowledge that the brightness of the monitors used in the TREYESCAN setup is lower than the actual brightness experienced when driving outdoors in daylight. Consequently, this difference affects the actual hindrance of relative scotomas as assessed through visual field testing and might result in an underestimation of the visual field's impact during the test when compared to daylight driving conditions. Moreover, it is worth mentioning that a recent study introduced the Night-time Hazard Visibility Test (NHVT).[20] This novel test proposes an evaluation of hazard visibility during night-time conditions, introducing an interesting domain for future research.

Eye Tracking

As previously mentioned, our research methodology employed the Pupil Core eye tracker[21] due to its integration with apriltags,[22] which enables the calculation of gaze coordinates related to a specific surface. This eye tracker uses one scene camera and two eye cameras situated diagonally beneath the eyes. In instances where participants wore their own spectacles or a trial frame, these were positioned underneath the eye tracking cameras. It is crucial to note that reflections or glints may introduce substantial disruptions to the eye tracking signal, impacting accurate pupil detection.[10] Notably, Pupil Labs has recently introduced the Neon eye tracker as an alternative,[23] a promising calibration free system with an accuracy that exceeds the Pupil Core. The design of the Neon eye tracker includes eye cameras placed on the inner side of the frame, eliminating the necessity to measure through spectacles and preventing glint interference. Given that our study predominantly involves an elderly population often requiring prescription glasses and a presbyopic correction at the distance of the TREYESCAN monitors (65 cm), this design consideration is particularly relevant. Neon also has a broader horizontal measuring span of 132° compared to

the Pupil Core lens used in our research, which has a measuring span of 103°. The compatibility of Neon with Apriltags, coupled with the other advantageous features, makes it a promising alternative to use in future TREYESCAN studies. However, as of this moment, there are no peer-reviewed publications available of Pupil Labs or other researchers using the Neon eye tracker, so this should be awaited.

In an ideal scenario, measurements should be conducted without requiring participants to wear additional devices. The presence of a head-mounted eye tracker could potentially influence participants' viewing behavior, by introducing non-naturalistic elements. Especially slippage can be an issue, due to participant movements, affecting the quality of data.[24,25] In turn, our research group is currently developing an innovative remote eye tracking system with multiple cameras. The system is designed to capture a wide field of view, without the need of extensive calibration routines.

AOI Measures

In the case-control study, we mainly relied on AOI analyses, which involves identifying specific regions in the stimulus important to the research objective. A noteworthy strength of our study was the determination of AOIs by an expert panel, with further validation through the reassessment of chosen AOIs in a pilot study involving normally-sighted individuals. This approach ensured that AOIs were not arbitrarily selected. Metrics such as AOI hits (indicating if gaze coordinates fall within an AOI) and dwell times (the duration of AOI visits, from entry to exit) were calculated.[26] The challenge with the analysis dynamic AOIs, which are moving areas of interest during video or animated elements, is caused by the relative movement of objects in relation to the coordinate system in which the gaze positions are recorded.[27] Consequently, it is difficult to make definitive statements regarding AOI size in the analysis.

To address the inherent inaccuracy of the eye tracker, we incorporated margins around AOIs. Recognizing that accuracy is highest in the center and poorest at the edges of the screen,[26] we applied larger margins towards the sides of the screen based on the object's position. However, by applying larger margins, gaze can be erroneously linked to the viewing of an AOI when a participant may be looking at something else. Additionally, overlapping AOIs introduce another limitation, as our assumption that a participant is looking at both AOIs simultaneously may not accurately reflect their visual attention.

In the dynamic AOI analyses, we decided to use dwell times with a frame-by-frame method instead of fixation measures. Previous research suggested that reporting

either measure is sufficient,[28] and a high correlation was found when comparing fixation-by-fixation analysis to a frame-by-frame method.[29] In our study, we were interested in differentiating eye movements that serve to maintain the present area of the visual scene or object on the fovea (e.g. fixation of a stationary object or smooth pursuit), or serve to bring a new area of the visual scene or object to the fovea (e.g. saccades to a new area of the visual scene).[30] It was therefore not essential for the research aim to make a distinction between fixations and smooth pursuits. Moreover, it is a difficult task to classify fixations in the presence of smooth pursuits, since signal characteristics of fixations and smooth pursuits are often overlapping.[31,32] Smooth pursuit movements may typically be erroneously classified as very long fixations with very short saccades in between. The frame-by-frame method with dwell times allowed us to measure if an object was looked at without introducing potential errors associated with misclassifying fixations and smooth pursuits.

Furthermore, in eye tracking research, employing the most accurate system available is essential for ensuring robust data collection.[26] In our research setup, enhanced accuracy would not only lead to more precise event classification, but also more exact calculations of dwell times and entry times, since the estimation of when the gaze falls within the borders of an AOI would be more accurate. Improved measurement accuracy would also allow for the possibility of using smaller margins around objects, enabling the inclusion of more AOIs in the analysis compared to our present study.

Additional Measurements

In our case-control study, we conducted additional measurements to assess visual function, visual fields, and quality of life, enabling a comparison of various metrics between glaucoma patients and control subjects.

Due to time restraints, cognitive assessments were not conducted. However, it is possible that cognitive decline may influence the outcomes of the TREYESCAN. Furthermore, considering the cognitive demands associated with driving, and that evidence suggests that mild cognitive impairment could potentially exacerbate the effects of declined vision on driving,[33] there is a need to explore the interaction between cognitive impairment and the ability to perform compensatory scanning. In the selection of cognitive tests, it is recommended to include those that are not dependent on vision.[34,35] Considering the association between visual impairment and declining cognitive function,[36] it is important to study the impact of cognition on the results of TREYESCAN in future research. Moreover, cognitive abilities might

contribute to some of the variations observed in the TREYESCAN results among individuals with visual field loss, necessitating further investigation.

Since the TREYESCAN exclusively involves visual stimuli, auditory assessments were intentionally excluded. However, it is important to recognize that individuals with reductions in visual acuity or visual fields may also encounter additional sensory impairments, such as hearing impairment, resulting in dual sensory impairment. This dual sensory impairment has been associated with an increased incidence of motor vehicle collisions.[37] Building upon the point mentioned above, it is noteworthy that dual sensory loss also has a higher impact on cognition than a visual impairment alone.[38,39] Nevertheless, the primary objective of TREYESCAN was to isolate and evaluate the skill of compensatory eye movements, and we believe that auditory impairment would not influence the outcomes of TREYESCAN, as auditory stimuli are not incorporated into the test.

Selection of Participants

For the selection of our case-control study, participants were selected from the ophthalmology clinics of two hospitals in Amsterdam, The Netherlands. It is noteworthy that not all glaucoma patients were routinely invited, and a potential selection bias may have occurred during the ophthalmologists' invitation process. Additionally, an alternative recruitment approach involved advertising in the glaucoma newsletter of The Eye Association Netherlands (Oogvereniging), and some participants self-referred after encountering study information in online articles. This introduces another potential source of selection bias, as individuals with a pre-existing interest in driving may have been more inclined to participate compared to other glaucoma patients who did not self-refer. This may have led to the inclusion of glaucoma patients who are potentially more capable than the general glaucoma population. Additionally, the members of The Eye Patient Association Netherlands may not represent the entire population of glaucoma patients, as the majority of individuals with glaucoma are not affiliated with this association.

Our sample comprised an older and experienced group of drivers. Previous research has indicated that experienced drivers demonstrate more extensive scanning than novice drivers, with experienced drivers making more horizontal eye movements.[40,41] Moreover, experienced drivers make more use of a wide field of view than novice drivers, when compared to a narrow view condition.[42] In our sample, we compared the glaucoma patients to a control group of similar age and driving experience.

However, it is the question if the TREYESCAN is suitable for younger individuals with visual field defects seeking to obtain a driver's license for the first time.

TREYESCAN

As a result of our research, we developed the TREYESCAN setup, designed to be implemented in a straightforward way across different settings. The comprehensive description of TREYESCAN provided below is intended to provide information for replication purposes.

Figure 1 presents the setup, which consists of three HP EliteDisplay 24-inch monitors arranged in a linear configuration. Seamless extension of the traffic scenes across the three monitors was realized with Nvidia Surround, resulting in minimal occlusions at the bezel intersections. An additional screen, not visible to participants, is used for experiment control. The TREYESCAN setup uses two separate computers. Firstly, an Acer Nitro N50-600 I92060 PC (8GB memory) with a NVIDIA GeForce RTX 2060 video card and Intel Core i5 processor is used for stimulus presentation. It is important to employ a computer with a powerful video card which is able to connect four monitors and present a video smoothly across multiple monitors. Additionally, an Apple MacBook Pro with an M1 chip (2020, 16GB memory) is connected to the Pupil Core and is used for gaze recording, following Pupil Labs' recommendation. This dual-computer setup minimizes latencies in both stimulus presentation and data recording.

Whilst performing the TREYESCAN, the participant sits on a car seat positioned 65 cm away from the central screen, offering a 100° field of view. The table height is adjustable to ensure the participants' eyes are centered on the middle of the screen, and allowing head movements in all directions. The TREYESCAN task comprises of two videos of approximately 8 minutes, each with 12 real-world traffic scenes separated by a gray screen. Between the two videos participants are offered a short break. Task 1 features 63 objects (34 Must-Be-Seen, 29 May-Be-Seen objects) and Task 2 incorporates 61 objects (30 Must-Be-Seen, 31 May-Be-Seen objects). Participants' eye movements are recorded as they watch the videos without accompanying traffic sounds. They are instructed to imagine themselves as the vehicle's driver and press a button when identifying objects requiring some form of action, such as reducing speed or changing lanes.[43]

The TREYESCAN is accompanied by custom software, written in Python 3.8.3[44] and relies on various libraries including NumPy,[45] Pandas,[46] OpenCV,[47] Matplotlib,[48] and SciPy.[49] The TREYESCAN toolkit is open source and available on GitHub (*https://github.com/treyescan/dynamic-aoi-toolkit*).[15] It includes tools for dynamic AOI allocation

using semi-automatic and manual methods, measurement of AOI parameters such as dwell times and entry times, and the visualization of gaze and AOIs. For event classification, the TREYESCAN software incorporates an adapted version of the REMoDNaV algorithm,[50] specifically modified to account for the larger viewing angles inherent in the TREYESCAN setup (*https://github.com/treyescan/event-classifier*).[16] An additional tool was developed, enabling the identification of AOIs by a panel of experts. This tool presents videos in an online environment (Fig. 2), allowing raters to click on objects they consider important and differentiate between Must-Be-Seen objects and May-Be-Seen objects (*https://github.com/treyescan/marking-aois*).[51]

Figure 1. Picture of TREYESCAN setup. Participants were seated in front of three display monitors whilst wearing the Pupil Core eye tracker.

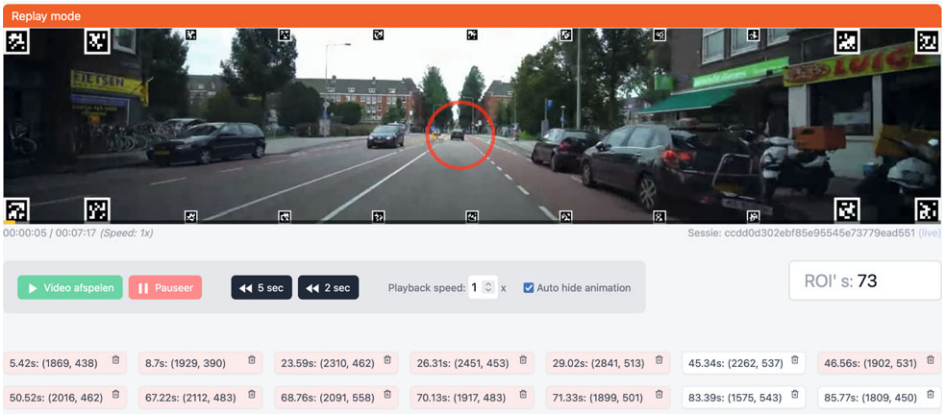

Figure 2. Screenshot of the marking AOIs tool. Experts can assess traffic scenes through a web browser in an online environment. While viewing the video, experts can click on objects, differentiating between Must-Be-Seen (Red) and May-Be-Seen (White) objects. The tool allows playback of the video with circle animations highlighting the clicks for easy verification of ratings. Additionally, experts can use features such as slower playback and the ability to remove AOI clicks through the list below the video.

Future Research

After considerable effort in developing the TREYESCAN, including building the setup, programming the software, and the selection of scenes and AOIs, valuable insights have emerged that can be utilized for patients with visual field loss, as evidenced by pilot and case-control studies. These advancements open up possibilities for future research. As previously highlighted, it is recommended to include cognitive tasks in future studies. Additionally, the exploration of the novel Neon eye tracker with the TREYESCAN setup might be beneficial.

It is essential to acknowledge the limited task demands associated with the observation of traffic scenes in the TREYESCAN without actual vehicle control. This limitation may create an impression of capable driving performance that does not necessarily align with actual driving capabilities. In future studies, a comparative analysis between TREYESCAN outcomes and on-road driving is essential. For the TREYESCAN test, an interesting approach involves administering the test to individuals with visual field loss scheduled for an on-road driving examination at the CBR. This would enable a systematic comparison between TREYESCAN results and on-road driving test performance. Additionally, it would be insightful to assess and compare the predictive value of the TREYESCAN with the Esterman visual field test. Furthermore, integrating mobile eye tracking to measure eye movements during real driving scenarios and correlating them with those observed during TREYESCAN would provide valuable insights. Such an analysis is important to assess the extent to which a favorable outcome in the TREYESCAN aligns with success in on-road driving.

The applicability of TREYESCAN could extend beyond glaucoma patients to encompass other groups with visual field impairment, such as individuals with hemianopia[52] or retinitis pigmentosa.[53] It might also be interesting to explore its relevance in other ophthalmological patient cohorts, including those with central scotomas due to macular degeneration,[54] or even beyond ophthalmology, in patients with mild cognitive impairment or dementia.[55-57] Comparative assessments of TREYESCAN outcomes among these varied patient groups could present valuable insights.

For the sake of participant well-being and to prevent simulator sickness,[58] certain challenging traffic scenarios involving sharp turns or speed bumps, notably roundabouts, were deliberately excluded from the final version of the test. Despite these precautions, simulator sickness was reported by several participants in our study,[58] with one individual attributing it to a preexisting susceptibility to motion

sickness and an intolerance for 3D animation movies. It is advisable to incorporate susceptibility to simulator sickness as an exclusion criterion in future studies.[59] Moreover, a comprehensive evaluation of the prevalence of individuals experiencing such issues is essential, as the widespread implementation of the TREYESCAN test may be hindered if a substantial portion of the population is unable to perform the test due to these concerns.

Implications for Clinical Practice

It is crucial to emphasize that the majority of glaucoma patients experience mild visual field loss, and that with timely detection and intervention, the onset and impact of glaucoma can be delayed. Glaucoma patients with mild visual field loss can drive safely, which is also suggested by the results of our case-control study, where those with mild visual field loss showed no significant differences compared to control participants in the viewing of AOIs. TREYESCAN is particularly designed for the group of glaucoma patients with moderate to severe visual field loss, where concerns about safe traffic participation arise based on their static visual field test results or experiences while driving.

Prior research indicates that older adults alter their driving behavior based on their perceptions of how physical health, medication, and cognitive and sensory decline might affect their driving competence.[33] TREYESCAN presents an opportunity for positive self-monitoring in individuals with glaucoma by visually illustrating their gaze patterns in traffic scenes. It has the potential to highlight instances when glaucoma patients, who may pose a risk on the road, have overlooked essential objects. This visual presentation has the potential to facilitate a better acceptance of driver's license revocation, compared to presenting static visual field test results to the affected individual.[60] Additionally, TREYESCAN has the potential to instill confidence in glaucoma patients who are hesitant to drive but exhibit adequate compensatory viewing behavior, by visually demonstrating their effective strategies.

Some patients could benefit from rehabilitation programs designed to train effective scanning techniques. Presently, compensatory scanning training is offered to patients with hemianopia, in which a participant learns to consistently make large eye and head movements in the blind part of the visual field.[61] This enables the patient to expand the functional visual field and minimize the loss of visual information as much as possible. With effective scanning, individuals with hemianopia have demonstrated to be safe drivers.[62-64] TREYESCAN could play an important role in identifying

patients who would benefit from a training program in a more tailored manner than solely looking at the visual fields. Additionally, it could serve as a before and after measurement to evaluate the progress of the training. Rehabilitation programs for glaucoma patients can include training in effective scanning techniques, and enhancing saccadic eye movements. By integrating these approaches, individuals with glaucoma could maintain functional independence and improve their quality of life despite the challenges posed by the disease. It is important to recognize that besides viewing strategies, other compensatory driving strategies exist, across strategic, tactical, and operational levels, according to Michon's Hierarchy of Driving Behavior.[65,66] The outcome of TREYESCAN could provide insights into determining the necessity of compensatory vision training.

In the event that future studies establish a correlation between compensatory eye movements in TREYESCAN and the outcomes of on-road driving tests, the potential of TREYESCAN lies in predicting compensatory viewing behaviors in driving situations. This applicability could extend to diverse contexts, including ophthalmology clinics and vision rehabilitation centers.

Conclusion

The primary aim of this thesis was the development of a test for investigating and analyzing compensatory eye movements in individuals with glaucoma, allowing for unrestricted head and eye movements. To achieve this goal, we created the TREYESCAN, a novel setup accompanied by self-developed analysis software. Additionally, further aims were investigated, including an examination of the predictive value of the Esterman visual field test, a pilot study involving individuals with normal vision to evaluate scenes and AOIs, and a case-control study comparing the TREYESCAN results between glaucoma patients and normally-sighted individuals.

The results of the case-control study demonstrated that glaucoma patients with varying degrees of visual field loss show considerable variability in saccade rates and the identification of AOIs, not evidently due to increasing visual field loss. There was a significant association between the saccade rate and the number of detected AOIs, highlighting the potential effectiveness of saccadic viewing training in this population. Recognizing the importance of compensatory viewing in individuals with visual field loss, we underscore the need for a comprehensive approach that extends beyond static visual field testing.

Although future research is needed to investigate the TREYESCAN on a larger scale, our efforts have laid the foundation for a test to measure compensatory eye movements. By overcoming challenges inherent with screen-based eye tracking on wide screens and conducting dynamic AOI analyses, this thesis provides a framework for researchers interested in studying compensatory eye movements in individuals with visual field loss. Furthermore, the TREYESCAN can be implemented as an assessment instrument in rehabilitation centers to assist clients with visual field loss in mobility-related needs. Moreover, the setup and software introduced in the dynamic AOI toolkit extend their utility beyond the field of ophthalmology, serving as a valuable open-source resource for researchers across diverse fields, including psychology, transportation, and low vision research.

References

1. Wood JM, Black AA, McGwin G, Jr., Owsley C. Challenges and perspectives of vision standards for driver licensing. *Ophthalmic Physiol Opt*. Jan 2024;44(1):1-4. doi:10.1111/opo.13254
2. Patterson G, Howard C, Hepworth L, Rowe F. The Impact of Visual Field Loss on Driving Skills: A Systematic Narrative Review. *British and Irish Orthoptic Journal*. 2019;15(1):53-63. doi:10.22599/bioj.129
3. Ramrattan RS, Wolfs RC, Panda-Jonas S, et al. Prevalence and causes of visual field loss in the elderly and associations with impairment in daily functioning: the Rotterdam Study. *Archives of Ophthalmology*. 2001;119(12):1788-94. doi:10.1001/archopht.119.12.1788
4. Flaxman SR, Bourne RRA, Resnikoff S, et al. Global causes of blindness and distance vision impairment 1990-2020: a systematic review and meta-analysis. *The Lancet Global Health*. 2017;5(12):e1221-e1234. doi:10.1016/S2214-109X(17)30393-5
5. Zhang N, Wang J, Li Y, Jiang B. Prevalence of primary open angle glaucoma in the last 20 years: a meta-analysis and systematic review. *Scientific Reports*. 2021;11(1):13762. doi:10.1038/s41598-021-92971-w
6. Jonas JB, Aung T, Bourne RR, Bron AM, Ritch R, Panda-Jonas S. Glaucoma. *The Lancet*. 2017;390(10108):2183-2193. doi:10.1016/S0140-6736(17)31469-1
7. Rein DB, Wittenborn JS, Lee PP, et al. The cost-effectiveness of routine office-based identification and subsequent medical treatment of primary open-angle glaucoma in the United States. *Ophthalmology*. 2009;116(5):823-32. doi:10.1016/j.ophtha.2008.12.056
8. Hoste AM. New insights into the subjective perception of visual field defects. *Bulletin de la Societe Belge d'Ophtalmologie*. 2003;(287):65-71.
9. Crabb DP, Smith ND, Rauscher FG, et al. Exploring eye movements in patients with glaucoma when viewing a driving scene. *PLoS One*. 2010;5(3):e9710. doi:10.1371/journal.pone.0009710
10. Kasneci E, Black AA, Wood JM. Eye-Tracking as a Tool to Evaluate Functional Ability in Everyday Tasks in Glaucoma. *Journal of Ophthalmology*. 2017;2017:6425913. doi:10.1155/2017/6425913
11. Esterman B. Functional scoring of the binocular field. *Ophthalmology*. 1982;89(11):1226-1234.
12. Faraji Y, Tan-Burghouwt MT, Bredewoud RA, van Nispen RMA, van Rijn LJR. Predictive Value of the Esterman Visual Field Test on the Outcome of the On-Road Driving Test. *Translational Vision Science & Technology*. 2022;11(3):20. doi:10.1167/tvst.11.3.20
13. Faraji Y, van Rijn JW, van Nispen RMA, et al. A toolkit for wide-screen dynamic area of interest measurements using the Pupil Labs Core Eye Tracker. *Behavior Research Methods*. 2023;55(7):3820-3830. doi:10.3758/s13428-022-01991-5
14. Faraji Y, van Rijn JW, van Nispen RMA, et al. TREYESCAN: configuration of an eye tracking test for the measurement of compensatory eye movements in patients with visual field defects. *Scientific Reports*. 2023;13(1):20479. doi:10.1038/s41598-023-47470-5
15. Faraji Y, van Rijn JW. Dynamic AOI Toolkit v1.2.0. Computer software. 2024;doi:https://doi.org/10.5281/zenodo.10535707
16. Faraji Y, van Rijn JW. treyescan/event-classifier: v1.0.0. Computer software. 2024;doi:https://doi.org/10.5281/zenodo.10535679
17. Shahar A, Alberti CF, Clarke D, Crundall D. Hazard perception as a function of target location and the field of view. *Accident Analysis & Prevention*. 2010;42(6):1577-84. doi:10.1016/j.aap.2010.03.016
18. Vlakveld WP. A comparative study of two desktop hazard perception tasks suitable for mass testing in which scores are not based on response latencies. *Transportation research part F: traffic psychology and behaviour*. 2014;22:218-231.
19. Prado Vega R, van Leeuwen PM, Rendon Velez E, Lemij HG, de Winter JC. Obstacle avoidance, visual detection performance, and eye-scanning behavior of glaucoma patients in a driving simulator: a preliminary study. *PLoS One*. 2013;8(10):e77294. doi:10.1371/journal.pone.0077294
20. Wood JM, Black AA. Development and validation of a novel Night-time Hazard Visibility Test. *Investigative Ophthalmology & Visual Science*. 2023;64(8):1983-1983.

21. Kassner M, Patera W, Bulling A. Pupil: an open source platform for pervasive eye tracking and mobile gaze-based interaction. *Proceedings of the 2014 ACM international joint conference on pervasive and ubiquitous computing: Adjunct publication*. 2014:1151-1160.
22. Wang J, Olson E. AprilTag 2: Efficient and robust fiducial detection. *2016 IEEE/RSJ International Conference on Intelligent Robots and Systems (IROS)*. 2016:4193-4198.
23. Baumann C, Dierkes K. Neon Accuracy Test Report. *Pupil Labs*. 2023;doi:https://doi.org/10.5281/zenodo.10420388
24. Ehinger BV, Gross K, Ibs I, Konig P. A new comprehensive eye-tracking test battery concurrently evaluating the Pupil Labs glasses and the EyeLink 1000. *PeerJ*. 2019;7:e7086. doi:10.7717/peerj.7086
25. Niehorster DC, Santini T, Hessels RS, Hooge ITC, Kasneci E, Nystrom M. The impact of slippage on the data quality of head-worn eye trackers. *Behavior Research Methods*. 2020;52(3):1140-1160. doi:10.3758/s13428-019-01307-0
26. Holmqvist K, Andersson R. Eye tracking: A comprehensive guide to methods, paradigms and measures. *Lund, Sweden: Lund Eye-Tracking Research Institute*. 2017;
27. Hessels RS, Benjamins JS, Cornelissen THW, Hooge ITC. A Validation of Automatically-Generated Areas-of-Interest in Videos of a Face for Eye-Tracking Research. *Frontiers in Psychology*. 2018;9:1367. doi:10.3389/fpsyg.2018.01367
28. Susac A, Bubic A, Planinic M, Movre M, Palmovic M. Role of diagrams in problem solving: An evaluation of eye-tracking parameters as a measure of visual attention. *Physical Review Physics Education Research*. 2019;15(1):013101.
29. Vansteenkiste P, Cardon G, Philippaerts R, Lenoir M. Measuring dwell time percentage from head-mounted eye-tracking data--comparison of a frame-by-frame and a fixation-by-fixation analysis. *Ergonomics*. 2015;58(5):712-21. doi:10.1080/00140139.2014.990524
30. Hessels RS, Niehorster DC, Nystrom M, Andersson R, Hooge ITC. Is the eye-movement field confused about fixations and saccades? A survey among 124 researchers. *Royal Society Open Science*. 2018;5(8):180502. doi:10.1098/rsos.180502
31. Larsson L, Nyström M, Andersson R, Stridh M. Detection of fixations and smooth pursuit movements in high-speed eye-tracking data. *Biomedical Signal Processing and Control*. 2015;18:145-152.
32. Komogortsev OV, Karpov A. Automated classification and scoring of smooth pursuit eye movements in the presence of fixations and saccades. *Behavior Research Methods*. 2013;45:203-215.
33. Anstey KJ, Wood J, Lord S, Walker JG. Cognitive, sensory and physical factors enabling driving safety in older adults. *Clinical Psychology Review*. 2005;25(1):45-65.
34. Dupuis K, Pichora-Fuller MK, Chasteen AL, Marchuk V, Singh G, Smith SL. Effects of hearing and vision impairments on the Montreal Cognitive Assessment. *Neuropsychology, development, and cognition Section B, Aging, neuropsychology and cognition*. 2015;22(4):413-37. doi:10.1080/13825585.2014.968084
35. Stark Z, Morrice E, Murphy C, Wittich W, Johnson AP. The effects of simulated and actual visual impairment on the Montreal Cognitive Assessment. *Neuropsychology, development, and cognition Section B, Aging, neuropsychology and cognition*. 2023;30(4):523-535. doi:10.1080/13825585.2022.2055739
36. Zheng DD, Swenor BK, Christ SL, West SK, Lam BL, Lee DJ. Longitudinal Associations Between Visual Impairment and Cognitive Functioning: The Salisbury Eye Evaluation Study. *JAMA Ophthalmology*. 2018;136(9):989-995. doi:10.1001/jamaophthalmol.2018.2493
37. Green KA, McGwin Jr G, Owsley C. Associations between visual, hearing, and dual sensory impairments and history of motor vehicle collision involvement of older drivers. *Journal of the American Geriatrics Society*. 2013;61(2):252-257.
38. Ge S, McConnell ES, Wu B, Pan W, Dong X, Plassman BL. Longitudinal association between hearing loss, vision loss, dual sensory loss, and cognitive decline. *Journal of the American Geriatrics Society*. 2021;69(3):644-650.

39. Liu CJ, Chang PS, Griffith CF, Hanley SI, Lu Y. The Nexus of Sensory Loss, Cognitive Impairment, and Functional Decline in Older Adults: A Scoping Review. *Gerontologist*. 2022;62(8):e457-e467. doi:10.1093/geront/gnab082
40. Underwood G. Visual attention and the transition from novice to advanced driver. *Ergonomics*. 2007;50(8):1235-1249.
41. Garay-Vega L, Fisher DL, Pollatsek A. Hazard anticipation of novice and experienced drivers: empirical evaluation on a driving simulator in daytime and nighttime conditions. *Transportation Research Record*. 2007;2009(1):1-7.
42. Alberti CF, Shahar A, Crundall D. Are experienced drivers more likely than novice drivers to benefit from driving simulations with a wide field of view? *Transportation Research Part F: Traffic Psychology and Behaviour*. 2014;27:124-132.
43. Young AH, Crundall D, Chapman P. Commentary driver training: Effects of commentary exposure, practice and production on hazard perception and eye movements. *Accident Analysis & Prevention*. 2017;101:1-10.
44. Van Rossum G, Drake Jr FL. *Python tutorial*. vol 620. Centrum voor Wiskunde en Informatica Amsterdam; 1995.
45. Harris CR, Millman KJ, van der Walt SJ, et al. Array programming with NumPy. *Nature*. 2020;585(7825):357-362.
46. McKinney W. Data structures for statistical computing in python. *Proceedings of the 9th Python in Science Conference*. 2010;445:51-56.
47. Bradski G. The OpenCV Library. *Dr Dobb's Journal: Software Tools for the Professional Programmer*. 2000;25(11):120-123.
48. Hunter JD. Matplotlib: A 2D graphics environment. *Computing in science & engineering*. 2007;9(03):90-95.
49. Virtanen P, Gommers R, Oliphant TE, et al. SciPy 1.0: fundamental algorithms for scientific computing in Python. *Nature methods*. 2020;17(3):261-272.
50. Dar AH, Wagner AS, Hanke M. REMoDNaV: robust eye-movement classification for dynamic stimulation. *Behav Res Methods*. Feb 2021;53(1):399-414. doi:10.3758/s13428-020-01428-x
51. Faraji Y, van Rijn JW. Marking AOIs v1.0.0. Computer software. 2022;doi:https://doi.org/10.5281/zenodo.7022592
52. Goodwin D. Homonymous hemianopia: challenges and solutions. *Clinical Ophthalmology*. 2014:1919-1927.
53. Hartong DT, Berson EL, Dryja TP. Retinitis pigmentosa. *The Lancet*. 2006;368(9549):1795-1809.
54. Fletcher DC, Schuchard RA, Renninger LW. Patient awareness of binocular central scotoma in age-related macular degeneration. *Optometry and vision science*. 2012;89(9):1395-1398.
55. Wadley VG, Okonkwo O, Crowe M, et al. Mild cognitive impairment and everyday function: an investigation of driving performance. *Journal of Geriatric Psychiatry and Neurology*. 2009;22(2):87-94. doi:10.1177/0891988708328215
56. Devlin A, McGillivray J, Charlton J, Lowndes G, Etienne V. Investigating driving behaviour of older drivers with mild cognitive impairment using a portable driving simulator. *Accident Analysis & Prevention*. 2012;49:300-7. doi:10.1016/j.aap.2012.02.022
57. Martin AJ, Marottoli R, O'neill D. Driving assessment for maintaining mobility and safety in drivers with dementia. *Cochrane database of systematic reviews*. 2013;(5)
58. Balk SA, Bertola DB, Inman VW. Simulator sickness questionnaire: twenty years later. University of Iowa; 2013:
59. Brooks JO, Goodenough RR, Crisler MC, et al. Simulator sickness during driving simulation studies. *Accident Analysis & Prevention*. 2010;42(3):788-96. doi:10.1016/j.aap.2009.04.013
60. Nyberg J, Strandberg T, Berg H-Y, Aretun Å. Welfare consequences for individuals whose driving licenses are withdrawn due to visual field loss: a Swedish example. *Journal of Transport & Health*. 2019;14
61. Postuma E, Heutink J, Tol S, et al. A systematic review on visual scanning behaviour in hemianopia considering task specificity, performance improvement, spontaneous and training-induced adaptations. *Disability and Rehabilitation*. 2023:1-22. doi:10.1080/09638288.2023.2243590

62. Wood JM, McGwin G, Jr., Elgin J, et al. On-road driving performance by persons with hemianopia and quadrantanopia. *Investigative Ophthalmology & Visual Science*. 2009;50(2):577-85. doi:10.1167/iovs.08-2506
63. Elgin J, McGwin G, Wood JM, et al. Evaluation of on-road driving in people with hemianopia and quadrantanopia. *The American Journal of Occupational Therapy*. 2010;64(2):268-278.
64. De Haan GA, Melis-Dankers BJ, Brouwer WH, Bredewoud RA, Tucha O, Heutink J. Car driving performance in hemianopia: an on-road driving study. *Investigative Ophthalmology & Visual Science*. 2014;55(10):6482-6489.
65. Michon JA. A Critical View of Driver Behavior Models: What Do We Know, What Should We Do? In: Evans L, Schwing RC, eds. *Human Behavior and Traffic Safety*. Springer US; 1985:485-524.
66. Dickerson AE, Bedard M. Decision tool for clients with medical issues: a framework for identifying driving risk and potential to return to driving. *Occup Ther Health Care*. Apr 2014;28(2):194-202. doi:10.3109/07380577.2014.903357

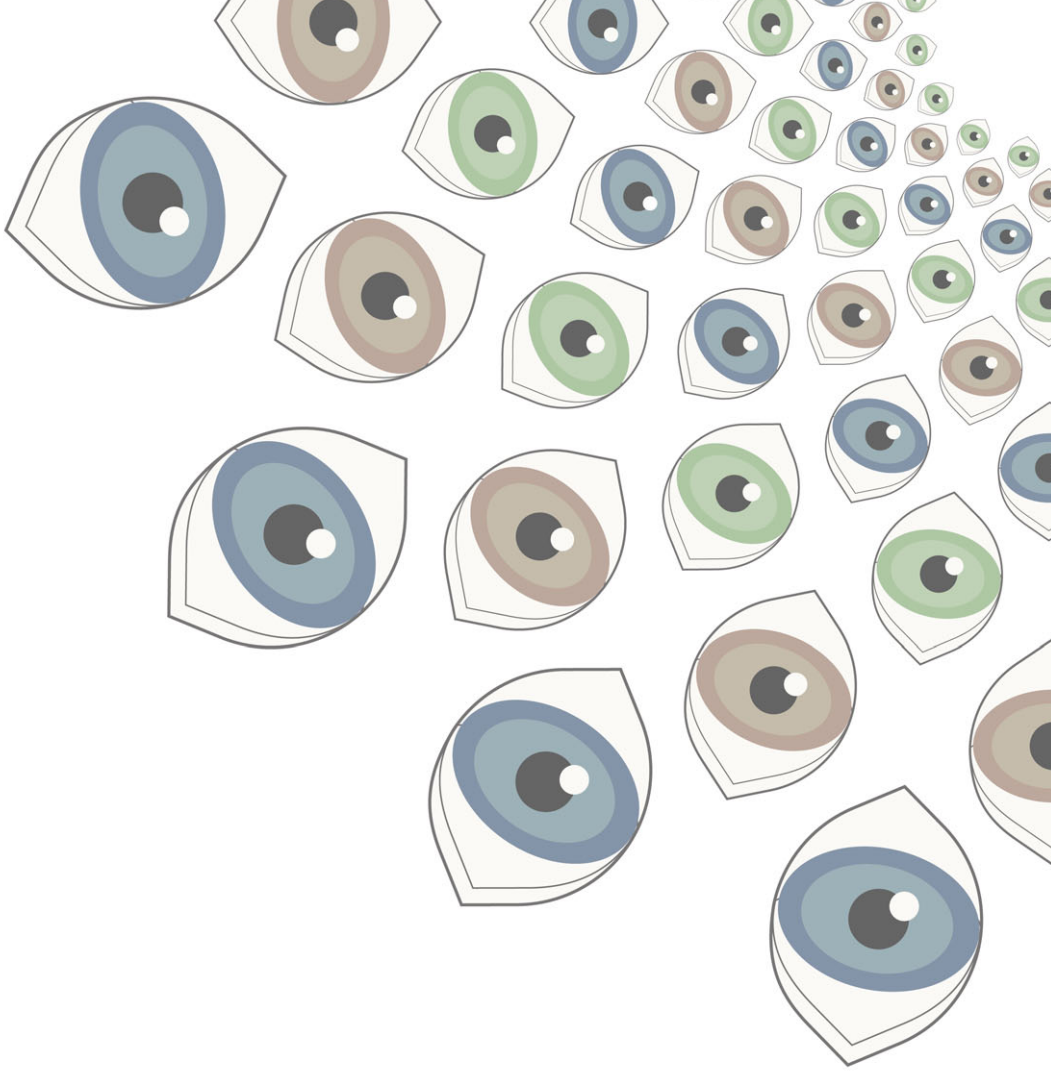

Annex 1

Nederlandse samenvatting (Dutch summary)

Onafhankelijkheid en mobiliteit zijn onlosmakelijk met elkaar verbonden. Het bezit van een rijbewijs en de mogelijkheid om een auto te besturen spelen daarbij een belangrijke rol, vooral wanneer de lichamelijke mobiliteit afneemt of wanneer men in gebieden woont waar openbaar vervoer niet vanzelfsprekend is.

Ongeveer 2% van de bevolking ouder dan 40 jaar lijdt aan glaucoom, een oogaandoening waarbij de oogzenuwen geleidelijk hun functie verliezen. Deze onomkeerbare schade leidt tot gezichtsveldverlies en kan uiteindelijk zelfs resulteren in blindheid. Glaucoom wordt vaak pas in een laat stadium ontdekt, doordat de hersenen in staat zijn om de ontbrekende delen van het gezichtsveld logisch in te vullen, waardoor mensen zich niet bewust zijn van het gezichtsveldverlies. Gelukkig kan de progressie van het verlies vaak worden afgeremd, maar bij sommige patiënten is de aandoening desondanks progressief.

Zowel Europese als Nederlandse wetgeving stelt eisen aan het gezichtsvermogen om veilig auto te mogen rijden. Voor de gezichtsscherpte gold tot voor kort een minimum van 50%, maar wetenschappelijk onderzoek heeft ertoe geleid dat men mag rijden als dit percentage met behulp van een telescoopje kan worden bereikt. Dergelijk telescoopje kan bovenin een brillenglas bevestigd worden waardoor bijvoorbeeld de plaatsnamen op ANWB borden vergroot kunnen worden gezien. Ook voor het gezichtsveld gelden eisen, maar de vraag is of ook deze wel realistisch zijn. Enerzijds blijkt dat mensen met grotere defecten in het gezichtsveld vaak zonder problemen en veilig kunnen autorijden. Anderzijds is de manier waarop het gezichtsveld wordt gemeten, niet representatief voor hoe iemand daadwerkelijk kijkt. Tijdens de meting moeten zowel het hoofd als de ogen volledig stil worden gehouden, terwijl men in het dagelijks leven juist het hoofd en de ogen beweegt om waar te nemen wat men wil zien.

Op dit moment dient dit Esterman binoculaire gezichtsveldonderzoek als de standaard voor het beoordelen van het gezichtsveld bij glaucoompatiënten die rijbewijskeuringen ondergaan in Nederland. Bij dit onderzoek kijkt iemand met beide ogen voortdurend naar een punt middenin een halve bol. Als er in die halve bol buiten dat punt een lichtje wordt geprojecteerd moet men op een knop drukken, maar de ogen en het hoofd mogen niet worden bewogen. Het probleem is dat als men autorijdt zowel de ogen als het hoofd voortdurend worden bewogen.

In **hoofdstuk 2** werd de relatie tussen het Esterman gezichtsveldonderzoek en de praktische rijtest onderzocht met gegevens van het Centraal Bureau

Rijvaardigheidsbewijzen (CBR). Aan de hand van al eerder verzamelde gegevens van mensen die op basis van hun gezichtsveld een rijtest op de weg moesten afleggen, werd een zogenaamd retrospectief dossieronderzoek uitgevoerd. De resultaten toonden een duidelijk verband tussen het aantal gemiste punten in het gezichtsveldonderzoek en de kans op het niet slagen van de praktische rijtest. Dit benadrukt het belang van het gezichtsveld voor rijprestaties. Echter, bleek ook dat het Esterman gezichtsveldonderzoek in onze groep geen onderscheidend vermogen had om rijprestaties op individueel niveau te voorspellen. Dit resultaat benadrukt de noodzaak voor een toegankelijke en betrouwbare test die beter de uitkomst van de praktische rijtest kan voorspellen. Idealiter zou een dergelijke test gestandaardiseerd en kosteneffectief zijn, zoals een gezichtsveldtest, maar daarnaast ook meer aansluiten bij het werkelijke kijkgedrag tijdens het autorijden, net zoals de praktische rijtest bij het CBR.

In dit proefschrift wordt de ontwikkeling van een nieuwe test beschreven waarbij wij met een systeem dat oogbewegingen kan registreren (ook wel een eye-tracker genoemd) het kijkgedrag hebben gemeten van mensen met en zonder glaucoom, terwijl zij op een breed beeldscherm naar verkeerssituaties keken. We noemden deze test de Traffic Eye Scanning and Compensation Analyzer (TREYESCAN). Gedetailleerde beschrijvingen van de ontwikkelingsfasen van de TREYESCAN worden gepresenteerd in **hoofdstuk 3 en 4**.

In **hoofdstuk 3** wordt beschreven hoe wij de TREYESCAN opstelling hebben ontworpen om oogbewegingen te kunnen meten en analyseren op een breed scherm. De analyseprogramma's van dit systeem zijn voor iedereen toegankelijk gemaakt zodat ook andere onderzoekers dit kunnen gebruiken. In ons systeem hebben wij ons gericht op zaken waarvan experts vonden dat het belangrijk was dat deze gezien werden, zogenaamde "Areas Of Interest" (AOI). Een AOI in eye-tracking onderzoek verwijst dus naar een specifiek gedeelte van een visuele stimulus dat van bijzonder belang is voor de analyse. Een AOI kan stil staan (statisch zijn) zoals een deel van een afbeelding of tekstvak, of bewegen (dynamisch zijn), zoals in de TREYESCAN een auto of fietser in een verkeersscène. Bij eye-tracking onderzoek wordt het kijkgedrag van personen geregistreerd, inclusief waar ze naar kijken (fixaties) en hoe hun ogen bewegen tussen verschillende fixaties (saccades). Een AOI stelt de onderzoeker in staat om binnen deze gegevens zich te richten op specifieke onderdelen van de visuele stimulus, waardoor men kan bepalen hoe lang een persoon naar een bepaald gebied kijkt (dwell time) en hoe snel hun blik naar dat gebied wordt getrokken (entry

time). Door deze gerichte analyse kunnen waardevolle inzichten verkregen worden in hoe visuele aandacht wordt verdeeld en welke elementen het meeste aandacht trekken.

Het doel om kijkgedrag op een breed scherm met onbeperkte hoofdbewegingen te meten, vormde een uitdaging vanwege de beperkingen van de op dat moment beschikbare eye-trackers. Deze hebben doorgaans een beperkte hoofdbewegingsvrijheid en een beperkt meetbereik. In onze opstelling hebben we dit probleem opgelost door te kiezen voor een eye-tracker die als bril op het gelaat gedragen kan worden (Pupil Core Eye Tracker) en deze te integreren met op het beeldscherm geplaatste referentiepunten, zogenaamde apriltags (tekens die lijken op QR-markers). Hierdoor werd het mogelijk om een breed gebied te meten met onbeperkte hoofdbewegingen. De openbare testopstelling biedt essentiële hulpmiddelen voor het bepalen van dynamische AOI's met verschillende methoden. Bovendien biedt de testopstelling ook visualisatiehulpmiddelen. Vervolgens hebben we gecontroleerd of de opstelling werkte door metingen te doen bij 11 deelnemers zonder visuele beperking. Dat leverde veelbelovende resultaten op. Onze geteste opstelling kan worden gebruikt door onderzoekers die de Pupil Core Eye Tracker gebruiken in verschillende onderzoeksgebieden, met name in onderzoeksopstellingen die brede schermafmetingen vereisen.

In **hoofdstuk 4** wordt een pilotstudie beschreven, waarin wij geschikte scènes en AOI's voor de uiteindelijke versie van de TREYESCAN selecteren. De verkeersscènes werden met een groothoeklens vanuit een rijdende auto opgenomen in Amsterdam, waarbij de gereden routes in samenwerking met het CBR werden ontworpen. Vervolgens werden interessante verkeersscenario's geïdentificeerd en samengevoegd tot zes video's van ongeveer 8 minuten. Een panel van beoordelaars, bestaande uit CBR-experts op het gebied van praktische rijgeschiktheid en ervaren chauffeurs, beoordeelde deze video's. De beoordelaars categoriseerden AOI's in Must-Be-Seen objecten (vereisen actieve of passieve actie) en May-Be-Seen objecten (relevant om gezien te worden maar vereisen geen verandering in rijgedrag). De locatie van geselecteerde dynamische AOI's werd in elk frame gevolgd met behulp van de programma's die in **hoofdstuk 3** werden beschreven. Om de scène- en AOI-selectie voor TREYESCAN te verbeteren, werden de zes video's getoond aan 20 mensen zonder visuele beperking tijdens twee meetmomenten. Aan de hand van de ervaring van deze deelnemers werden verkeerssituaties met snelle bochten en hoge snelheidsdrempels verwijderd omdat mensen vertelden daar duizelig of

misselijk van te worden. Bovendien werden scènes waarin een AOI plotseling in beeld verscheen uitgesloten, gezien mogelijke schrikreacties bij deelnemers en het ontbreken van zijspiegelinformatie. Scènes met uitsluitend centrale AOI's en een groot aantal overlappende AOI's werden ook verwijderd. Als gevolg hiervan bestond de uiteindelijke versie van TREYESCAN uit twee video's van ongeveer 8 minuten, namelijk de eerste en tweede taak. De gegevens van de eye-tracker metingen binnen de overgebleven verkeersscènes werden bestudeerd. Zo werd bepaald welke AOI's geschikt waren voor gebruik in de uiteindelijke versie van de TREYESCAN. Uiteindelijk bleven er 124 AOI's over in de TREYESCAN, waarvan 64 objecten als Must-Be-Seen werden geclassificeerd en 60 als May-Be-Seen objecten.

In **hoofdstuk 5** worden de resultaten van een zogenaamde "case-control studie" gepresenteerd, waarin de TREYESCAN werd afgenomen bij 50 glaucoompatiënten met verschillende mate van gezichtsveldverlies en 26 deelnemers zonder visuele beperking (controle deelnemers). Glaucoompatiënten werden verdeeld in de categorieën "Mild", "Matig" en "Ernstig" op grond van de ernst van het gezichtsveldverlies. Niet alle eye-tracking metingen van de glaucoompatiënten en controledeelnemers bleken bruikbaar. Uiteindelijk konden we de metingen van 40 glaucoompatiënten en 23 controledeelnemers voor de eerste taak, en 37 glaucoompatiënten en 23 controledeelnemers voor de tweede taak, gebruiken. De resultaten toonden aan dat controledeelnemers meer AOI's bekeken en meer saccades maakten dan glaucoompatiënten. Er werd een significant verschil waargenomen in de snelheid van het bekijken van AOI's voor Must-Be-Seen objecten, waarbij controledeelnemers sneller keken. Glaucoompatiënten met ernstig gezichtsveldverlies presteerden echter niet significant slechter dan glaucoompatiënten met mild gezichtsveldverlies, en er was aanzienlijke overlap en variabiliteit in de resultaten van de glaucoompatiënten. Ook werd een verband tussen het totale aantal saccades en het aantal waargenomen objecten gezien, wat suggereert dat glaucoompatiënten het zien van objecten kunnen verbeteren door meer saccades te maken.

Hoewel toekomstig onderzoek nodig is om de TREYESCAN op grotere schaal te onderzoeken, hebben onze inspanningen de basis gelegd voor een test om compenserende oogbewegingen te meten. Door de uitdagingen die gepaard gaan met eye-tracking op brede schermen te ondervangen en dynamische AOI-analyses uit te voeren, biedt dit proefschrift een kader voor onderzoekers die geïnteresseerd zijn in het bestuderen van compenserende oogbewegingen bij personen met gezichtsveldverlies. Bovendien kan de TREYESCAN ook in de praktijk gaan worden

gebruikt als een beoordelingsinstrument in revalidatiecentra om cliënten met gezichtsveldverlies te ondersteunen bij mobiliteitsgerelateerde hulpvragen. De opstelling en software die in de dynamische AOI-toolkit openbaar zijn aangeboden, reiken verder dan het vakgebied van de oogheelkunde en dienen als een waardevolle bron voor onderzoekers in diverse disciplines, waaronder psychologie, transport en low-vision onderzoek.

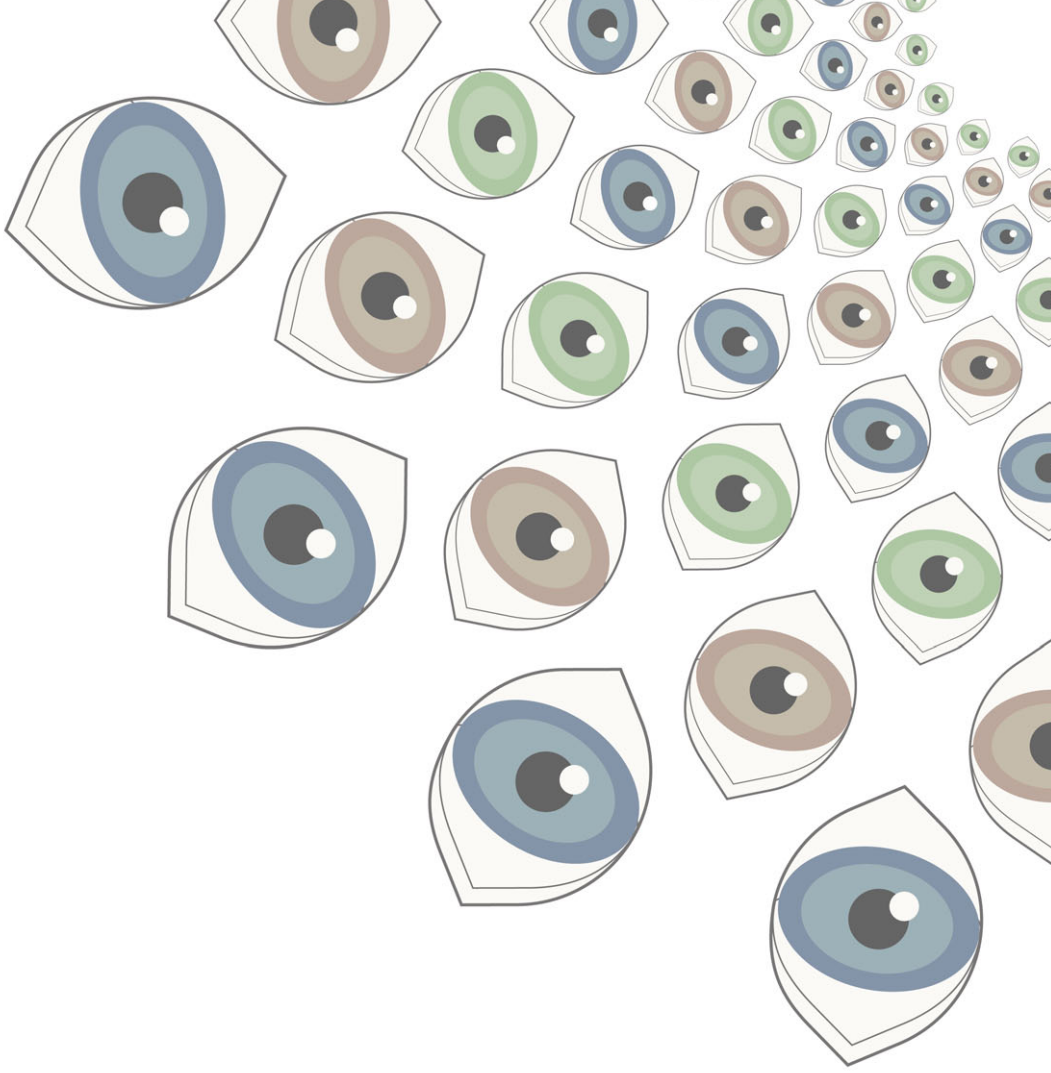

Annex 2

PhD Portfolio

Name: Yasmin Faraji–Hoogvliet
PhD Period: February 2020 – January 2024
Promotors: Ger H.M.B. van Rens & Ruth M.A. van Nispen
Co-promotors: L.J. (René) van Rijn & Jan Koopman
Department: Ophthalmology, Amsterdam UMC location VUmc

PhD training	Year	EC
Courses & workshops		
Introduction to Systematic Review and Meta-Analysis, Coursera	2020	0.46
Work smarter, not harder, Coursera	2020	0.29
Writing in the Sciences, Coursera	2020	1.07
Basic course for clinical investigators (BROK), NFU	2020	1.50
Crash course on Python, Coursera	2020	0.93
Python3 Course, Codecademy	2020	0.89
Course on Scientific Integrity, VUmc	2020	2.00
Castor EDC Beginner Course	2020	0.07
Castor EDC Advanced Course	2020	0.07
Discover your qualities during corona times, APH	2020	0.10
V20: Principles of Epidemiological Data Analysis, EpidM	2020	3.00
V30: Regression Techniques, EpidM	2021	5.00
Het Vrouwenbrein: Vrouwen zijn anders, SheAcademy	2021	0.21
Mindfulness-based stress reduction (MBSR) Training, Pluk	2021	0.71
Getting Published, Nature Research	2022	0.43
Presentations		
VVAO Gooi en Eemland, Online. *Oral Presentation*	2021	0.50
Rotary Laren Blaricum, Online. *Oral Presentation*	2021	0.50
CBR (Dutch driving test organization), Online. *Oral Presentation*	2021	0.50
Dutch Ophthalmology PhD Students Congress (DOPS), Nijmegen. *Oral Presentation*	2021	0.50
European Society for Low Vision Research and Rehabilitation, Online. *Oral Presentation*	2021	2.00
Noordelijke Oogheelkunde Nascholing, Online. *Oral Presentation*	2022	0.50
Dutch Ophthalmology Congress, Groningen. *Oral Presentation*	2022	1.00
Symposium Low Vision Research, Vrije Universiteit Amsterdam. *Poster Presentation*	2022	1.00
Meeting Day, Kennis over Zien, Utrecht. *Poster Presentation*	2022	1.00
Dutch Ophthalmology PhD Students Congress (DOPS), Nijmegen. *Poster Presentation*	2022	1.00
Science & Awards Day, Amsterdam UMC. *Poster Presentation*	2022	0.90
The Eye, The Brain, The Auto, Detroit, USA. *Invited Oral Presentation*	2022	2.00
Dutch Glaucoma Working Group, Utrecht. *Oral Presentation*	2023	0.50
Association for Research in Vision and Ophthalmology, New Orleans, USA. *Poster presentation*	2023	2.00
Dutch Ergophthalmology Working Group, Amersfoort. *Oral Presentation*	2023	0.50

PhD Portfolio (Continued)

PhD training	**Year**	**EC**
Dutch Ophthalmology PhD Students Congress (DOPS), Nijmegen. *Oral Presentation*	2023	0.50
Dutch Ophthalmology Congress (NOG), Groningen. *Oral Presentation*	2024	0.50
Symposium Vereniging voor Revalidatie Bij Slechtziendheid (NOG), Zeist. *Oral Presentation*	2024	0.50
Meeting Stichting Uitzicht, Utrecht. *Oral Presentation*	2024	0.50
OptiVisT Functional Vision Congress, Aberdeen, *Poster Presentation*	2024	2.00
Conference Attendance without Presentation		
Dutch Ophthalmology Congress (NOG), Maastricht	2020	0.29
The Car, The Eye & The Brain, Online	2020	0.57
Spring Sessions, APH, Online	2022	0.25
Teaching & Supervising		
Working on digitizing the ophthalmology rotation for the Master Medicine amid the COVID-19 pandemic	2020	1.25
Bachelor thesis medical student, 1x	2021	1.00
Master thesis medical student, 1x	2021	1.00
Bachelor 2nd year medical students, 6x	2021	1.00
Awards		
Best Oral Presentation Award, DOPS	2021	–
Best Oral Presentation Award, DOPS	2023	–
Other		
Intervision Meetings, Year 1-4, APH	–	0.50
Research Meetings, Department Meetings, Journal Club, Year 1-4	–	2.00

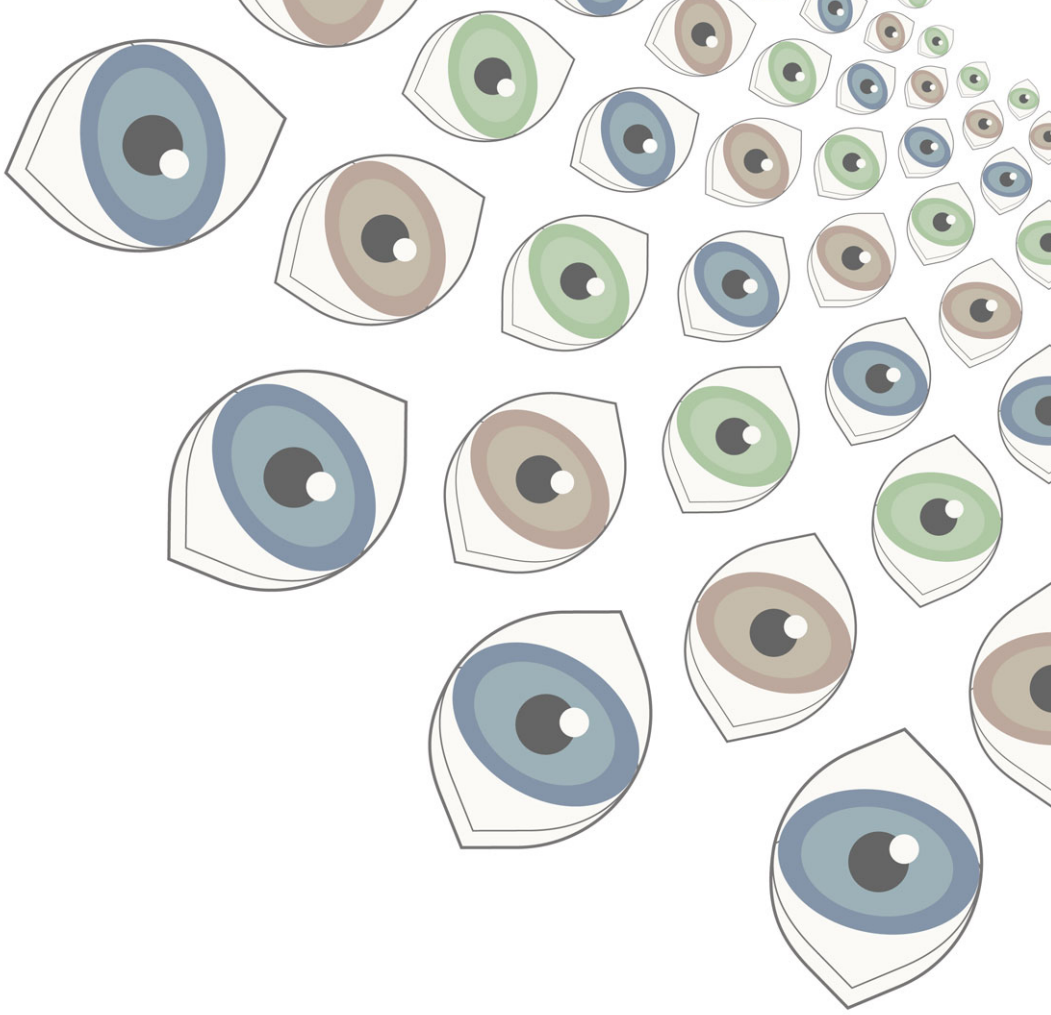

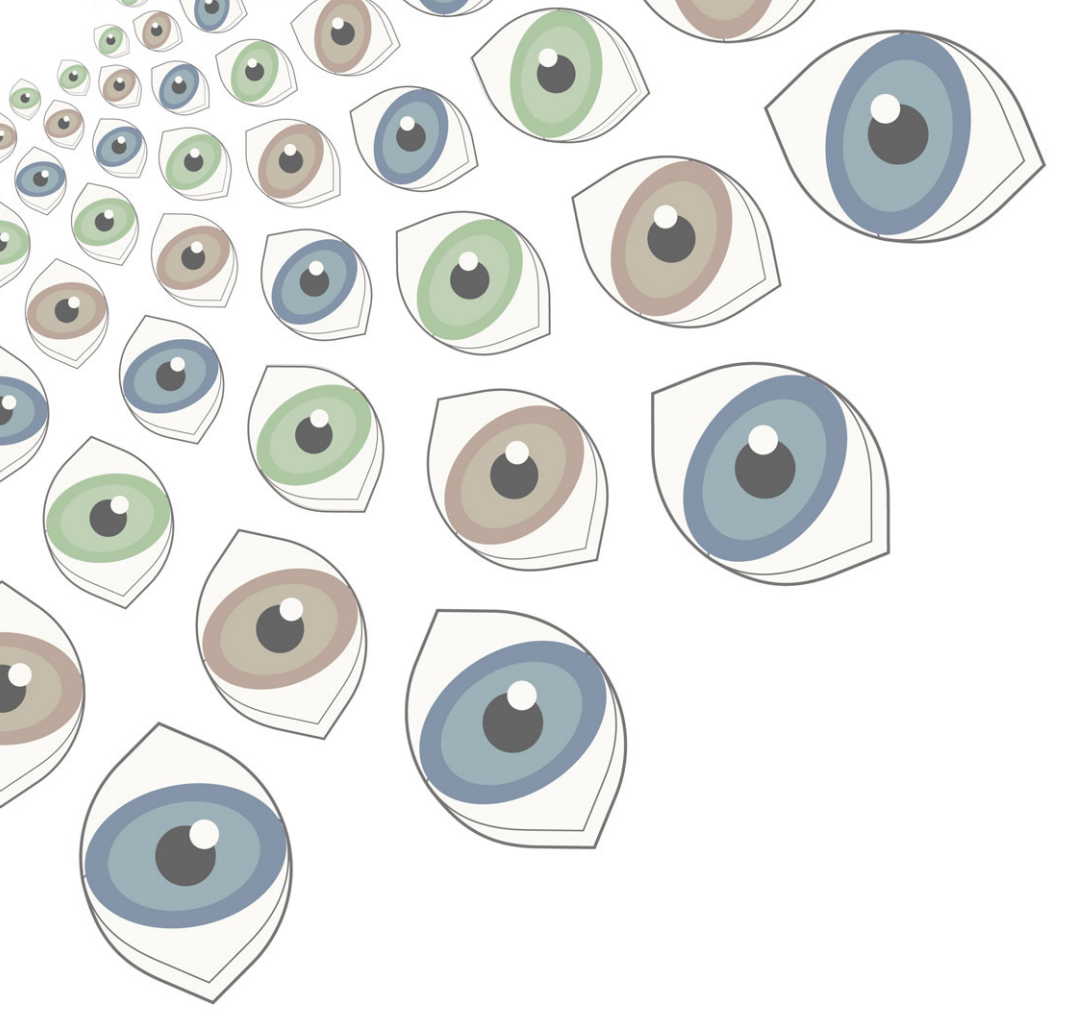

Annex 3

List of publications & List of co-authors

List of publications

Faraji Y, Tan-Burghouwt MT, Bredewoud RA, van Nispen RMA & van Rijn LJ (2022). Predictive Value of the Esterman Visual Field Test on the Outcome of the On-Road Driving Test. Translational Vision Science & Technology, 11(3):20

Faraji Y, van Rijn JW, van Nispen RMA, van Rens GHMB, Melis-Dankers BJM, Koopman J & van Rijn LJ (2022). A Toolkit for Wide-Screen Dynamic Area of Interest Measurements Using the Pupil Labs Core Eye Tracker. Behavior Research Methods, 1-11

Faraji Y, van Rijn JW, van Nispen RMA, van Rens GHMB, Melis-Dankers BJM, Koopman J & van Rijn LJ (2023). TREYESCAN: Configuration of an Eye Tracking Test for the Measurement of Compensatory Eye Movements in Patients with Visual Field Defects. Scientific Reports, 13:20479

Faraji Y, van Rijn JW, van Nispen RMA, van Rens GHMB, Melis-Dankers BJM, Koopman J & van Rijn LJ (2024). Traffic Scene Perception Utilizing TREYESCAN: A Comparative Study between Glaucoma Patients and Normally-Sighted Individuals. *Manuscript under review*

List of co-authors

Bredewoud, R.A.
CBR – Division Fitness to Drive, Rijswijk, The Netherlands

Koopman, J.
Royal Dutch Visio, Centre of Expertise for Blind and Partially Sighted People, Huizen, The Netherlands

Melis-Dankers, B.J.M.
Royal Dutch Visio, Centre of Expertise for Blind and Partially Sighted People, Huizen, The Netherlands

Nispen van, R.M.A.
Amsterdam UMC location Vrije Universiteit Amsterdam, Ophthalmology, Amsterdam, The Netherlands
Amsterdam Public Health, Quality of Care, Societal Participation & Health, Mental Health, Aging and Later Life, Amsterdam, The Netherlands

Rens van, G.H.M.B.
Amsterdam UMC location Vrije Universiteit Amsterdam, Ophthalmology, Amsterdam, The Netherlands
Amsterdam Public Health, Quality of Care, Societal Participation & Health, Mental Health, Aging and Later Life, Amsterdam, The Netherlands

Rijn van, J.W.
Amsterdam UMC location Vrije Universiteit Amsterdam, Ophthalmology, Amsterdam, The Netherlands

Rijn van, L.J.
Amsterdam UMC location Vrije Universiteit Amsterdam, Ophthalmology, Amsterdam, The Netherlands
Department of Ophthalmology, Onze Lieve Vrouwe Gasthuis, Amsterdam, The Netherlands
Amsterdam Neuroscience, Systems & Network Neurosciences, Amsterdam, The Netherlands

Tan-Burghouwt, M.T.
Previous affiliation: CBR – Division Fitness to Drive, Rijswijk, The Netherlands

Authors' contributions per chapter

Chapter 2 Predictive Value Esterman Visual Field

Authors: Y Faraji, MT Tan-Burghouwt, RA Bredewoud, RMA van Nispen & LJ van Rijn
MTTB, RAB and LJvR contributed to the conception and the design of the study. Data was collected by YF with supervision of MTTB. YF, RMAvN and LJvR analyzed the data and interpreted the results. YF drafted the manuscript. All authors critically reviewed the initial manuscript and revised manuscripts. All authors approved the final version of the manuscript and take responsibility for its content.

Chapter 3 Dynamic Area of Interest Toolkit

Authors: Y Faraji, JW van Rijn, RMA van Nispen, GHMB van Rens, BJM Melis-Dankers, J Koopman & LJ van Rijn
YF, RMAvN, GHMBvR, BJMMD, JK and LJvR contributed to the concept and design of the study. Software was written by YF and JWvR. Data was collected by YF. YF, RMAvN and LJvR analyzed the data. YF, RMAvN, GHMBvR, BJMMD, JK and LJvR interpreted the results. YF drafted the manuscript. All authors critically reviewed the initial manuscript and revised manuscripts. All authors approved the final version of the manuscript and take responsibility for its content.

Chapter 4 Configuration of TREYESCAN

Authors: Y Faraji, JW van Rijn, RMA van Nispen, GHMB van Rens, BJM Melis-Dankers, J Koopman & LJ van Rijn

YF, RMAvN, GHMBvR, BJMMD, JK and LJvR contributed to the concept and design of the study. Software was written by YF and JWvR. Data was collected by YF. YF, RMAvN and LJvR analyzed the data. YF, RMAvN, GHMBvR, BJMMD, JK and LJvR interpreted the results. YF drafted the manuscript. All authors critically reviewed the initial manuscript and revised manuscripts. All authors approved the final version of the manuscript and take responsibility for its content.

Chapter 5 TREYESCAN Case-Control Study

Authors: Y Faraji, JW van Rijn, RMA van Nispen, GHMB van Rens, BJM Melis-Dankers, J Koopman & LJ van Rijn

YF, RMAvN, GHMBvR, BJMMD, JK and LJvR contributed to the concept and design of the study. Software was written by YF and JWvR. Data was collected by YF. YF, RMAvN and LJvR analyzed the data. YF, RMAvN, GHMBvR, BJMMD, JK and LJvR interpreted the results. YF drafted the manuscript. All authors critically reviewed the initial manuscript and revised manuscripts. All authors approved the final version of the manuscript and take responsibility for its content.

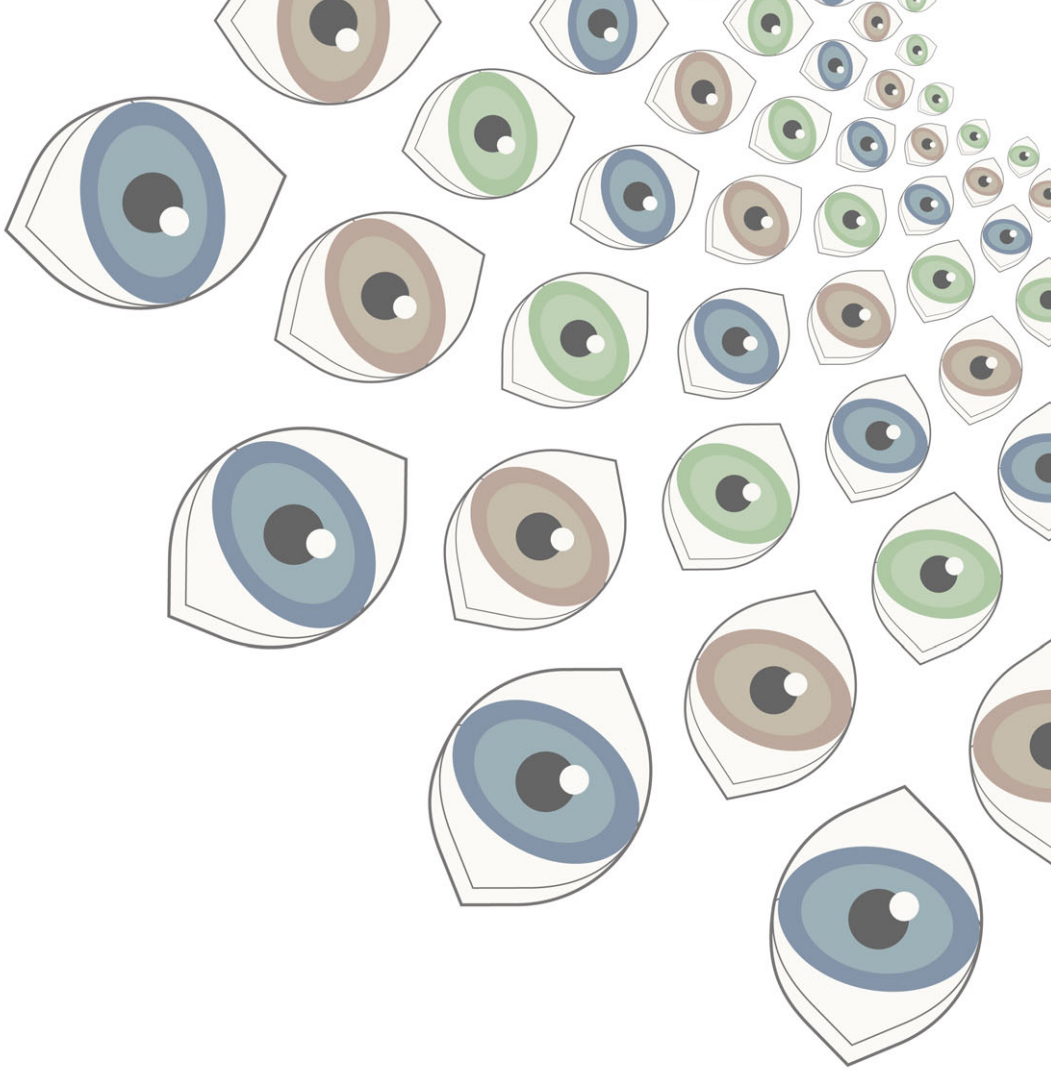

Annex 4

About the Author

Yasmin Faraji-Hoogvliet was born on February 21, 1995, in Sari, Iran. Three weeks later, she immigrated to The Netherlands with her parents, so her father, Farid Faraji, could pursue his PhD in the field of Acarology at the University of Amsterdam. Meanwhile, her mother, Atoosa Familian, completed her PhD in Immunology as a medical doctor at the VU University Amsterdam.

Growing up in Amsterdam, Amstelveen, and Uithoorn, Yasmin completed her secondary education at Hermann Wesselink College in Amstelveen in 2013 (*Bilingual Gymnasium*). She then pursued a degree in medicine at the VU University Amsterdam. During her studies Yasmin actively engaged in various extracurricular activities, including working as a teaching assistant pharmacotherapy, serving as a nurse at an elderly home, and working as a triage nurse (*triagist*) at the GP emergency service (*Huisartsenpost*). Additionally, she served as a teaching assistant and board member at the Basic Suturing Course Amsterdam, and held a position as a board member and violinist at the VU Student Orchestra (*VU-Orkest*).

After graduating from medical school in 2019, Yasmin started her career as a medical doctor at the ophthalmology department of Jeroen Bosch Hospital in Den Bosch. In 2020, she began her PhD research at Amsterdam UMC, to develop "TREYESCAN". Her primary objective was to create a test capable of measuring the compensatory eye movements of glaucoma patients while they view traffic scenes. Her goal was to make a positive impact on the mobility challenges faced by visually impaired individuals.

Throughout her PhD, Yasmin continued working as an instructor at the Basic Suturing Course, where she provided training to medical students and professionals seeking to enhance their suturing skills. She also played violin in the VU Chamber Orchestra (*VU-Kamerorkest*). Furthermore, she held a board member position for the "Stichting Maten" of the VU-Orchestra.

Currently, Yasmin is participating in the ophthalmology residency program at Amsterdam UMC to further her medical training.

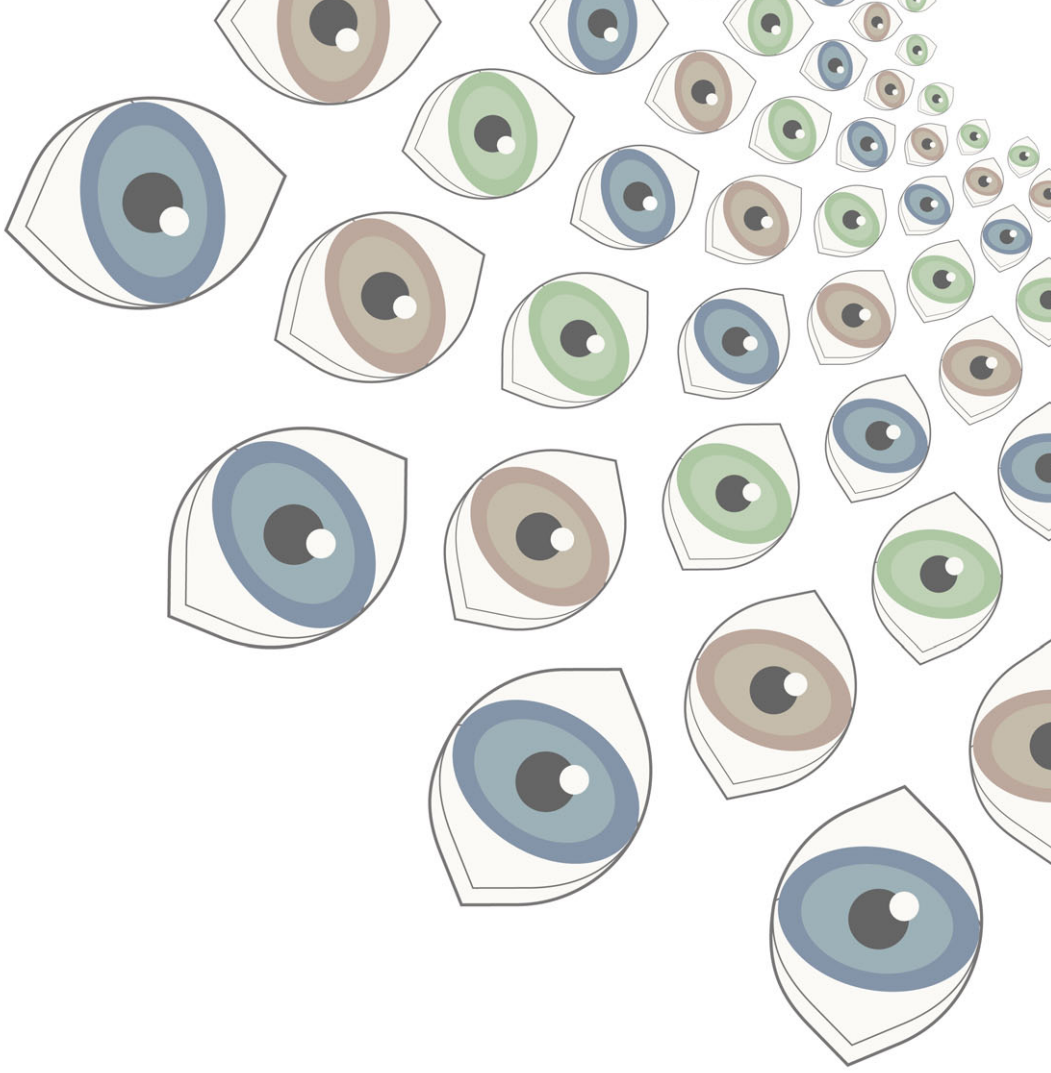

Annex 5

Dankwoord (acknowledgements)

Hoewel mijn naam op de kaft staat, is dit proefschrift het resultaat van een gezamenlijke inspanning. Daarom wil ik graag iedereen bedanken die mij bij de totstandkoming van dit proefschrift heeft ondersteund.

Allereerst wil ik graag mijn dank uitspreken aan alle **deelnemers** die met zoveel inzet betrokken waren bij de verschillende stadia van dit onderzoek. Hun toewijding waardeer ik enorm. Het enthousiasme voor de TREYESCAN en de persoonlijke verhalen over het belang van autorijden en mobiliteit, hebben mij de motivatie gegeven om dit project af te ronden.

Ontzettend veel dank aan mijn promotieteam. Beste **Ger**, ik ben je enorm dankbaar dat ik mijn semi-arts stage op de poli Oogheelkunde van het Elkerliek ziekenhuis in Helmond mocht lopen, de plek waar ons avontuur samen begon. In die periode heb ik waardevolle lessen van je geleerd, vooral over het belang van persoonlijke aandacht voor elke patiënt, zelfs als het spreekuur overvol is. Dankzij jou kreeg ik de kans om als wetenschappelijke stage student deel uit te maken van de low-vision onderzoeksgroep in Amsterdam UMC, met de mogelijkheid om door te stromen naar een promotietraject. Ik ben je dankbaar voor de kansen die je me hebt gegeven en voor de levenslessen die ik tijdens dit traject dankzij jou heb opgedaan.

Lieve **Ruth**, bedankt dat ik altijd bij jou terechtkon voor een fijn en gezellig gesprek, vooral wanneer ik weer eens beren op de weg zag. Jouw rustige uitstraling gaf me telkens weer vertrouwen. Het is bewonderenswaardig hoe jij elke PhD-student persoonlijke aandacht geeft. Ondanks je drukke agenda, maak je toch altijd tijd vrij voor iedereen. Ik hoop dat deze afronding niet het einde van onze samenwerking betekent.

Beste **René**, door jouw nuchtere en praktische blik, bleef ik vertrouwen houden in het project en in mijn eigen kunnen. Sinds de start van mijn opleiding tot oogarts, heb ik een beter beeld gekregen van hoe druk jouw werkdagen daadwerkelijk zijn. Toch maakte je altijd tijd voor mij vrij, of het nu ging om een overleg, het uitvogelen van de eye tracker, of het kijken naar de TL-verlichting in het plafond. Ik zal nooit vergeten hoe we samen door de straten van Amsterdam reden en hebben zitten juichen wanneer een scooter plotseling de weg op kwam rijden.

Beste **Bart** en **Jan**, bedankt voor jullie betrokkenheid bij dit project en voor de technische expertise die jullie hebben ingebracht op het gebied van verlichting, eye tracking en mobiliteit. Jullie hielden altijd het revalidatieaspect in gedachten, wat mij veel heeft geleerd over de hulpvragen van personen met een visuele beperking.

Onze overleggen waren vaak online, maar het was altijd een plezier om jullie bij een congres of symposium in levende lijve te ontmoeten.

Beste **Marianne** en **Ruud**, jullie staan als coauteur op het eerste artikel in deze thesis. Bedankt dat jullie mij, toen ik nog een derdejaars geneeskundestudent was, de kans gaven om onderzoekservaring op te doen en de dataverzameling bij jullie op de Naritaweg uit te voeren. Het is bijzonder en toevallig dat ik dit artikel later in mijn PhD-traject heb kunnen publiceren, en dat het nu deel uitmaakt van deze thesis.

Hartelijk dank aan de promotiecommissie, **Prof.Dr. Moll**, **Dr. Goossens**, **Prof.Dr. Cornelissen**, **Prof.Dr. Beckers**, en **Prof.Dr. de Waard**, voor het zorgvuldig en kritisch beoordelen van dit proefschrift. Ik kijk ernaar uit om tijdens de verdediging met jullie van gedachten te wisselen over mijn werk.

Arman en **Priti**, bedankt voor jullie betrokkenheid bij mijn onderzoek en het verwerken van data. **Arman**, ik heb veel geleerd in de tijd dat ik jou als stagiair mocht begeleiden. Je was een zeer gemotiveerde student, wat het samenwerken met jou bijzonder prettig maakte. Ik hoop dat we onze opgebouwde vriendschap nog lang kunnen voortzetten!

Sinds mei 2024 ben ik gestart met de opleiding tot oogarts in Amsterdam UMC. Ik wil **Annette** en **Ivanka**, mijn opleiders, enorm bedanken voor de kans en de ruimte die zij mij hebben geboden om de afronding van mijn PhD te combineren met het begin van de opleiding. Ook wil ik mijn **collega AIOS** en de **stafartsen** bedanken voor de warme ontvangst en het begrip voor de afronding van dit project. Er komen nog hele mooie tijden aan samen, dat weet ik zeker!

Dan mijn geweldige paranimfen. Lieve **Joris,** bedankt voor je betrokkenheid bij dit project. Ik kwam bij jou aankloppen als goede vriend die mij al sinds de middelbare school uit de brand helpt met computerproblemen. In die eerste fase, heb je me ontzettend fijn op weg geholpen met het programmeren in Python en was je altijd enorm geduldig, zelfs wanneer je voor de zoveelste keer dezelfde uitleg moest geven aan iemand zonder technische achtergrond. Ik ben er trots op dat ik nu, als medicus, aardig kan programmeren, en dat heb ik volledig aan jou te danken. Uiteindelijk groeide dit uit tot een waardevolle samenwerking, waarbij ik je mijn collega mocht noemen en we officiële wekelijkse werkmeetings inplanden. Deze meetings waren voor mij erg waardevol, niet alleen vanwege jouw kennis als programmeur, maar ook vanwege het vriendschappelijke bijpraatmomentje.

Lieve **Arthur**, al snel ontdekten we dat we op dezelfde dag jarig zijn, maar daarna bleken er meer overeenkomsten tussen ons te zijn. Jij ging mee naar het congres *The Eye, The Brain & The Auto* in Detroit, waar ik was uitgenodigd om een praatje te houden. Samen met jou en Anton heb ik daar een geweldige tijd beleefd en onvergetelijke herinneringen gemaakt (iets met breedsprakige Amerikanen en indrukwekkende flitsende auto's). Het was ontzettend gezellig met jou en Rob op kantoor. Ik hoop dat we elkaar nog vaak zullen zien!

Tijdens mijn traject heb ik veel gezellige collega-onderzoekers leren kennen: **Aleid**, **Annabel**, **Arthur**, **Buket**, **Edine**, **Ellen**, **Esther**, **Hilde**, **Katie**, **Laura**, **Lia**, **Jenny**, **Jonathan**, **Katie**, **Leo**, **Lorenzo**, **Manon**, **Marc**, **Maria**, **Mariska**, **Marjolein**, **Mieke**, **Milo**, **Miriam**, **Petra**, **Richard**, **Rob**, **Vera**, **Wouter, en Yvonne**. Bedankt voor de leuke tijden op en buiten kantoor. Ik realiseer me goed dat het niet vanzelfsprekend is om met een aantal collega's ook buiten kantoor een vriendschap op te bouwen, en ik waardeer dat enorm. **Esther**, wij zaten in hetzelfde uitdagende schuitje: een onderzoeksproject opstarten terwijl de wereld op slot ging door een pandemie. Het was een geruststelling om de onzekerheden die daarmee gepaard gingen met jou te kunnen delen. **Katie**, ik bewonder jouw drive en enthousiasme, zelfs in moeilijke tijden. Het laatste NOG-congres voelde als een mooie afsluiting van de PhD-periode, en ik heb enorm genoten van de tijd die we daar met **Mariska** en **Vera** hebben doorgebracht. **Rob**, ik ben blij dat ik jou heb leren kennen en dat we zo'n leuke klik hebben. Je was een geweldig kamergenootje, en ik heb vaak vol bewondering opzij gekeken naar hoe jij met je werk aan de slag was. Bedankt dat je altijd een luisterend oor voor mij had, ook al kwebbelde (en zong) ik vaak je oren van je hoofd. Ik hoop dat we nog contact zullen houden, maar dat moet vast lukken aangezien je tegenover ons woont. **Miriam**, wat was jij een fijne collega en ben je een lieve vriendin. Bedankt dat we altijd alles konden bespreken in de treinrit terug naar Utrecht. Ik ben blij dat we goed contact hebben gehouden sinds onze beide trajecten zijn afgelopen, en ik weet zeker dat we dat in de toekomst ook zullen blijven doen. **Petra**, wat hebben wij het leuk gehad samen in de PhD-tijd, van het delen van hotelkamers (of enge airbnb kamers) tot de eer dat ik jouw paranimf mocht zijn. Bedankt voor jouw wijze inzichten en adviezen, die hebben veel voor mij betekend. Wat was het geweldig om jou en je leuke gezin in Oostenrijk te bezoeken. Hopelijk blijven we elkaar nog lang opzoeken.

Mijn lieve vrienden, ik wil jullie allemaal bedanken voor de aanmoedigingen en de gezelligheid. Hoewel ik niet iedereen persoonlijk kan noemen, wil ik een aantal van jullie in het bijzonder bedanken. **Eloise** (baelo), wat was het fijn om tijdens de corona periode

samen aan ons werk te zitten. Bedankt dat ik ook af en toe bij je mocht aankloppen voor video-edit advies. **Melania** (my sister from another mother), ook al woon je aan de andere kant van de wereld (aka Maastricht), stond je altijd voor mij klaar. Ik heb veel gehad aan onze wekelijke podcasts, die ik opnam tijdens mijn loopje van het station naar mijn werkplek. Liefste **Besties**, het is zo bijzonder dat we nog steeds zo'n hechte groep zijn sinds de middelbare school. Elk jaar besef ik me weer hoe bijzonder dat is. **Inge**, bedankt dat je altijd zo'n betrokken vriendin bent en dat je zo enthousiast mensen hebt geworven voor mijn studies. Ik ben blij dat onze partners het zo goed met elkaar kunnen vinden en dat we het altijd gezellig hebben met zijn vieren. **Jelmi**, het was fijn om met jou te kunnen praten over PhD-life, ook al werk jij in een heel ander vakgebied in het verre Zurich. Dank voor je goede adviezen, zoals: "praat eens met mijn broer, hij is wiskundige". **Thijs**, bedankt dat ik altijd bij jou terechtkon voor computer gerelateerde vragen, en voor het maken van de prachtige knop voor de opstelling. **Nelle**, bedankt voor de gezellige werkdagen bij mij thuis. Je was altijd bereid een stukje na te lezen en was welwillend proefpubliek wanneer ik een presentatie wilde oefenen. Ik heb veel bewondering voor hoe jij deze periode van je leven aanvliegt en ik ga onze woensdagen missen. **Mandy** en **Annabel**, ik ben blij dat we hechte vriendinnen zijn gebleven sinds de bachelor geneeskunde. Bedankt voor de leuke avondjes en de steun die jullie mij hebben gegeven. Lieve **VU-Orkest buddies**, bedankt voor alle muziek die we samen hebben mogen maken, de leuke tijden op tournee en in verschillende bestuursformaties, en vooral dat we zulk leuk contact met elkaar hebben gehouden.

Mijn lieve **familie** en mijn **opa's** en **oma's**, verspreid over de hele wereld met kilometers afstand tussen ons in, jullie waren op afstand de beste cheerleaders die ik me maar kon wensen. Het was een groot geluk dat een deel van de familie in 2023 bij onze bruiloft samen kon komen, en ik hoop dat het in de toekomst makkelijker zal worden om elkaar te zien.

Anja, **Jan**, **Wouter**, **Opa** en **Oma** (en Teuntje), wat is het fijn om me ook bij jullie zo thuis te voelen. Bedankt voor jullie oprechte interesse in mijn werk en hoe het ervoor stond met mijn artikel(tjes). **Jan**, toen ik ineens met een Volvo-autostoel zonder onderstel zat, wist jij daar gelukkig wel raad mee. Dankzij jouw ingenieuze creatie konden meer dan 100 mensen toch comfortabel naar de verkeersscènes kijken.

Atoosa en **Farid**, mijn lieve ouders, ik ben jullie ontzettend dankbaar voor alles wat jullie voor mij hebben gedaan. Jullie hebben mij van jongs af aan geïnspireerd en het vertrouwen gegeven dat ik mijn doelen kan waarmaken. In maart 1995 verhuisden

jullie naar Nederland met een baby van 3 weken voor Farid's PhD-onderzoek. Naarmate ik ouder word, besef ik steeds meer hoe dapper jullie waren om deze stap te zetten en hoe onwijs knap jullie het hebben gedaan. Daarop volgde Atoosa's PhD-onderzoek en jullie verdedigingen staan me nog heel goed bij (ook al was ik toen een meisje van 5 en 10 jaar). Ik vind het heel bijzonder dat ik in jullie voetsporen mag treden en het met deze verdediging voelt alsof de cirkel rond is. Doostetoon daram ghade ye donya.

Last but certainly not least, lieve **Anton**, zonder jouw onvoorwaardelijke steun, rust, humor, en liefde was dit proefschrift nooit tot stand gekomen. Ik ben enorm dankbaar voor hoe ons leven zich heeft ontvouwd tijdens mijn promotietraject, van onze eerste stappen als samenwonend stel in een bescheiden appartementje van 36 m^2 tot onze prachtige bruiloft. In jou heb ik de perfecte combinatie van een veilige haven en geweldig avontuur gevonden. Ik kijk enorm uit naar alles wat het leven ons nog zal brengen.
Ik hou van joes.